NCHRP Project 12-103

Phase I Report

"Bridge Superstructure Tolerance to Total and Differential Foundation Movements"

4/14/2014

David Masceri, John Braley, Nick Romano, and Franklin Moon
Drexel University

Dennis Mertz, PhD, PE
Professor, University of Delaware

Naresh Samtani, PhD, PE
President, NCS Consultants, LLC

Submitted to

Waseem Dekelbab, PhD, PE, PMP
Senior Program Officer
National Cooperative Highway Research Program

Table of Contents

NCHRP Project 12-103

"Bridge Superstructure Tolerance to Total and Differential Foundation Movements"

Phase I Report

1 Introduction

Currently, there is little rational and practical guidance available to bridge designers as to what constitutes tolerable differential support movements for various bridge types/configurations. The semi-empirical and anecdotal evidence available from past research (e.g., Moulton et al. 1985) suggests that large relative movements may be tolerable from a structural safety perspective, but designating such large movements as "tolerable" runs contrary to many designers' sensibilities. While current practice can vary significantly from state to state, it is not uncommon for arbitrarily small differential support movements to be specified by bridge designers. Depending on the specific case, this excessive conservatism can lead to a significant increase in cost (e.g. through precluding the use of certain foundation types) with no clear evidence that it produces a commensurate improvement in long-term bridge performance.

1.1 Research Objectives

Motivated by this knowledge gap, the overarching aim of this research is to develop a more sound and comprehensive understanding of the levels of differential support movements that bridges may tolerate without performance problems. More specifically, this research was devised to satisfy the following two objectives:

1) Develop procedures to determine the acceptable levels of bridge foundation movements based upon superstructure tolerance to total and differential movements considering service and strength limit states

2) Propose revisions to the AASHTO LRFD Bridge Design Specifications related to foundation movement limits that shall include vertical, horizontal, and rotational movements.

1.2 Summary of Work Plan

To satisfy these objectives, a work plan was developed and organized into four phases as shown in Figure 1-1. The specific objectives for each phase are given in Table 1-1.

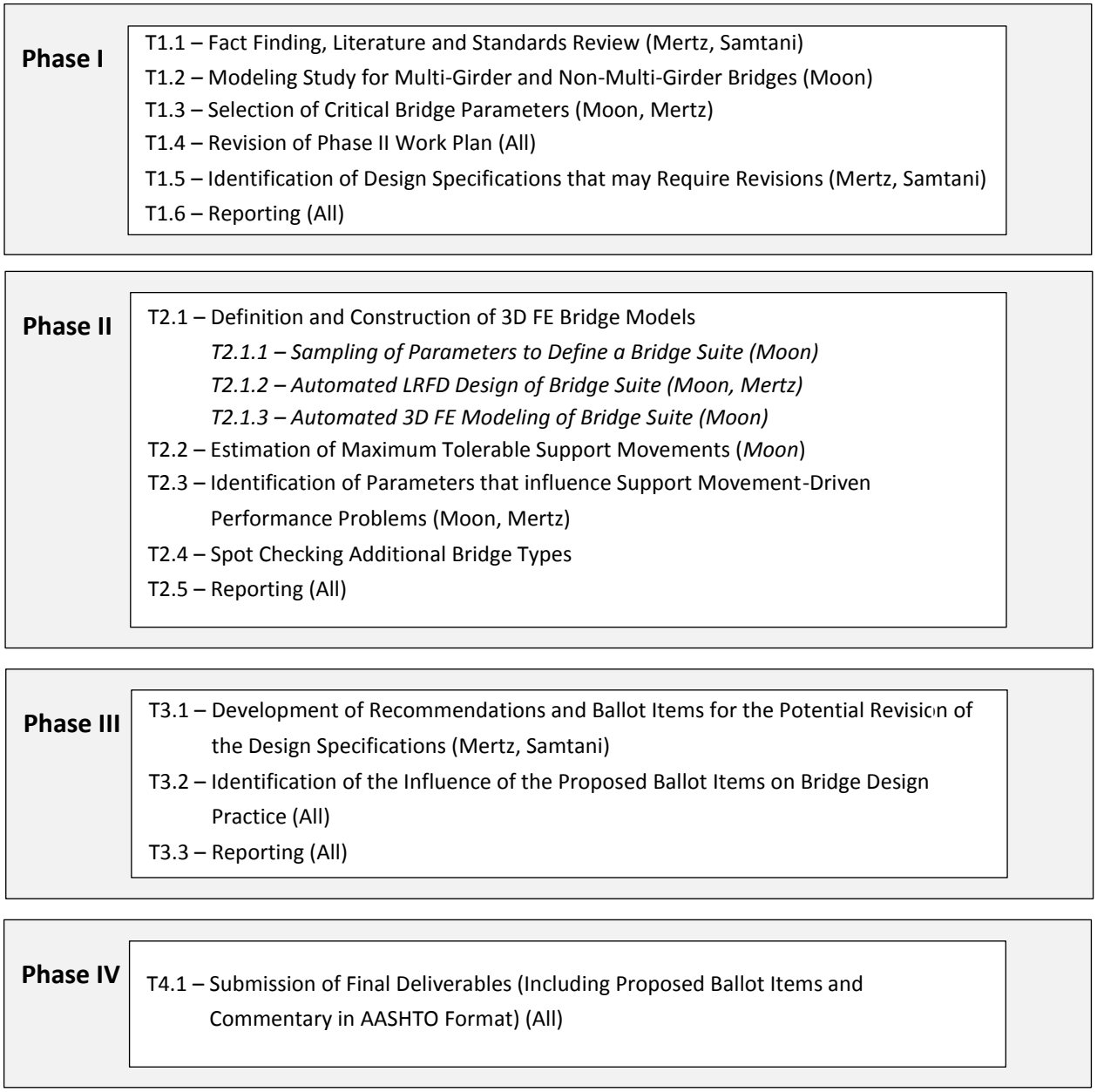

Figure 1-1 – Schematic of Proposed Research Plan

Table 1-1 – Summary of Phase-Specific Objectives

Phase	Principal Objectives
I	(a) Establish the state-of-the-knowledge related to total and differential support movements (b) Develop efficient and accurate modeling approaches capable of simulating the response of common bridge types to support movements (c) Examine the sensitivity of the initial set of parameters to responses generated from support movements (d) Revise the proposed work plan based on the results of (b) and (c) (e) Identify design provisions that may require revisions based on the results of this research program
II	(a) Develop estimates of tolerable support settlements for both strength and serviceability limit states for common bridge types (b) Identify the critical parameters that influence tolerable support movements (c) Develop simple expressions to estimate the level of tolerable support movement based on the identified influential parameters
III	(a) Develop recommendations and associated ballot items for the inclusion of Phase II results within the AASHTO LRFD Specifications (b) Identify the influence of the proposed recommendations on current practice
IV	Develop a comprehensive report documenting the entire research project

1.3 Overview of Research Team

To carry out the research plan outlined above, a team of three individuals with complementary expertise was formed. The team consists of Dr. Franklin Moon (Associate Professor, Drexel University) who has expertise related to bridge performance, FE modeling and computational tools; Dr. Dennis Mertz (Professor, University of Delaware) who brings expertise related to the AASHTO LRFD Design Specifications, bridge performance, and current bridge engineering practice; and Dr. Naresh Samtani (President, NCS Consultants, LLC) who has expertise related to bridge substructure performance and design, current geotechnical engineering practice, and the AASHTO LRFD Design specifications. Figure 1-2 provides a summary of the research team, their roles, and the proposed management/communication structure.

1.4 Outline of Report

The outline of the report follows directly from the work plan for Phase I shown in Figure 1-1. A brief summary of each section is provided below.

- Section 2 of the report provides an overview of the available literature related to the influence of differential and absolute foundation movements on the performance of short and medium span bridges.

- Section 3 presents a modeling study to determine the precise modeling approaches to be employed for both multi-girder and non-multi-girder bridges. This study examined several different modeling approaches through both mesh sensitivity studies and comparison with benchmark models.
- Section 4 presents a series of parametric studies carried out on multi-girder steel bridges to identify how various parameters influence the sensitivity of a bridge to support movements. Based on the results of this study, the final set of parameters to be included within the Phase II analyses was selected.
- Section 5 presents a revised Phase II work plan based on the results obtained during Phase I of the project.
- Section 6 provides a summary of the provisions within the AAHSTO LRFD Design Specifications that are related to support movements. Depending on the results of this research program, these provisions may be targeted for revision.

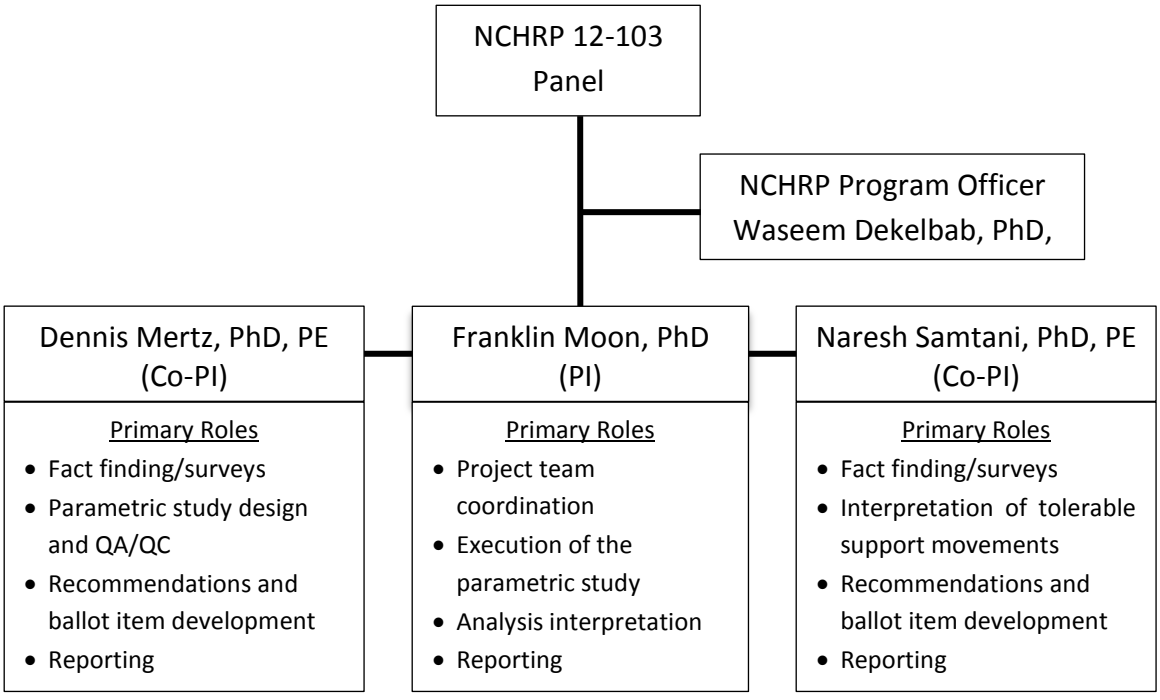

Figure 1-2 – Research Team Organization and Roles

2 Literature Review (T1.1)

Bridge foundations and geotechnical features should be designed so that their deformations or differential movements will not cause structural damage to the bridge or any of its auxiliary features. Uneven displacements of bridge abutments and pier supports can deteriorate the quality of the ride, public safety, aesthetics, and structural integrity of a bridge. These types of movements often lead to expensive maintenance and repairs. Therefore, geotechnical limit states with consideration of bridge structures are related to foundation deformations. Foundation deformations within the service limit states can be categorized into vertical, horizontal, and rotational movements. The following sections provide background information and design criteria regarding these limit states as well as issues related to construction sequencing.

2.1 Vertical Support Movement

Depending on the type of superstructure, the connection between the superstructure and substructure, and the span lengths and widths, the magnitudes of differential settlement that can cause damage to the bridge can vary significantly. In a continuous span bridge, differential settlements induce bending moments and shear in the superstructure and can potentially cause structural damage. They can also cause damage to a simple span bridge, although to a lesser extent. With simple span bridges the major concern is with ride quality and aesthetics. Without continuity over the supports, the change in slope of the riding surface near the supports may be more severe than those in a continuous span. It has been found in a number of studies (Grant et al., 1974 and Skempton and MacDonald, 1956) that the extent of damage of structures caused by differential settlement is roughly proportional to the angular distortion. The angular distortion is the normalized measure of differential settlement, including the distance over which the settlement occurs. For bridge structures, the two points to evaluate the differential settlement are commonly the distance between adjacent supports.

Currently, the only definitive guidance related to the effect of foundation deformations on bridge structures is based on a report by the FHWA (1985). From an evaluation of 314 bridges nationwide, FHWA (1985) arrived at the following conclusions:

> *The results of this study have shown that, depending on type of spans, length and stiffness of spans, and the type of construction material, many highway bridges can tolerate significant magnitudes of total and differential vertical settlement without*

becoming seriously overstressed, sustaining serious structural damage, or suffering impaired riding quality. In particular, it was found that a longitudinal angular distortion (differential settlement/span length) of 0.004 would most likely be tolerable for continuous bridges of both steel and concrete, while a value of angular distortion of 0.008 would be a more suitable limit for simply supported bridges.

Another study (NCHRP, 1983) states:

In summary, it is very clear that the tolerable settlement criteria currently used by most transportation agencies are extremely conservative and are needlessly restricting the use of spread footings for bridge foundations on many soils. Angular distortions of 1/250 of the span length and differential vertical movements of 2 to 4 inches (50 to 100 mm), depending on span length, appear to be acceptable, assuming that approach slabs or other provisions are made to minimize the effects of any differential movements between abutments and approach embankments. Finally, horizontal movements in excess of 2 in. (50 mm) appear likely to cause structural distress. The potential for horizontal movements of abutments and piers should be considered more carefully than is done in current practice.

Based on the above studies, AASHTO LRFD C10.5.5.2 indicates that angular distortions between adjacent foundations greater than 0.008 rad. in simple spans and 0.004 rad. in continuous spans should not be permitted in settlement criteria. This same article states that "other angular distortion limits may be appropriate after consideration of cost of mitigation through larger foundations, realignment or surcharge, rideability, aesthetics, and safety."

In a survey performed for SHRP 2 (2011) regarding the allowable movement of new structures, it was found that a majority of agencies are not following the guidance on tolerable movement provided in the AASTHO LRFD Specification. Agencies differed in their criteria for tolerable movement, with some on a case-by-case bases while others had general quantitative requirements. An example of the use of more stringent criteria can be found in the Pennsylvania Department of Transportation's (PennDOT) Structures Design Manual (2012), which states:

The allowable settlement for shallow footings supporting bridge structures shall be based on the angular distortion (δ'/l) between adjacent support units (i.e., between piers or piers and abutments) where δ' and l are the differential settlement and span between

adjacent units, respectively. In addition, the maximum net settlement of a footing shall not exceed 1 inch. The dimensionless ratio δ'/l shall be limited to 0.0025 and 0.0015 for simple and continuous span bridges, respectively.

Another example of the use of more stringent criteria is from Chapter 10 of the Arizona Department of Transportation (ADOT) Bridge Design Guidelines (ADOT 2009), which states the following:

The bridge designer should limit the total settlement of a foundation per 100 ft. span to 0.5 in. Linear interpolation should be used for other span lengths. Higher total settlement limits may be used when the superstructure is adequately designed for such settlements. The designer shall also check other factors such as rideability and aesthetics. Any total settlement that is higher than 2.5 in, per 100 ft. span, must be approved by the ADOT Bridge Group.

From a structural perspective, bridges can handle more movement that traditionally allowed. There are no technical reasons for agencies to set such arbitrary limitations to the criteria found in AASHTO LRFD C10.5.5.2. There are practical limits to limiting deformation based on other structures associated with a bridge, e.g., utilities, approach slabs, wingwalls, drainage grades, etc. It is understood that the differential movement limitations provided in AASHTO LRFD should be considered in conjunction with the movement tolerances of all bridge facilities. Comprehensive guidance in design, however, is currently lacking.

2.2 Horizontal (Lateral) and Rotational Support Movements

According to Moulton et al. (1985) both the frequency and magnitude of vertical movements are often substantially greater than horizontal movements, but horizontal movements tend to be more damaging to bridge superstructures. Herein the word “horizontal” is considered synonymous with “lateral” (i.e. in the out-of-plane direction of substructures; longitudinal to the superstructure). Tolerance of the superstructure to horizontal movement depends greatly on the bridge seat or joint widths, bearing type(s), structure type, and load distribution effects. In the ideal case, such deformations are accommodated by movement systems and thus do not deform or result in forces within the superstructure. As a result, the tolerances built into the movement systems define the degree to which they may isolate the superstructure from lateral and rotational support movements. If exceeding the isolation capability of movement systems

is defined as intolerable, then simple, rigid-body geometric models are sufficient to compute the associated limits (since the stiffness characteristics of the superstructure are not engaged).

Moulton et al. (1985) found that horizontal movements less than 1 in. were almost always reported as being tolerable, while horizontal movements greater than 2 in. were quite likely to be considered to be intolerable. Based on this observation, Moulton et al. (1985) recommended that horizontal movements be limited to 1.5 in. The data presented by Moulton et al. (1985) show that horizontal movements tended to be more damaging when they are accompanied by vertical movements than when they were not. This is likely because when horizontal movements are combined with vertical movements, they tend to create rotational demands which have different implications for various superstructure elements, e.g., simple shear deformations in elastomeric bearing pads, rotational considerations for pot bearings, cracking within tall (slender) substructure elements, etc.

For foundations, regardless of whether they are shallow (e.g., spread footings) or deep (e.g., driven piles or drilled shafts), horizontal and rotational deformations can occur because of either lateral loads or lateral squeeze of the foundation soil. The following two sections provide of details related to these two mechanisms.

2.2.1 Horizontal and Rotational Deformations Due to Lateral Loads

Assuming that adequate drainage features are in-place and functioning satisfactorily, the primary source of lateral loads at abutments is earth fill and any surcharges behind the abutment. If appropriate drainage is not provided, then additional lateral loads can occur due to the build-up of hydrostatic pressures and frost action. Assuming that the abutment walls are free to displace laterally and the foundation soils are competent, the minimum movement that can be anticipated for design is the movement required to mobilize the active earth pressure. Such lateral movements can occur by sliding at the base of the spread footing, rotation of pile/shaft caps, and/or by rotation of the abutment stem wall. In any case, the primary concern is the horizontal movement and rotation at the superstructure level.

Generally granular fills are used at abutment locations. For these types of materials, the typical horizontal movements that can be anticipated are in the range of 0.001 to 0.004 times the height of the abutment wall. Thus, for example, if the abutment is 20-ft tall, horizontal movements in the range of ¼ in. to 1 in. may be anticipated. In a general construction sequence, the earth fill behind the abutment is substantially complete prior to placement of the

superstructure. In this case, the horizontal movement at the superstructure level is virtually complete and should not be of concern assuming that the vertical joint between the end of the superstructure and the abutment back-wall was designed properly to accommodate the movement. However, the lateral movements caused by lateral loads due to surcharges, such as live loads and thermal effects, experienced by the abutment after the placement of the superstructure should be considered in the design of the bridge structure.

At pier locations, the primary source of lateral loading is from thermal effects, braking forces and forces due to unequal spans if any exist on either side of the pier. Assuming that the pier substructure has sufficient structural resistance, these lateral loads are primarily resisted by sliding resistance at the base of the spread footing or the structural resistance at the connection of the cap with the underlying deep foundations. Where the foundation soils are weak in shear strength (e.g., fine-grained clayey soils) the interface shear strength may be small which increases the potential for sliding. Once the interface shear strength is overcome by the horizontal forces, large sliding movements can occur.

2.2.2 Horizontal and Rotational Deformations Due to Lateral Squeeze

In addition to lateral forces, lateral squeeze is often a source of horizontal and rotational substructure movements (Samtani and Nowatzki, 2006; Samtani et al. 2010). Figure 2-1 shows schematics of such movements at pier and abutment locations. The lateral squeeze phenomenon is due to an unbalanced load at the surface of the relatively soft soil with the depth of significant influence (DOSI) of the foundation subsurface stresses. The lateral squeeze behavior may be: (a) short-term undrained deformation that results in horizontal deformation from a local bearing resistance type of failure, or (b) long-term drained, creep-type deformation. Creep refers to the slow deformation of soils under sustained loads. In addition to rigid-body deformation of the substructures, the flexibility of the substructures themselves can act to amplify the resulting support movements experienced by the superstructure.

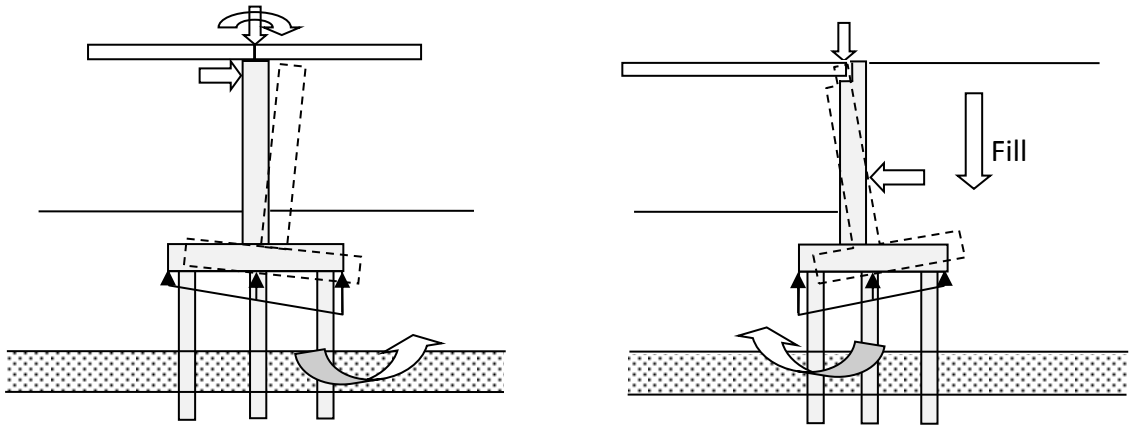

Figure 2-1 - Schematic of horizontal and rotational deformations due to settlement and rotation of foundations at (a) piers and (b) abutments.

2.3 Effect of Construction Sequencing

In order to appropriately model the effects of foundation deformation, the effect of construction sequencing on settlements must be taken into account. Most Designers use the criteria for tolerable movement described above as if the weight of a bridge structure was instantaneously placed. In reality, loads are applied gradually during construction. Subsequently, the foundation deformations also happen gradually. Figure 2-2 below shows some of the critical stages during construction that a designer can evaluate. Settlements that occur before the placement of the superstructure may not be relevant to the design of the superstructure. In Figure 2-2 it can be seen that the settlements that happen between points X and Z are the most relevant. Consideration of the applicable settlements along with the type of superstructure and bearings could lead to a more rational design approach.

2.4 Task 1.1 Conclusions

The following bullets summarize key aspects of the proposed approach that were directly dependent on the findings of the past research outlined in this section.

- Past research indicates that vertical support movements are unlikely to have a significant influence on structural stability/strength limit states. While these limit states will nonetheless be examined, the proposed approach includes numerous serviceability/durability limit states, including the performance of utilities.
- In the proposed approach, tolerable horizontal and rotational support movements will be defined as those that can be isolated from the superstructure by movement systems.

While it may be possible for superstructures to accommodate such movements through other means, given the more significant performance problems caused by horizontal and rotational movements, a stricter criterion appears appropriate.

- To develop rational guidance for multi-directional support movements, the general approach will be to condition the recommended tolerable vertical support movements based on the ability of movement systems to accommodate the associated levels of horizontal and rotational movements.
- The guidance to be developed through this research will focus on support movements that occur after the first superstructure elements are placed (points X to Z in Figure 2-2). Given the numerous construction sequences that may be employed, the proposed approach will assume all such support movements will be imposed on the complete superstructure. This is a conservative assumption since the complete superstructure will have a higher stiffness than at any stage during its construction

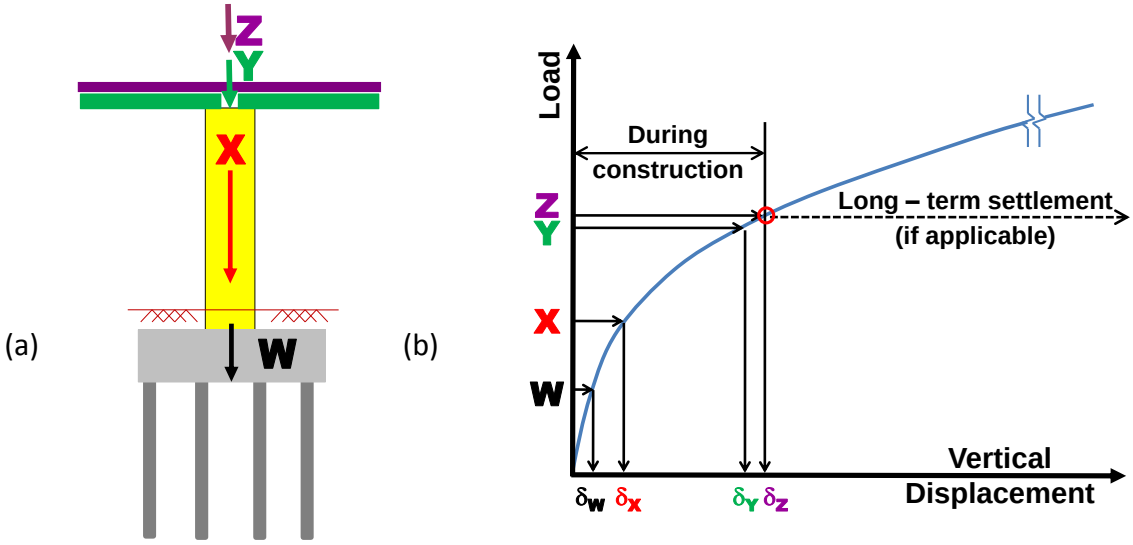

W	Load after footing construction
X	Load after pier column/wall construction
Y	Load after superstructure construction
Z	Load after wearing surface construction

δ_W	Displacement under load W
δ_X	Displacement under load X
δ_Y	Displacement under load Y
δ_Z	Displacement under load Z

Figure 2-2 Schematic of construction-point concept for a bridge pier. (a) Identification of critical construction points, (b) Conceptual load-displacement pattern for a given foundation.

3 Modeling of Multi-Girder and Non-Multi-Girder Bridges (T1.2)

3.1 Task 1.2 Objectives

The objectives of this task were to determine appropriate (in terms of both accuracy and efficiency) FE modeling approaches for both multi-girder bridges and box girder-type bridges. While the former are most prevalent within the U.S., various forms of concrete box girders remain popular in certain states and under certain circumstances (such as strict clearance constraints).

Multi-girder bridges have been commonly modeled using 2D grillage, 3D element-level models, shell element models, and solid element models. Given the monolithic nature of pre-cast and cast-in-place box girders, generally more refined models, such as the shell or solid element models are required. In the following study, both an archetypical multi-girder as well as box girder bridge form will be used to assess the trade-offs of various modeling approaches and select an appropriate model type. Specifically, this study examined various model forms, element types, boundary and continuity conditions, mesh size, results extraction approaches, etc., for each bridge type.

3.2 Background

Current practice in bridge design is heavily dependent upon single line girder (SLG) models, where bridges are analyzed as an "equivalent" single girder through making assumptions related to transverse distribution of forces based on various parameters (such as span length girder spacing, etc.). While SLG models have proved conservative for design related to live load and dead load actions, comparisons to field tests show such models significantly under-estimate stiffness and thus would be unconservative for certain support movement-induced actions. To illustrate the disparity, consider the MP28.9 Bridge (Figure 3.1) that the PI recently load-tested. This multi-girder steel bridge was composed of six plate girders with spans of 145 ft. and a 44^{o} skew.

Figure 3-1 – MP28.9 Bridge

Figure 3-2 shows a comparison between the simulated deflections of the bridge using 3D element-level FE model (see Section 3.3 for the details of this modeling approach) and the deflections measured during a load test. Specifically, this plot shows the mid-span deflection of each girder (i.e. the displacements across a transverse section of the bridge at mid-span) due to a single 65 kip tri-axle truck located over the edge girder at mid-span. As shown by this figure, the FE model captures the transverse deformed shape quite well, and generally over-predicts the measured displacements by 10% to 20%. Through a detailed model calibration these differences were traced primarily to the barrier stiffness and the stiffness of the asphalt overlay (the temperature at the time of test was below 40^{o} F), which were not included in the model shown in the comparison.

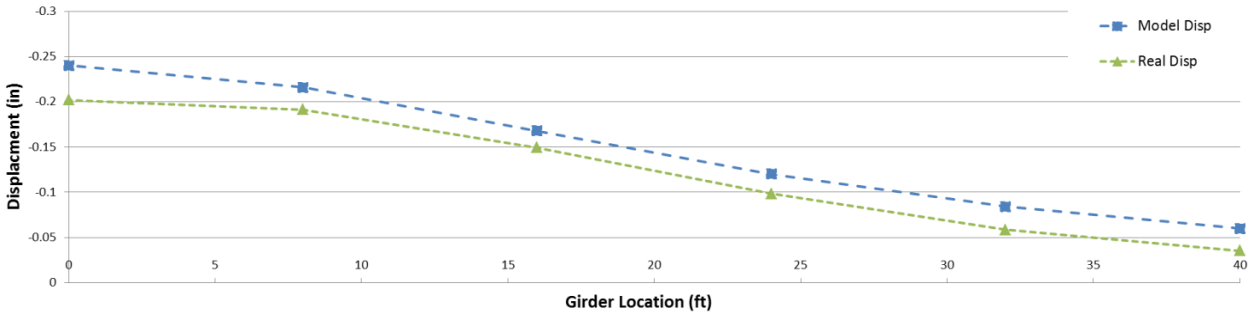

Figure 3-2 – Comparison of *A Priori* FEM Model and *In Situ* Bridge Test

An analysis was also carried out using a single-line girder model, and produced displacement predictions over two times larger than the displacements actually measured (110% to 150%

error). For this particular bridge, the single-line girder model had a stiffness consistent with a deflection limitation of L/2100, while the 3D FE model had a stiffness consistent with an L/5000 deflection limitation. This significant under-prediction of stiffness by the single-line girder modeling approach is not uncommon and in most cases it is conservative (Hevener 2003, Eom and Nowak 2001). For example, in the case of live load demands, the decreased stiffness of the single-line girder model adds an implicit level of conservatism during the design phase.

However, in the case of support movement demands, such an under-prediction of actual stiffness will translate into a similar under-prediction of the resulting forces. As a result, the single-line girder modeling approach can be significantly unconservative if used to assess the response of superstructures to support movements. As a result, this task aimed to determine the most appropriate modeling approaches to simulate the response of both multi-girder and non-multi-girder bridges to support movements.

3.3 Common Modeling Approaches for Multi-Girder Bridges

The behavior of common multi-girder bridges is frequently simulated using a wide range modeling techniques. The following sections provide a brief overview of commonly used modeling approaches to provide context to the investigation at hand.

3.3.1 Single-Line Girder Method of Analysis

This method is the most basic and commonly used approach for the design and performance evaluation of common bridge types within the U.S. This approach approximates structural phenomena through various equations to estimate the equivalent demands a single girder within the structural system will experience. As mentioned previously, this approach has been shown to under-estimate stiffness, but is generally conservative for the computation of dead and live load actions.

3.3.2 2D Grid Method of Analysis

The 2D grid method borrows assumptions from the classical “plane grid” analysis method, and is sometimes referred to as a grillage model. The girders and diaphragms are modeled as beam elements having three degrees of freedom (DOF) per node – specifically, two rotational and one translational DOF, with no depth information being explicitly represented. The two rotational degrees of freedom capture each girders’ major axis bending and torsional response. The single translational degree of freedom captures the vertical displacements of the girder.

With this method, all of the girders, diaphragms, and bearings are located at the same theoretical elevation in the model. Such models only permit the computation of vertical displacements and rotations within the plane of the bridge model.

3.3.3 2D Frame Method of Analysis

Similar to the 2D grid model, the 2D frame method of analysis ignores depth information. However, in this approach, the beam elements are equipped with six degrees of freedom at each node, three translational and three rotational. According to White et al. (2012), if there is no coupling between the degrees of freedom for the conventional 2D-grid and the three additional degrees of freedom, 2D-frame models actually do not provide any additional information beyond the ordinary 2D-grid solutions. That is, all of the displacements at the three additional nodal degrees of freedom will be zero, assuming gravity acts normal to the plane of the structure (i.e. the bridge does not have a significantly longitudinal slope).

3.3.4 Element-Level Method of Analysis

This type of model employs both one-dimensional (frame/beam elements) and two-dimensional elements (plate or shell elements) to model girders/diaphragms and the deck, respectively. Beam elements have either 2 or 3 nodes with 6 DOFs each. Plate/shell elements may have 3 (in the case of triangular elements), 4(in the case of rectangular elements), or up to 9 (in the case of 9-node rectangular shells) nodes with up to 6 DOFs each. In an effort to remain consistent with the three dimensional geometry of the structure, various link elements (to connect girders to the deck and diaphragm elements to the girders) and constraints (to simulate boundaries) are also employed. This model resolution is commonly termed “element-level” and is the most common class of 3D FE models employed for constructed systems (ASCE, 2013). The figure below shows a schematic illustrating how 3D geometry of the bridge is simulated using various elements and links.

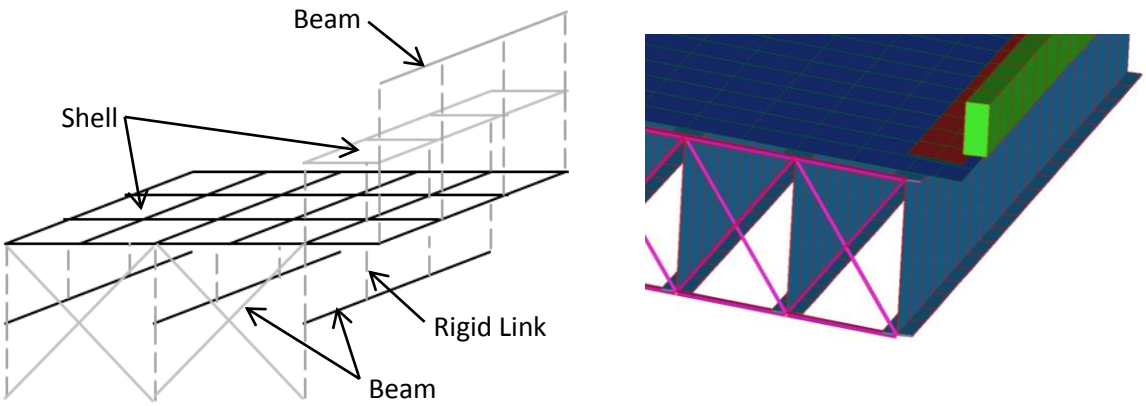

Figure 3-3 – Schematic of Generic Element-level FEM Model

In this model type a girder is discretized into 1D beam elements and the cross-sections are considered through the definition of geometric constants (e.g. area, moment of inertia, etc.). While an element-level FE model can reasonably simulate most bridge responses, it is not without its shortcomings, specifically: (1) an inability to effectively simulate warping deformation of girders (associated with torsion), and (2) an inability to simulate localized stresses (i.e. stress concentrations) associated with geometric discontinuities. While these shortcomings may be critical in the case of modeling specific construction sequences for complex bridges (White et al. 2012) and advanced fatigue/fracture assessment, they are not relevant for the global limits states to be investigated in this study.

3.3.5 Shell Element Method of Analysis

The most significant distinction between element-level and shell element models of multi-girder bridges is that the beams in shell element models are discretized vertically, laterally, and longitudinally using shell elements. This method of modeling girders allows for the accurate simulation of warping of the girders due to torsion. Computation time, model construction, and result extraction activities however, are more time consuming and more difficult than with element level models.

3.4 Modeling Study for Composite Multi-Girders

In order to investigate the efficacy of element-level and shell-element multi-girder bridge FE models, two benchmark structures were examined. First, a single 2-span continuous composite beam was modeled using both of the aforementioned methods. Second a multi-girder system

composed of two continuous beams with a contiguous deck as well as cross-bracing elements was studied to examine the modeling of transverse elements.

3.4.1 Overview of Composite Multi-Girder Modeling Study

For the two modeling approaches examined, the following aspects were studied for response convergence and/or consistency with the behavior mechanisms being simulated:

- Boundary conditions
- Continuity Conditions
- Model discretization
- Results extraction methods
- Beam-element shear deformation and response
- Computational efficiency

To examine these modeling aspects, the girder and deck responses for the two benchmark structures under dead load and support settlement were examined as described in Table 3-1. Table 3-2 provides the details of the benchmark structures.

Table 3-1 - Summary of Demands and Reponses Used in Benchmark Study

Dead Load	Support Settlement Applied to Exterior Support
Maximum Deflection	Girder total fiber stress over the center support
	Vertical reaction at the center support
	Deck stress over the center support
	Girder shear, axial, and moment actions

Table 3-2 – Details of the Benchmark Structures and Models

Type	Number of Girders	Deck Thickness	Total Deck Width	Span Length	Girder Depth
Element-level	1	8 in.	96 in.	960 in.	21 in.
Element-level	2	8 in.	96 in.	960 in.	21 in.
Shell Element	1	8 in.	96 in.	960 in.	21 in.
Shell Element	2	8 in.	96 in	960 in.	21 in.

The models used in the investigation were made up of 2-node beam elements with 6 DOFs at each node, 3-node triangular shell elements with 6 DOFs at each node, and 4-node rectangular

shell elements with 6 DOFs at each node. The following sections provide results related to each of the modeling aspects examined within this study.

3.4.2 Boundary and Continuity Conditions

3.4.2.1 Element-level Model

Boundary conditions for the element-level model were enforced by restricting all degrees of freedom except for rotation about the Z axis on each "pin" boundary, and all degrees of freedom except roation about Z axis and translation in the X (longitudinal) axis on each "roller" boundary. Instead of placing the boundary restrcition at the beam centroid, boundary nodes were placed at the bottom fiber of the beam section and rigid links were used to connected the beam element node to the boundary node. This boundary offset more closely mimics that of a real structure.

Girder/cross-bracing continuity was enfored for the two-girder models by the same rigid link construction. At each boundary as well as intermediate cross-bracing points, rigid links were connected to nodes located at the top and bottom of the girder cross-section. Deck/girder continuity was enforced by connecting rigid links between each of the nodes of the beams elements to nodes of the deck shell elements located directly above. Boundary and continuity contruction for a sample two-girder shell element model is shown in Figure 3-4.

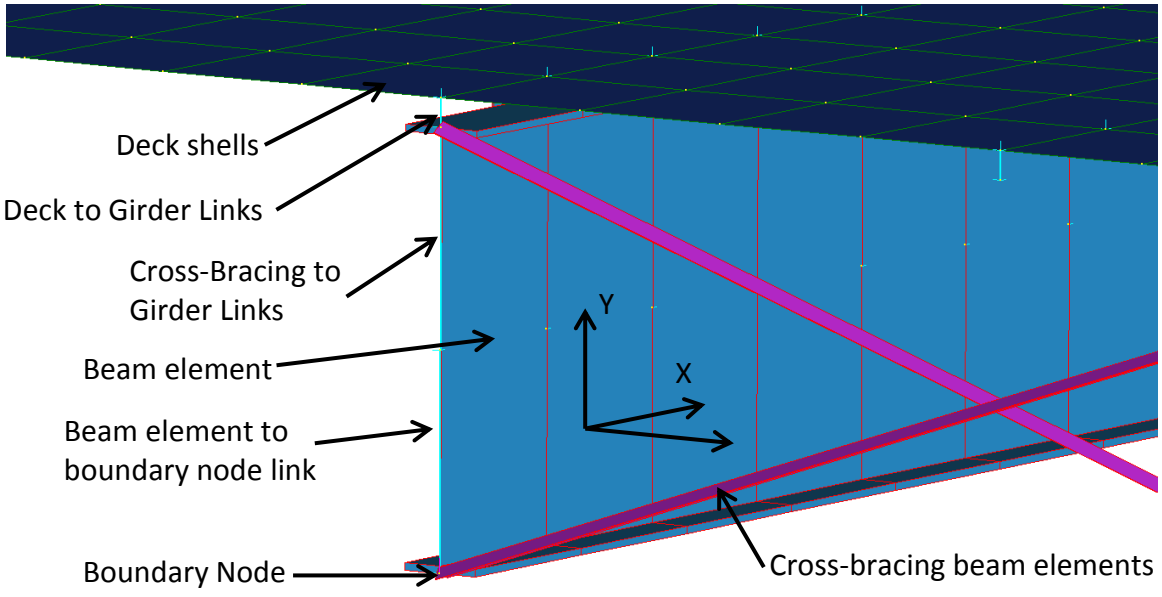

Figure 3-4 – Element-level Model Continuity and Boundary Conditions

3.4.2.2 Shell Element Model

Boundary conditions on the shell element model were enforced by restricting all degrees of freedom except for rotation about the Z axis on each “pin” boundary, and all degrees of freedom except rotation about Z axis and translation in the X axis on each “roller” boundary. Because shell element models are susceptible to local distortion due to point loads, rigid links were placed along the edge of each exterior shell element at each boundary, essentially rendering the cross-section at each boundary vertically rigid.

Girder/cross-bracing continuity was enfored for the two-girder models by the same rigid link construction: at each boundary as well as intermediate cross-bracing points, rigid links were connected between each node in the girder cross-section. Deck/girder continuity was enforced by connecting rigid links between each node of the top flange shells and each node of the deck shells located directly above. Boundary and continuity contruction for a sample two-girder shell element mdoel may be seen in Figure 3-5.

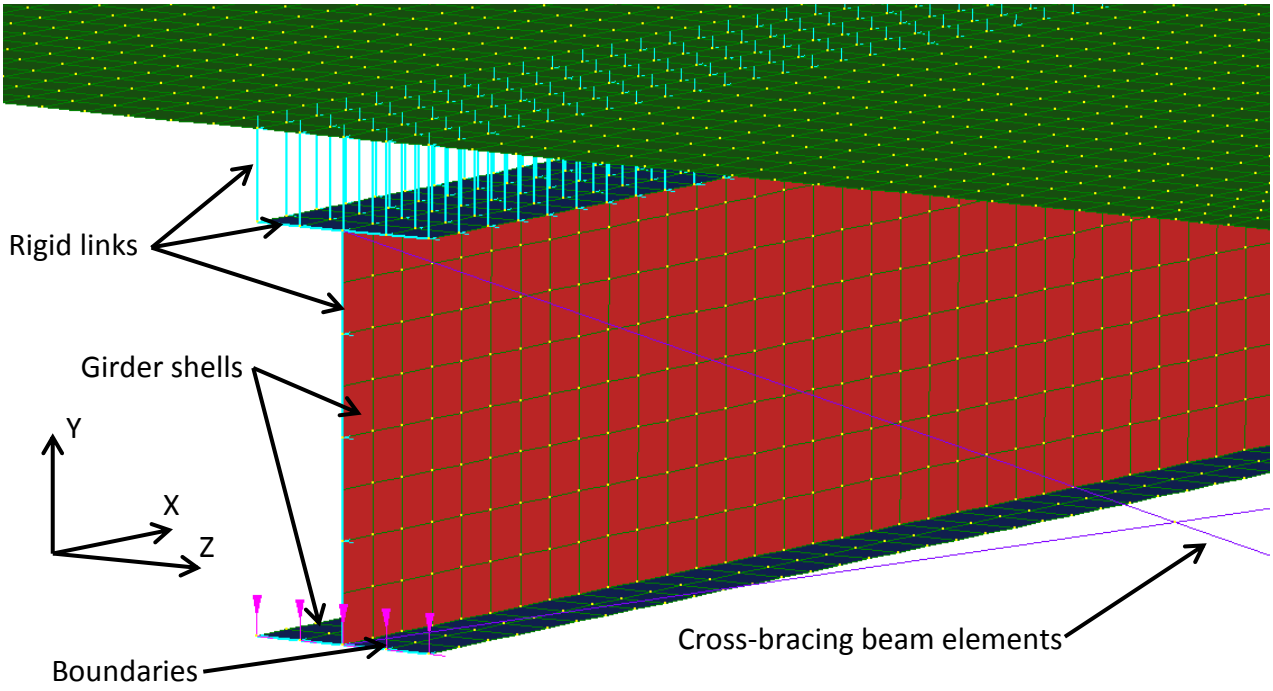

Figure 3-5 – Shell Element Model Continuity and Boundary Conditions

3.4.3 Model Discretization

Model discretization, or element size, was studied for both element-level and shell-element models to determine response convergence. Five levels of discretization were studied for the element-level models and three levels of discretization were studied for the shell-element models. Beam element sizes were given to the model building software as a target length. In the case of irregular geometry, skews, etc., the software will shorten or lengthen an element according to maximum and minimum element size criteria. No shell elements had an aspect ratio greater than 2:1, with most shell elements having an aspect ratio around 1:1. Table 3-3 provides the element sizes examined for both element-level and shell element models; the average element size is given as a length as well as the ratio of the beam depth to the element size. Figures 3-6, 3-7, 3-8, and 3-9 show schematics of each model included within this study for both modeling approaches and both benchmark structures.

Table 3-3 – Element Sizes for Discretization Study

Element-Level [in]	Element-Level [ratio]	Shell Element [in]	Shell Element [ratio]
2.5”	8	2.5”	8
5”	4	5”	4
10”	2	10”	2
20”	1	-	-
40”	0.5	-	-

Early in the discretization study it was evident that shear deformation of the beam elements within the element-level models was producing divergent results in many load cases. Due to this, the discretization study was modified to include the effects of shear deformation on mesh size convergence. The following sections provide representative results from these studies (complete results can be found in Appendix A).

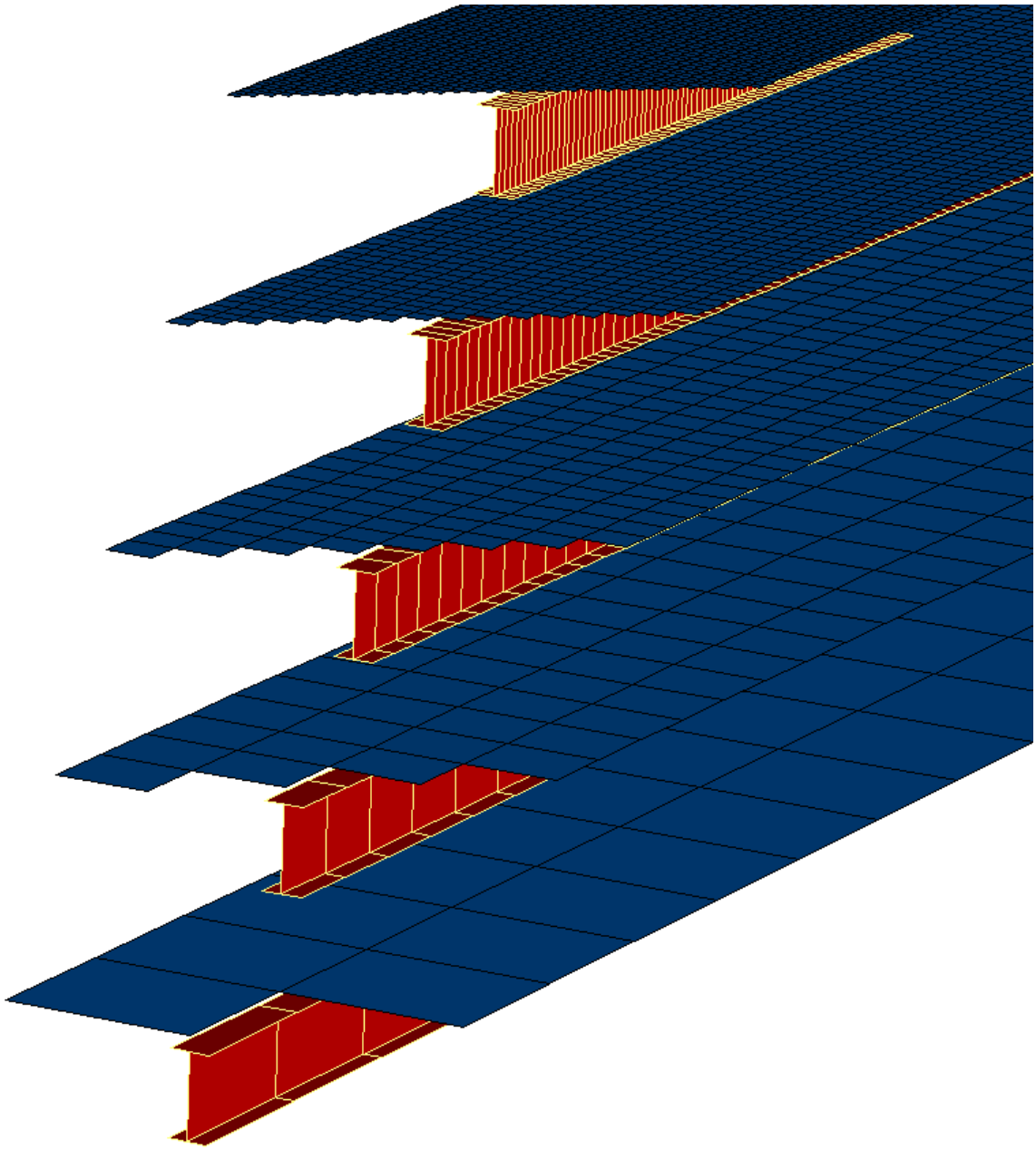

Figure 3-6 – Discretization Levels of Element-level Model

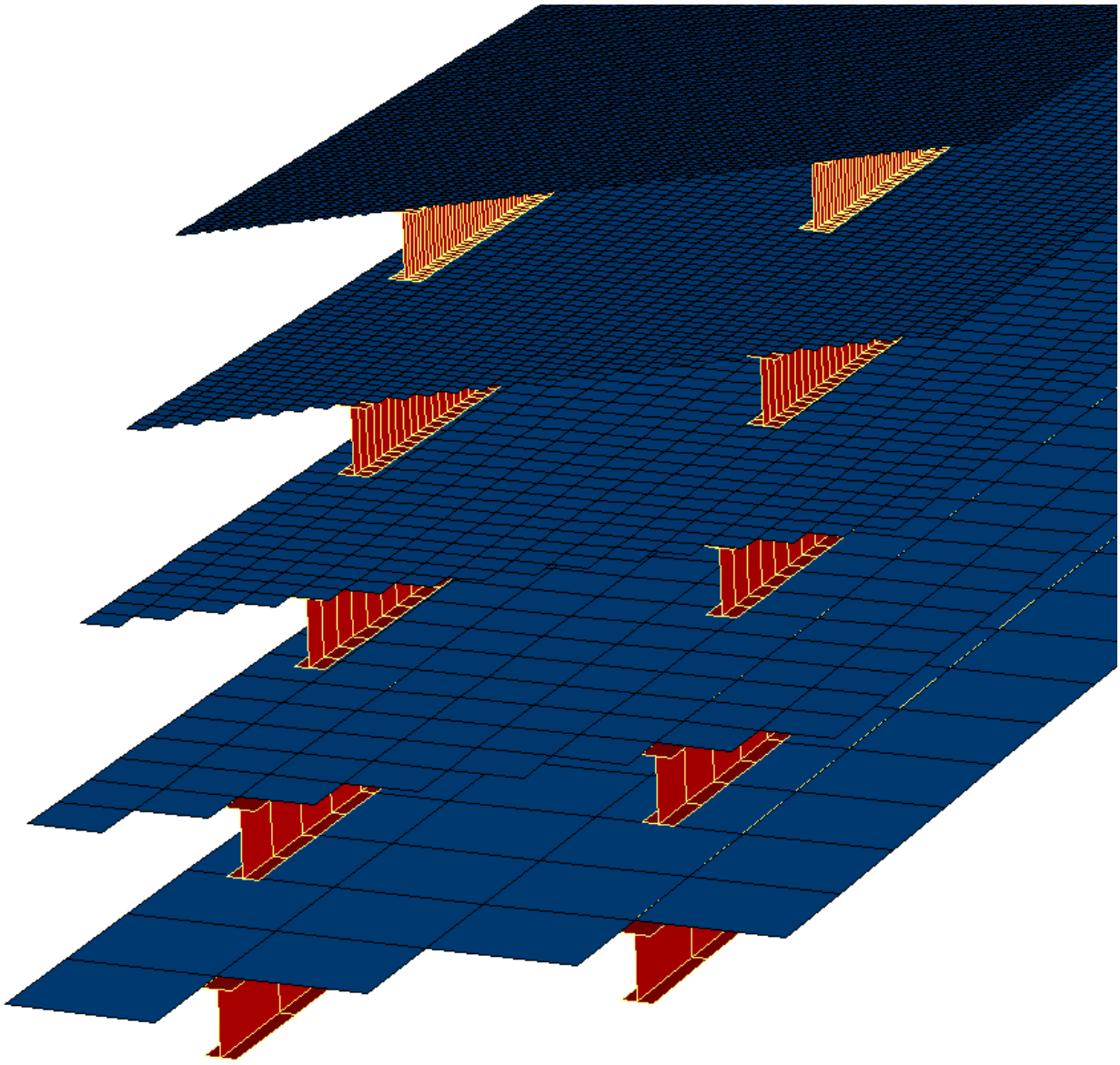

Figure 3-7 - Discretization Levels of Element-level Model

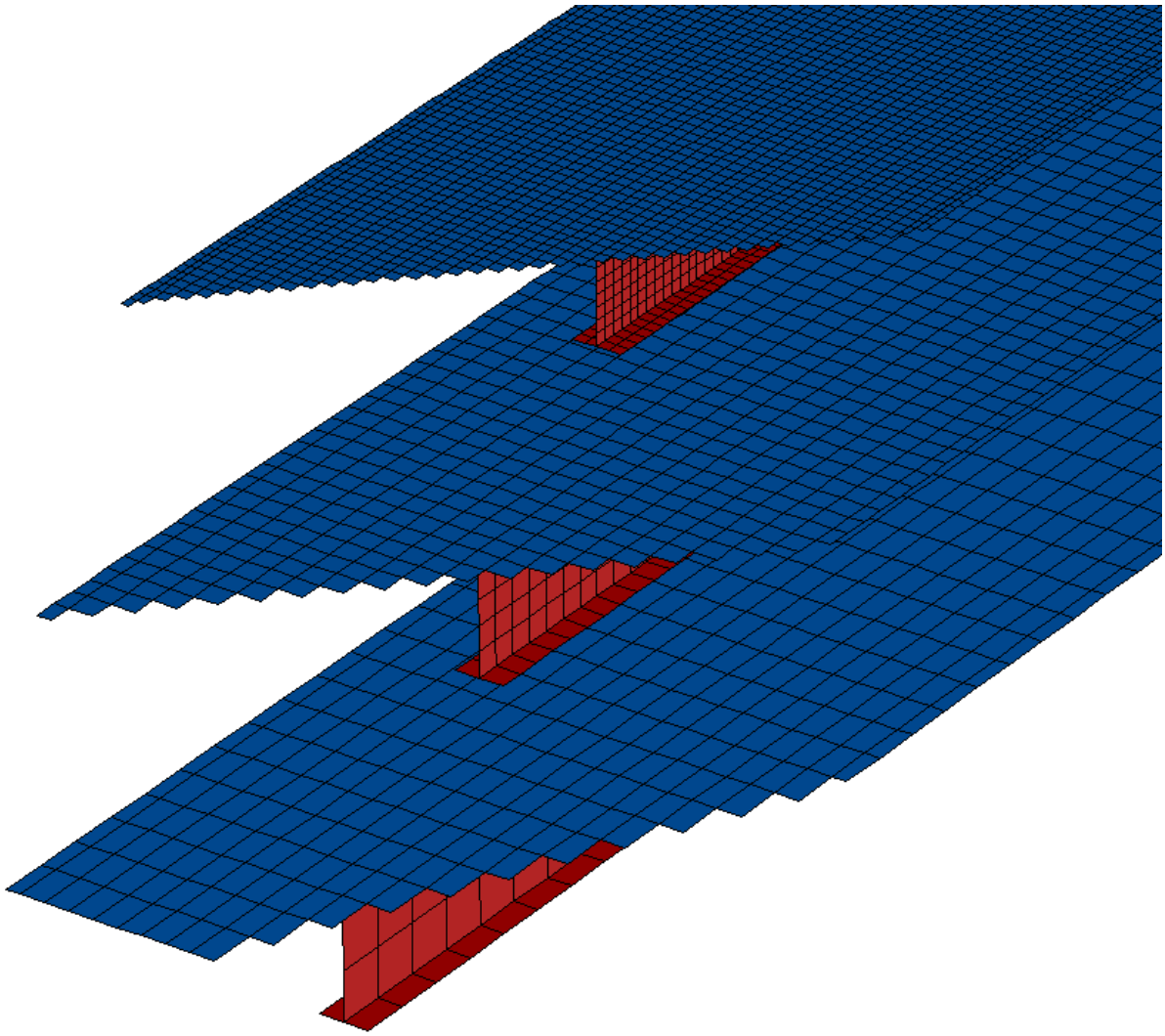

Figure 3-8 – Discretization Levels of Shell Element Models

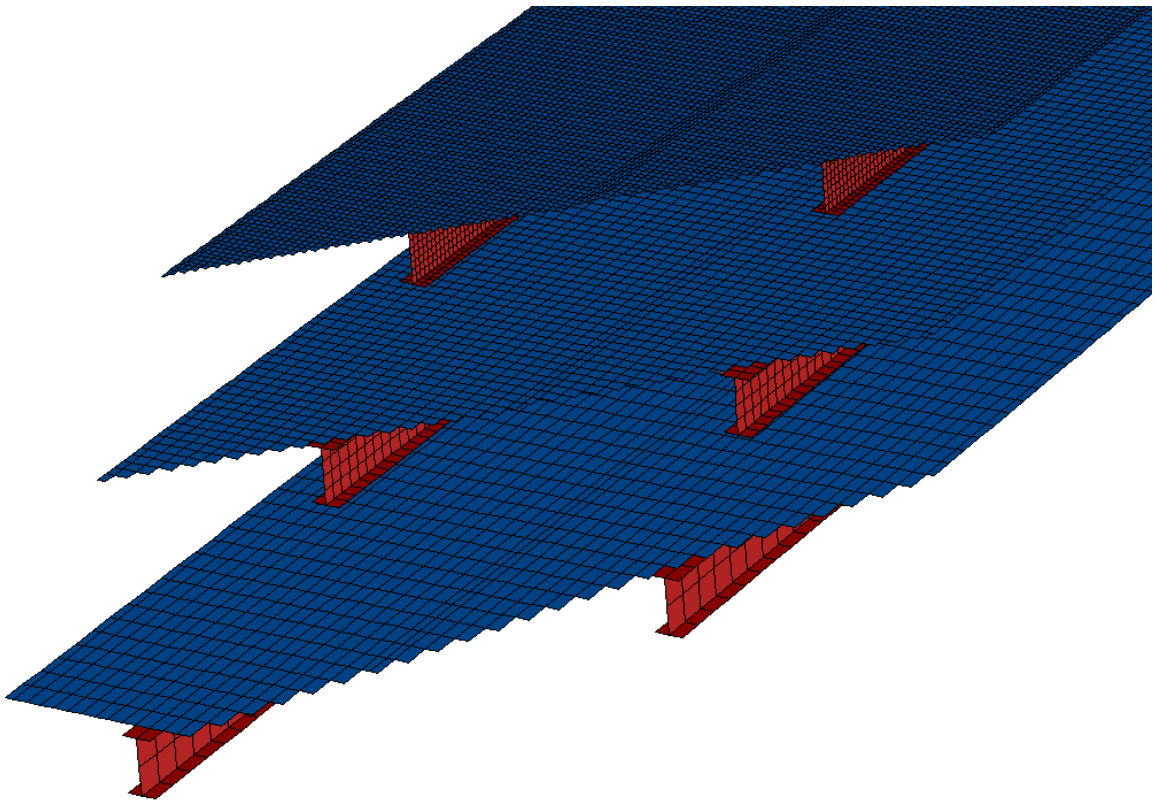

Figure 3-9 – Discretization Levels of Two-Girder Shell Element Model

3.4.4 Beam Element Shear Deformation

Element-level models are susceptible to mesh dependency due to the shear deformation of the beam elements. Discretization levels strongly influence the degree of composite action, and responses such as deformation under dead load as well as moment in the beam, axial force in the beam, and shear in the beam due to support settlement vary with mesh size. In order to assess the degree to which shear deformation causes divergence issues, a study was performed to compare the aforementioned responses when shear deformation in the beam elements was "turned" ON or OFF. In order to do this, the shear area of the beam element cross section was replaced with an artificially higher number (in the case of this study, $1x10^9$ in^2 was used).

Beam elements were discretized to the sizes listed in the previous section. For plotting purposes, the element size to beam depth ratio is used instead of the absolute value. This provides a more widely applicable metric for all future studies. It is the intention of this study

to determine the relative element size that will provide a converged solution while also allowing for computational efficiency.

Figure 3-10 illustrates the shear force in the girder versus relative element size, and indicates that that if shear deformation of the beam elements is considered, the results do not converge. In contrast, when shear deformation of the beam elements is ignored, convergence was observed at a beam depth to element length ratio of approximately four. In addition, when shear deformation of the beam elements is ignored, the shear force computed for the girders represents the majority of the shear force on the composite cross-section, which is consistent with the mechanics of materials solutions.

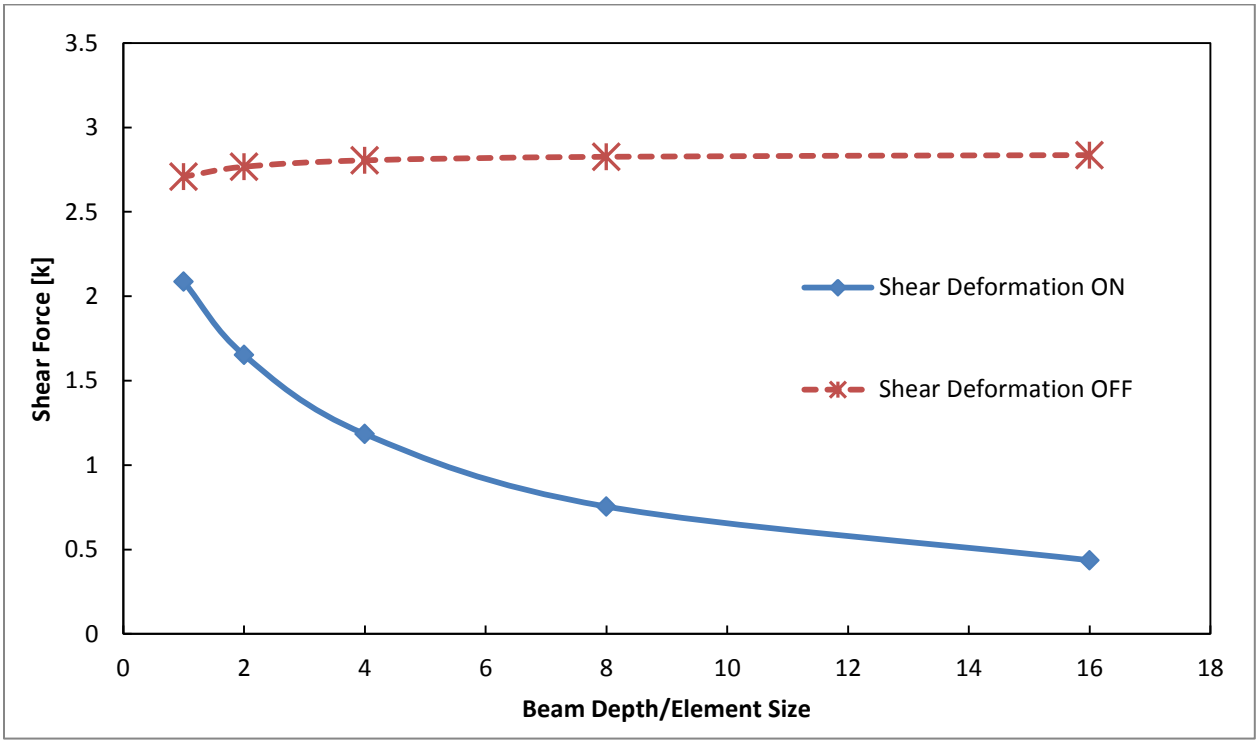

Figure 3-10 - Shear Response of Composite Beam Element Based on Section Depth to Element Length Ratio

3.4.5 Results Convergence and Model Type Agreement

This portion of the study examined the convergence of various responses for both element-level and shell element models and agreement between model types. Figure 3-11 and Figure 3-12 show convergence plots of deck stress for the element-level and shell element models, respectively. These figures illustrate three key points: (1) In the element-level model, with

shear deformation ignored, deck stress converges at an element ratio of approximately four; (2) Ignoring shear deformation results in convergence at a coarser mesh size; and (3) There is good agreement (under 5%) between the element-level and shell element model. This agreement is slightly better when shear deformation of the beam elements is ignored.

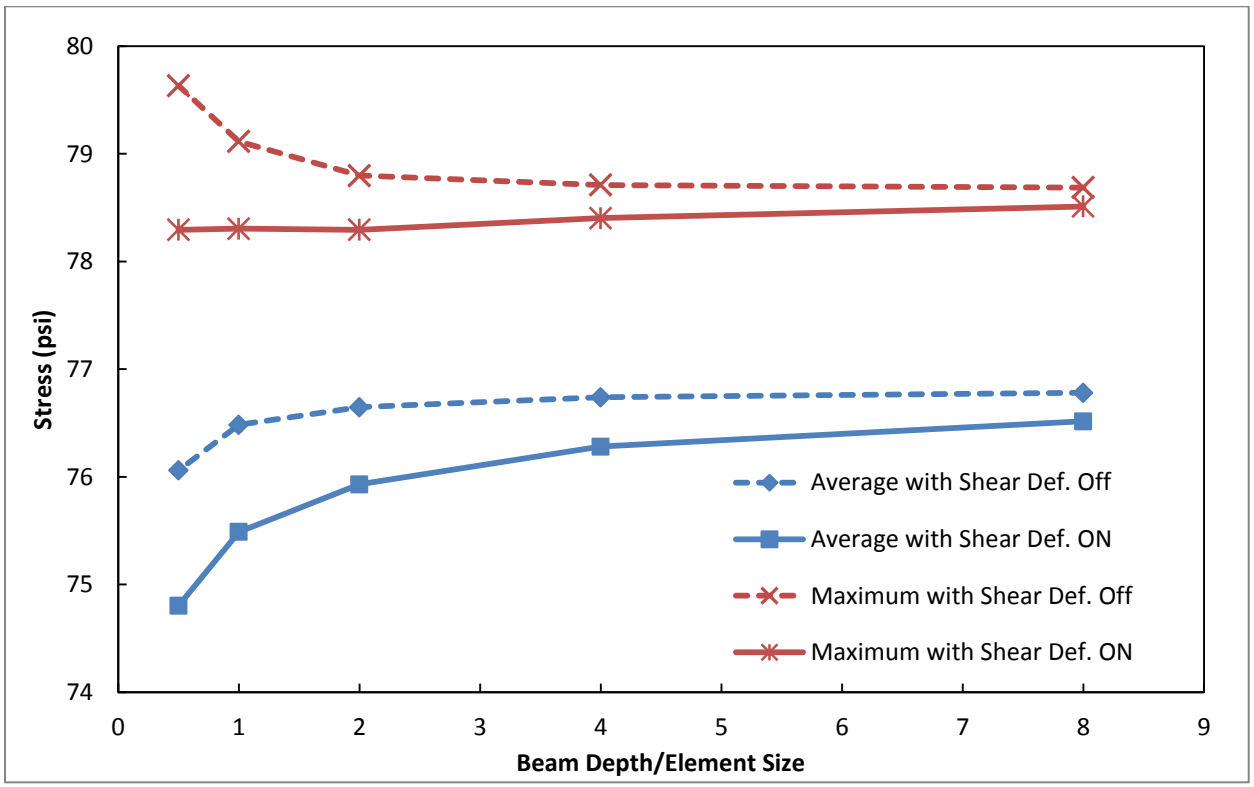

Figure 3-11 - Effect of Element Size on Deck Stress under a Vertical Settlement in Two Girder Beam Element Model

The other responses listed in Table 3-1 were also examined for both the element-level and shell element models, and the results were consistent with the trends shown in Figures 3-10 and 3-11. Specifically, results convergence occurred around an element ratio of four, and ignoring shear deformation within the element-level model produced more consistent results with the shell element model. The results illustrating this can be found in Appendix A.

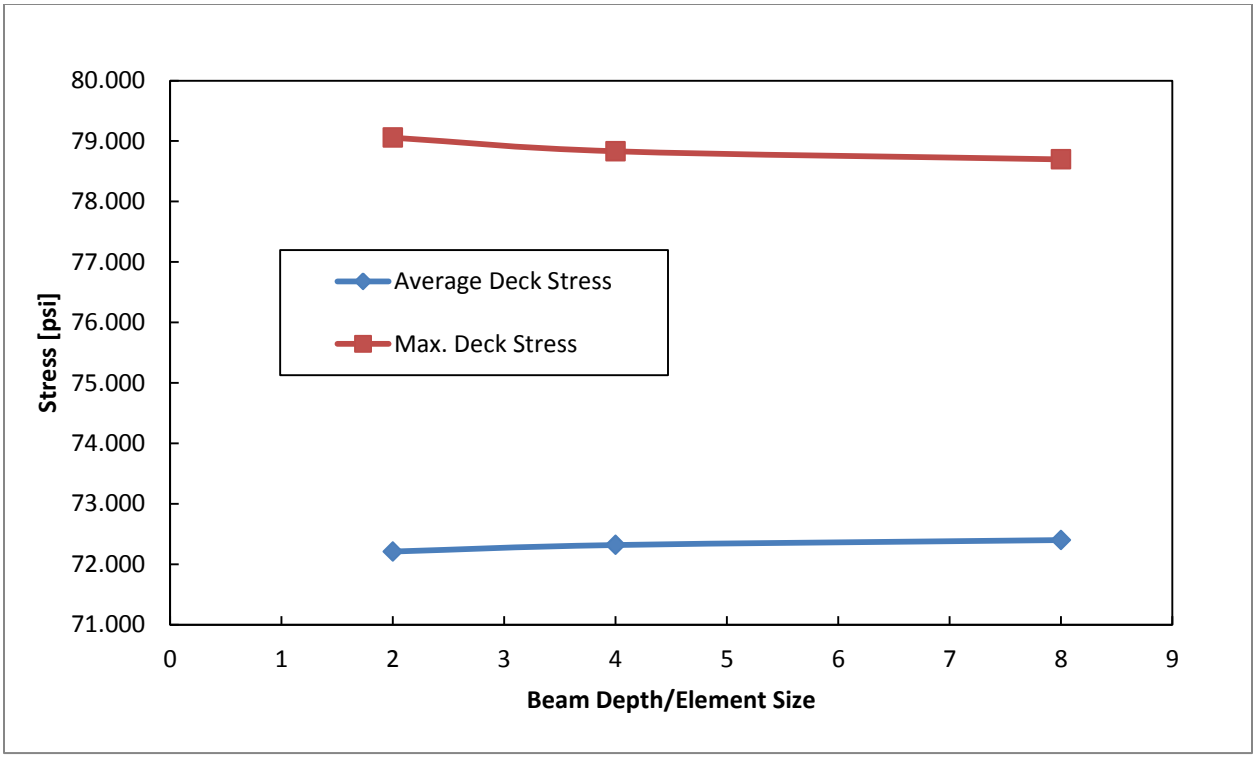

Figure 3-12 - Effect of Element Size on Deck Stress under a Vertical Settlement in Two Girder Shell Element Model

3.4.6 Results and Extraction Methods

3.4.6.1 Element-level Model

Results from the element-level models were extracted at the nodes above the center support. Stress results for the beam elements were computed using the calculated moment and the geometric constants that describe the cross-section. Shear in the beams were extracted in two ways: (1) It was taken as the shear within the beam element; (2) It was assumed to be equal to the reaction at the support. The first method of extracting shear proved to be dependent on the mesh size, and thus was deemed unreliable. The second method was conservative (in that it assumed the total shear force on the cross-section was resisted by the girder alone) and this approach converged at the element aspect ratio of four.

Deck stress over the center support was also computed based on the beam element response as opposed to directly extracted from the model. This was done to avoid the anomalous stress concentrations observed in the shell elements where the rigid links connect them to the beam elements. By assuming strain compatibility for the composite section, the nominal stresses in

the deck were computed by calculating the strain diagram for the beam and extrapolating this to the top of the deck (and the transforming this to stress using the elastic modulus of concrete).

3.4.6.2 Shell Element Model

The shell element model investigation required that the normal and shear forces from each element were extracted and then summed to obtain various member actions (moment, axial, shear). Because each girder is made up of individual shell elements, there is no direct way to extract member actions. This is in contrast to the element level model, where member actions are solved for directly.

Local stress concentrations are also an issue with shell elements. For example, Figures 3-13 and 3-14 show examples of how localized loading (either through a support reaction, point load, or rigid link connection) causes local distortion and stress concentrations. Such responses are strongly mesh dependent and are not realistic, since in the actual bridge structure such point loadings do not exist. As a result, when extracting results from shell elements, the analyst has to be careful to capture nominal responses and not those associated with these localized effects. This may be done by following Saint-Venant's Principle, i.e., extracting results at a sufficient distance from the concentrated force.

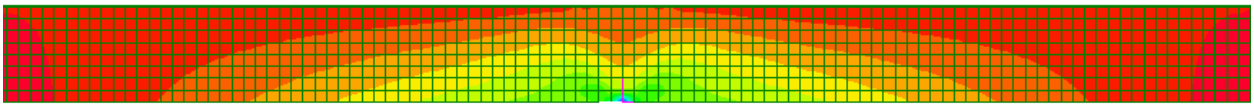

Figure 3-13 - Localized Stress Concentration over Support

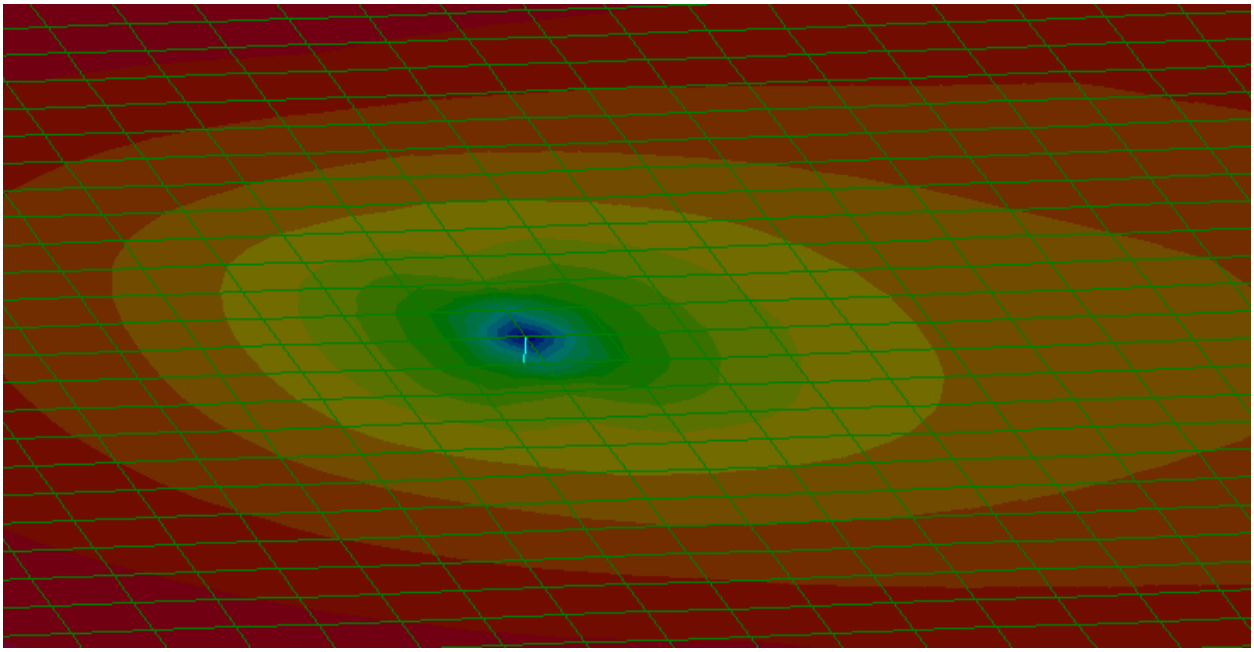

Figure 3-14 - Localized Stress Concentration on Deck at Point of Loading

3.4.7 Computational Efficiency

A study was conducted in order to compare the computing time for element-level and shell element models. As shown in Figure 3-15, the shell elements were found to be much more computationally expensive (e.g. requiring 800% more time for modeling with an element ratio of four). While the absolute times for these models may appear small, this factor is critical when large sensitivity studies are carried out (as proposed in Phase II).

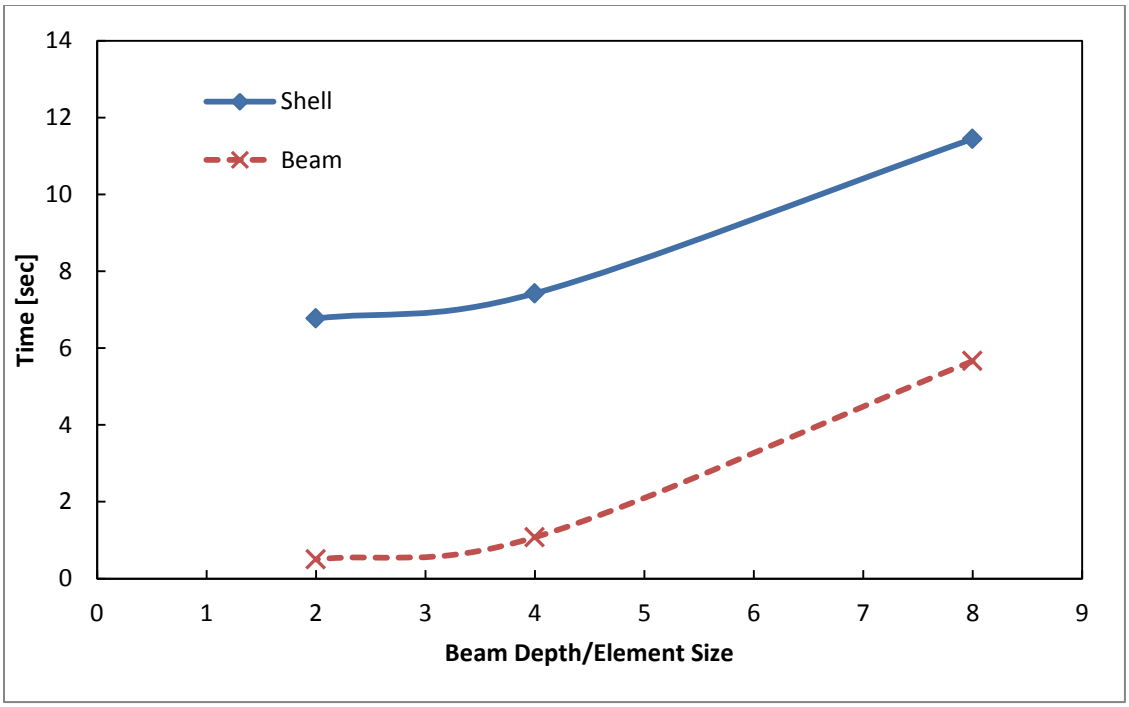

Figure 3-15 - Comparison of Computing Time for Shell and Beam Element Models

3.4.8 Summary and Conclusions of the Composite Multi-Girder Modeling Study

Based on the results of this modeling study, it is concluded that the element-level modeling approach (where the shear deformation of the beam elements is ignored) is the most appropriate approach for the simulation of multi-girder bridges. In comparing the element-level modeling approach to the shell element modelling approach, the following observations were made:

(1) The different approaches provided consistent results (approximately 5% difference) for the demands and responses examined
(2) Both modeling approaches converged at element ratios of approximately four (when the shear deformation of the beam elements was ignored)
(3) The element-level model allowed for easier and more consistent results extraction approaches
(4) The element-level modeling approach required less 15% of the computational time required by the equivalent shell element modelling approach

3.5 Multi-Girder Bridge Modeling Study

To extend the element-level model selected through the study in the previous section to complete bridge systems, an additional mesh sensitivity study is required. This study was carried out on a two-span continuous benchmark multi-girder bridge with 100 ft. spans. Since a 1:1 aspect ratio for shell elements was desired, a girder spacing of 10 ft. (which is a factor of the span length) was selected. The skew was set to zero to eliminate variably sized deck elements and to avoid non-rectangular elements. Boundary conditions were defined so as to provide the least restraint possible. This was achieved by restraining all supports in the vertical direction, restraining the exterior girders in the longitudinal direction at one abutment, and restraining the central girder in the transverse direction at that same abutment. In this manner local self-equilibrating forces were avoided.

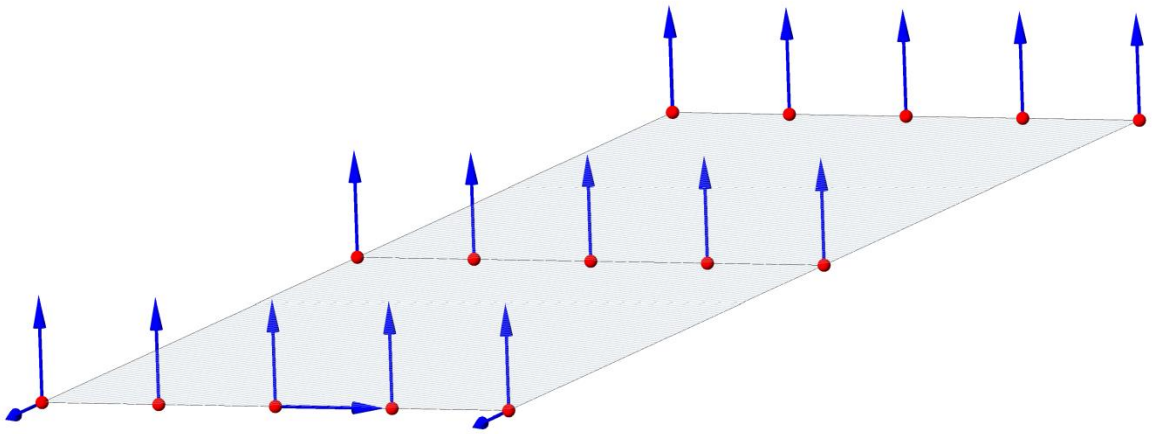

Figure 3-16 - Restrained Boundary Degrees of Freedom

Shear deformation was turned off by using the same artificially large shear area as employed in the previous study. As shown in the previously presented benchmark study, shear cannot be accurately modeled with an element-level model and the shear forces will be determined directly from the support reactions.

The bridge was designed with five 45 in. deep beams of 36 ksi steel. As used with the single and dual-girder composite models, an 8 in. deep concrete deck was connected to the girders through the use of rigid links to enforce composite action. Diaphragms were placed every 20 ft. Girders and barriers were modeled as beam elements

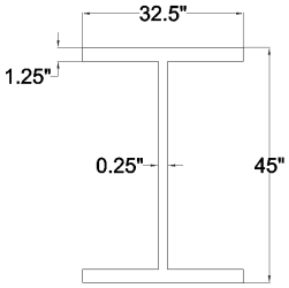

with the dimensions shown in Figure 3-17. The deck and sidewalk were modeled as shell elements.

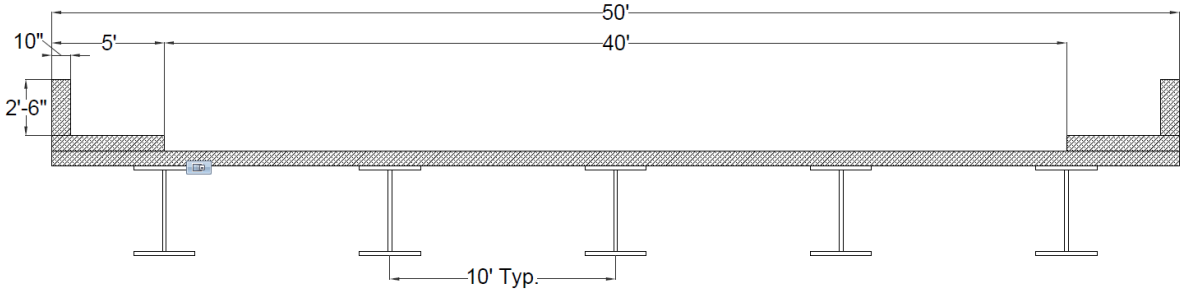

Figure 3-17 – Typical Multi-Girder Bridge Cross Section

Six levels of discretization were investigated, including 60 in., 30 in., 15 in., 12 in., 10 in., and 6 in. A separate model was created for each, with all other geometry and properties remaining constant. These models were analyzed under three loading cases: dead load, a point load, and a settlement. The dead load was based upon the material densities and geometry. A single point load of 32 kips was applied over the center girder 40 feet from the abutment. The vertical settlement was applied to each girder at the abutment and was set to one inch.

Linear static analysis was performed on each of these models under the three loading scenarios using Strand7 FE software. Moment and axial forces, as well as reactions were recorded for comparison. These results were located in the exterior and central girders over the center pier for dead load and settlement member actions. Under the point load, member actions of the center girder were recorded at the location of the applied point force. The reactions for the load scenarios were taken at the abutments.

Results of this study revealed that a girder spacing to mesh size ratio of ten (corresponding to a 12 in. discretization) provides convergence, with any further refinement not significantly effecting the results. Figures 3-18, 3-19, and 3-20 illustrate this convergence by providing a sample of the results obtained. As can be seen from these figures, the percentage differences quickly fall below one percent, thus indicating that little is gained from the increased discretization. Additional results from this study can be found in Appendix B. As a result of this study it is concluded that mesh size to girder spacing ratio of ten is sufficient to provide convergence of straight bridges. Prior to initiating the full parametric study proposed in Phase II, a similar study for skew bridges will be carried out.

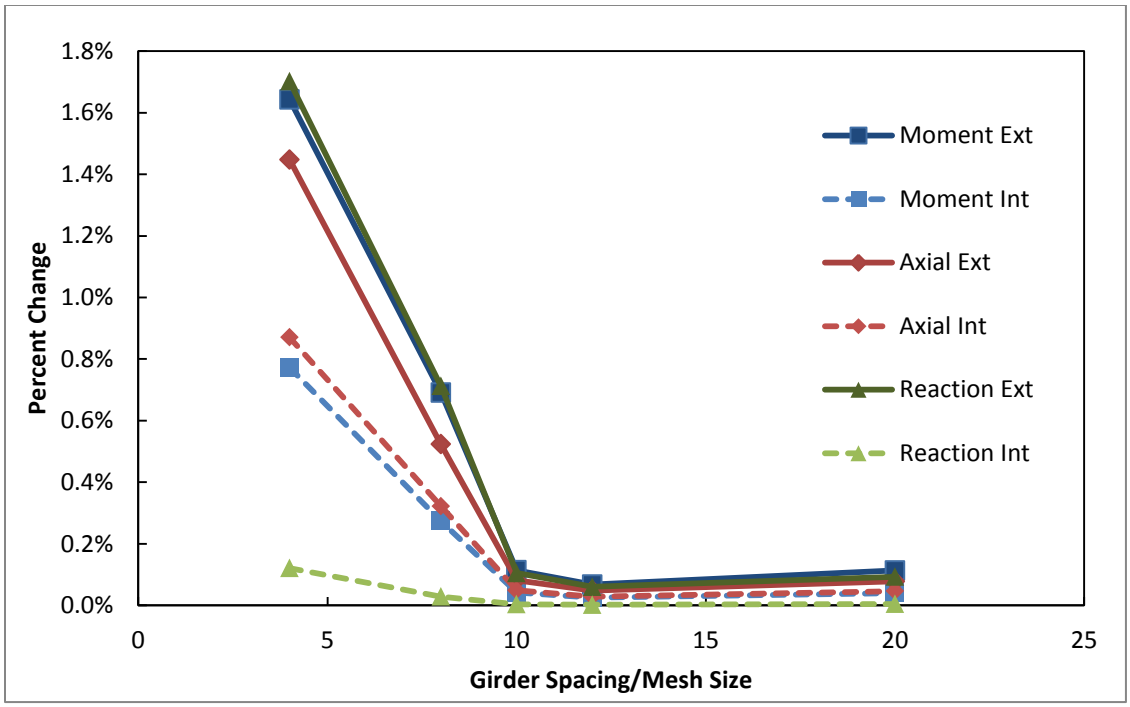

Figure 3-18 – Percent Change in Response to Support Settlement with Decreasing Mesh Size

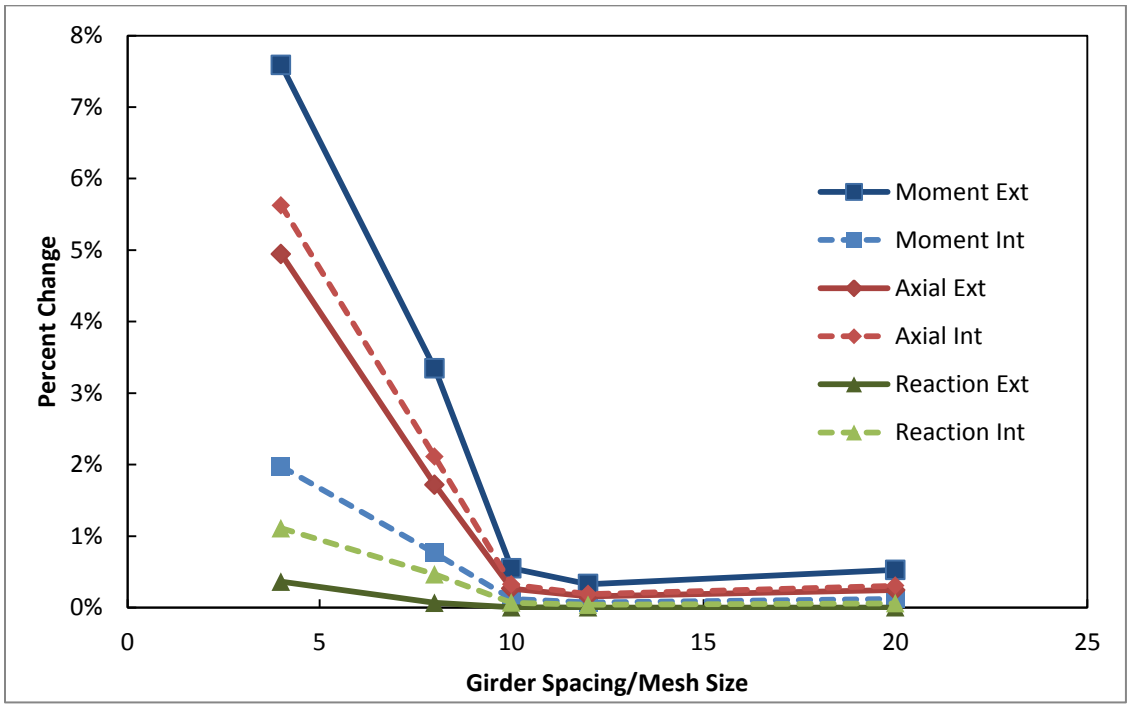

Figure 3-19 - Percent Change in Response to Dead Load With Decreasing Mesh Size

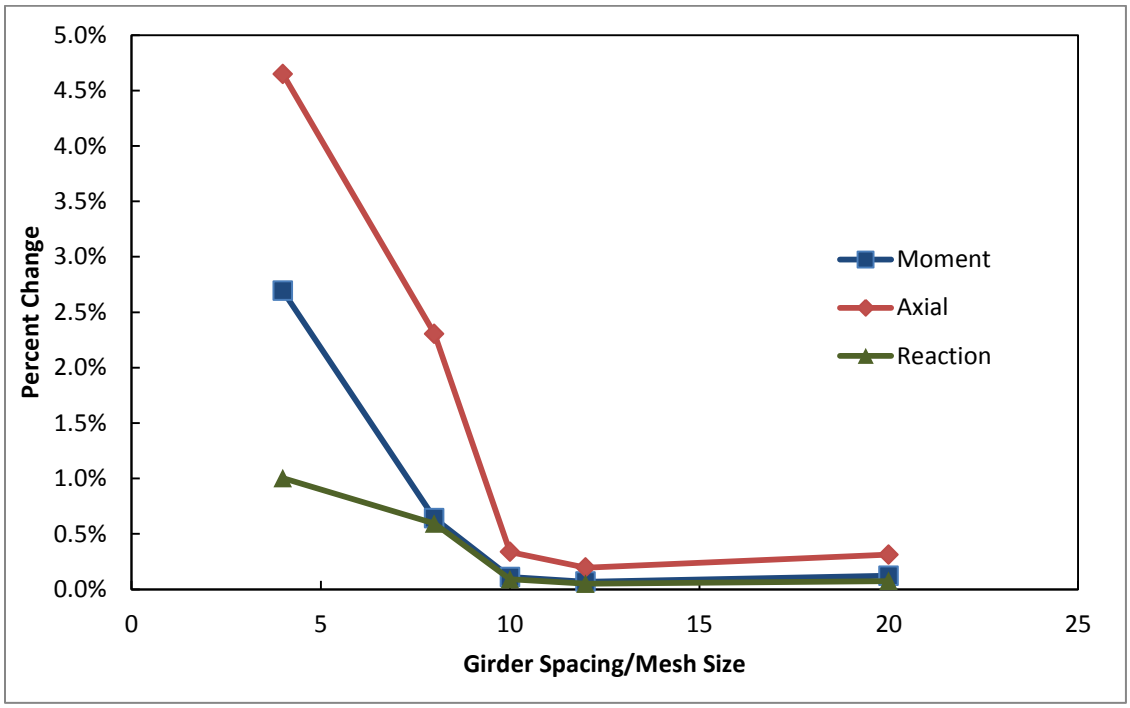

Figure 3-20 - Percent Change in Response to Point Load With Decreasing Mesh Size

3.6 Box Girder Bridge Modeling Study

The more complex geometry of a box girder bridge required further study to examine the necessary modelling techniques to accurately capture the structural response to a given loading scenario. While there are many different types of box girder bridges used, one frequently seen type is a monolithic box girder. For this modeling study, a California box girder bridge with the cross section shown in Figure 3-21 was examined within a two-span continuous bridge with 100 ft. spans. An additional complexity is introduced with this particular bridge geometry due to its canted exterior webs.

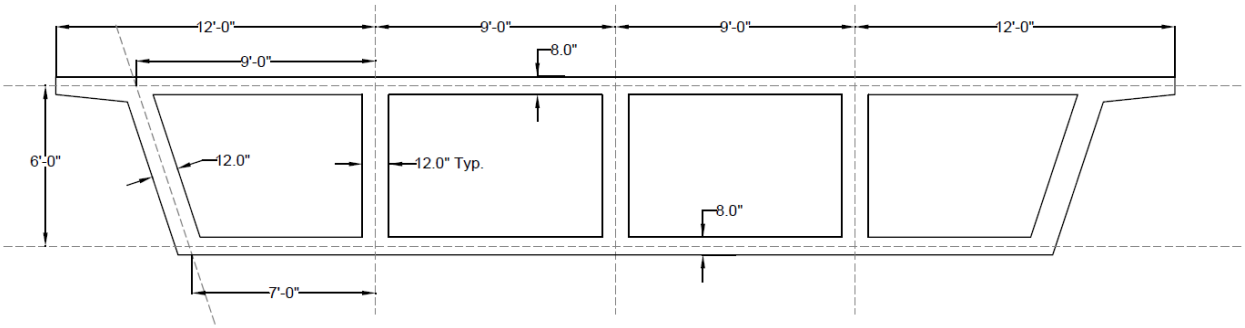

Figure 3-21 – Typical Box Girder Bridge Cross Section

3.6.1 Element Type

The bridge was modeled using a variety of elements, including brick, shell, and beam elements. In total, seven unique models were created which differed in how the cross section was represented with different element types. The following table summarizes differences of each of the seven models.

Table 3-4 – Overview of Elements Types for Box Girder Bridge Study

Model	Elements
1. Solid 20	20 Node Brick
2. Solid 8	8 Node brick w/ bubble function
3. Solid 8_2	8 node brick w/o bubble function
4. Shell	4 node shell
5. Beam Vertical	Webs: 2 node beam; Flanges: 4 node shells
6. Beam Canted	Webs: 2 node beam; Flanges: 4 node shells
7. Inverted T-Beam	Webs and bottom flange: 2 node beam; Top flange: 4 node shells

In models containing beam elements, compatibility was enforced through the use of rigid links. These links connect the centroids of elements and act like infinitely rigid bars, thus enforcing displacement compatibility of the connected elements. In the solid and shell element models, links were also used, but only at the supports to avoid local distortion. Pinned links were used in this case of the solid element models, since solid elements do not have rotational degrees of freedom.

Boundary conditions were consistent with those in the multi-girder models in which the bridge is in the most unrestrained state while remaining stable. Rather than locating the supports at

the center of beam elements, they were placed beneath the bottom flange in line with the webs at both abutments and the central pier. All supports have vertical translation restrained. At one abutment, the supports at the exterior webs are restrained from longitudinal translation, while the support at the center web is restrained from lateral translation.

The following images (Figures 3-22 through 3-26) show the manner in which the various models represent the geometry of the above cross section. The beam models are displayed with the beam elements extruded to show their assigned section geometry. The three solid element models are visually identical, and thus only one is displayed.

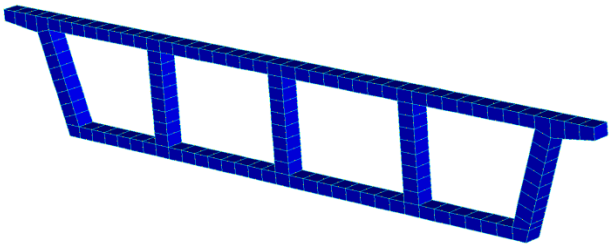

Figure 3-22 – Solid Element Model

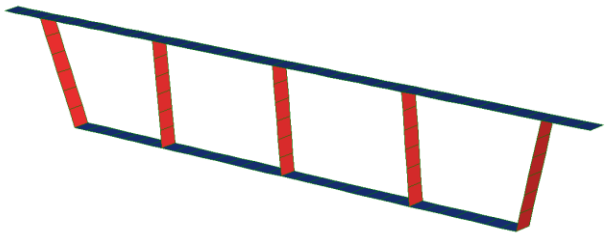

Figure 3-23 – Shell Element Model

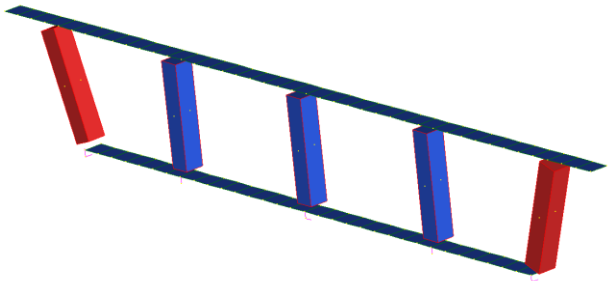

Figure 3-24 – Beam and Shell Element Model with Slanted Exterior Webs

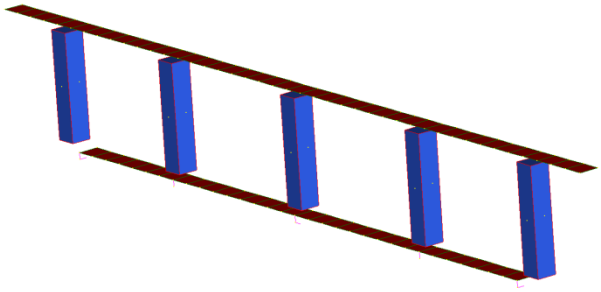

Figure 3-25 – Beam and Shell Element Model with Vertical Exterior Webs

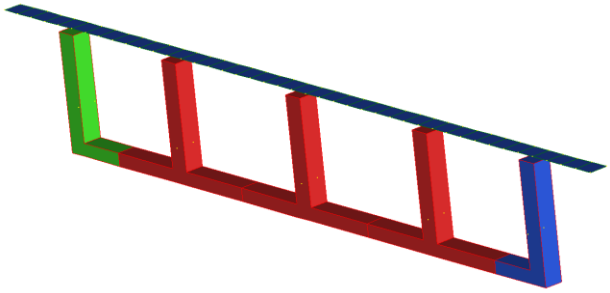

Figure 3-26 – Beam and Shell Model with Inverted T-Beam Cross Section

3.6.2 Mesh Size

The mesh size for each of the models described above were defined such that no element had any dimension larger than 12 in. In addition, the aspect ratios for all 2D and 3D elements were kept to 1:1 and 1:1:1, respectively. For the solid element models, these meshing rules resulted in over 20,000 brick elements. Any further refinement of the model exceeded the capabilities of the numerical precision of the FE software. Although strictly speaking, convergence for this model was not explicitly demonstrated, past experience of the investigators indicated that such a fine element mesh would not produce mesh-dependent results (for the responses of interest).

3.6.3 Model Comparison

The models were analyzed under dead load, a point load, and two settlement events. The point load was located at 0.4 of the span length from an abutment on the deck and above an interior (but not center) web. The first settlement was a vertical translation of 1 in for all supports at one abutment. The second was a continuous and linear differential settlement representing a

rotation of the abutment about the longitudinal axis such that the exterior webs moved upward and downward 0.5 in., respectively.

For the point load, stress was recorded at 0.4 of the span (parallel with the applied point load) at the top of the top flange and bottom of bottom flange at the center web. For all other loading scenarios, stresses were recorded along the width of the bridge at the interior pier on the top of the top flange and bottom of the bottom flange. The bottom reading was taken at a distance of 6 ft. from the supports (longitudinally) to avoid recording local distortions. The vertical reactions at the abutment where settlements were imposed were recorded for all load cases.

The following plots (Figures 3-27 through 3-30) show the percent deviation of the various modeling approaches from the responses obtained from the 20 node brick element solid model (assumed to be the ground-truth). The closer these values are to zero, the better the agreement of the model with the 20 node brick element model.

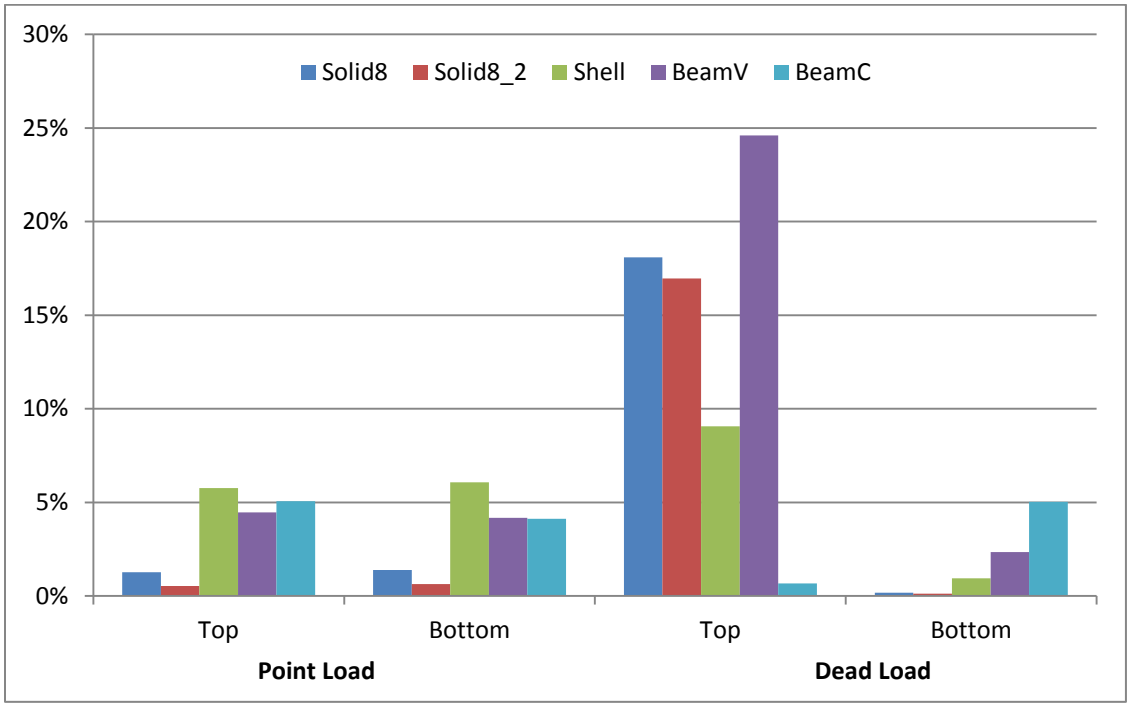

Figure 3-27 – Percent Agreement for Stresses between Model Types and 20 Node Solid Element Model

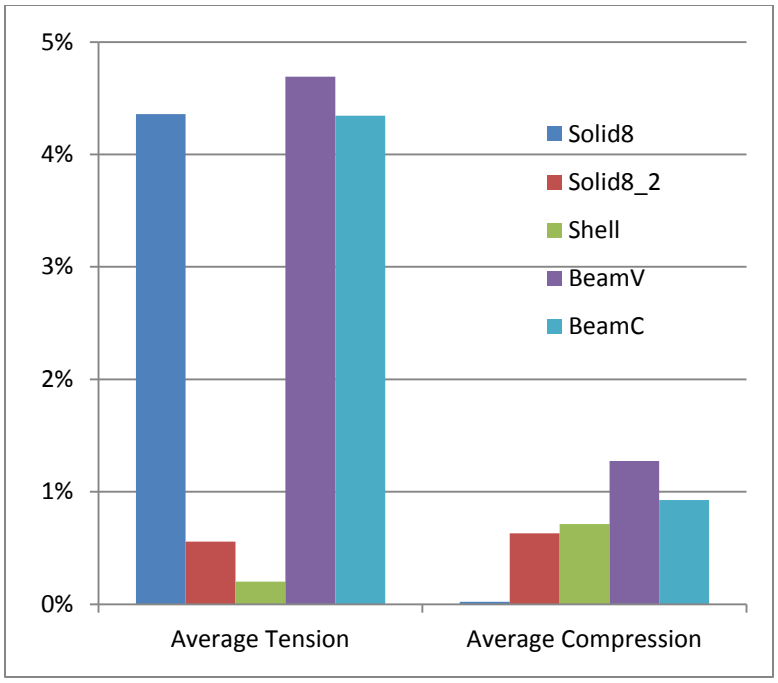

Figure 3-28 - Percent Agreement for Stresses between Model Types and 20 Node Solid Element Model due to Vertical Support Settlement

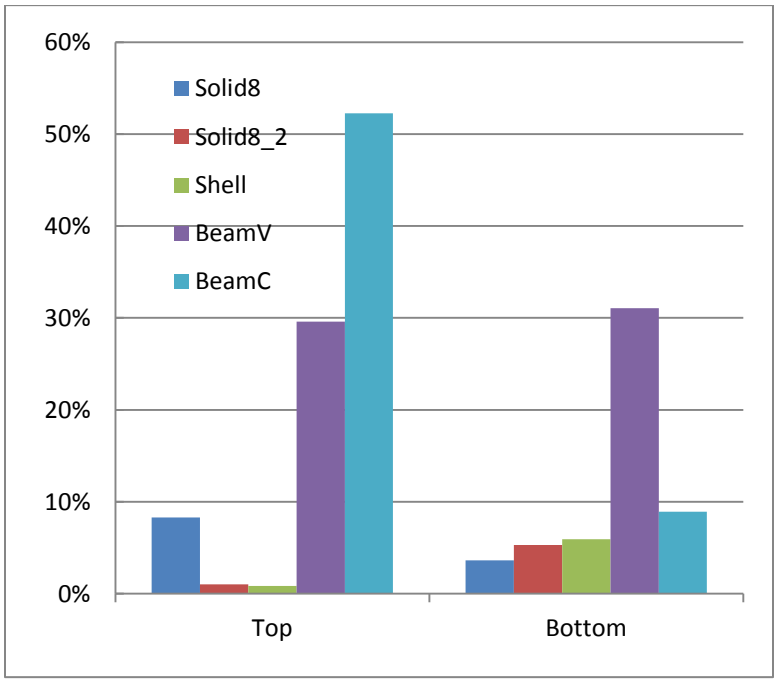

Figure 3-29 - Percent Agreement for Stresses between Model Types and 20 Node Solid Element Model Due to Differential Support Settlement

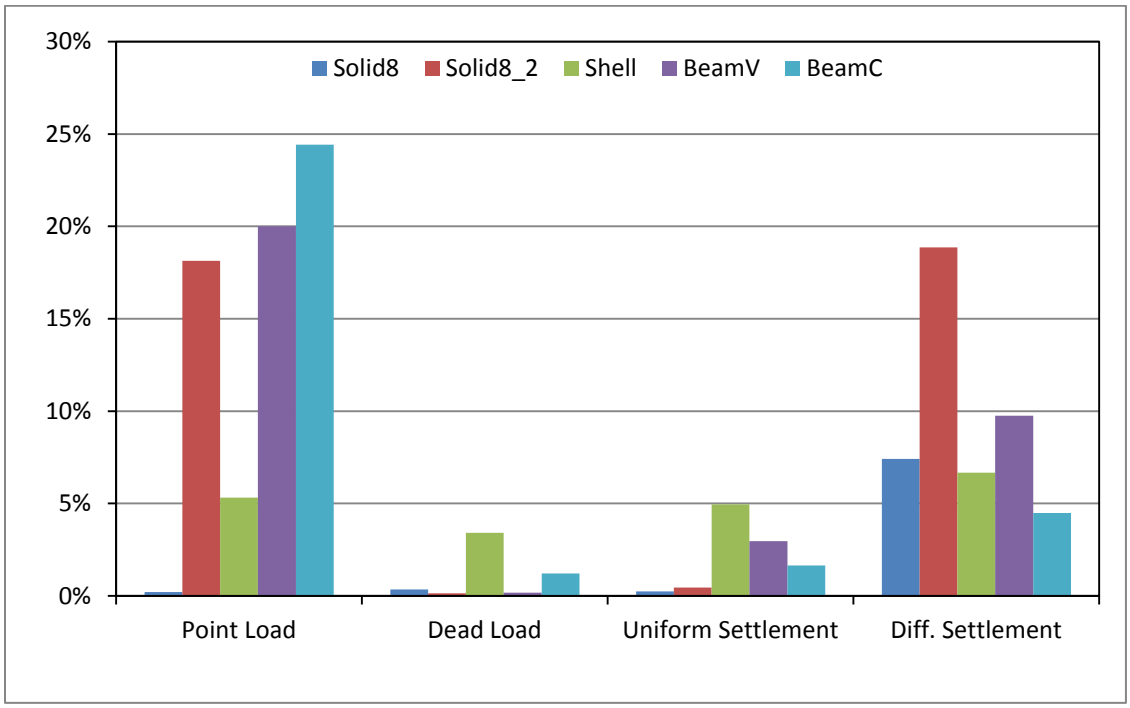

Figure 3-30 - Percent Agreement between Vertical Support Reactions for Various Model Types and 20 Node Solid Element Model

For these plots, the inverted T-beam model results have been omitted as they exhibited large errors and caused scaling/visualization issues with the plots. It is evident from these results that, of the remaining options, only the solid or shell elements can adequately represent the response of box girders bridges to the loading examined. For the purposes of this research, in light of the uncertainties associated with support movement predictions, "adequate" model accuracy is taken as less than 10% error from the most refined model. As a result, it is recommended that the model composed of shell elements be employed for the simulation of box girder bridges.

3.7 Task 1.2 Conclusions

3.7.1 Multi-Girder Bridges

Through a comparison of both single and two-girder element level and shell element model systems, it was determined that the element-level model was the best choice for the large

parametric study proposed for Phase II. This conclusion was based on (1) the good agreement (approximately 5% difference) between the element-level model and the more refined shell element model, (2) the more straightforward manner in which results may be extracted from the element-level model, and (3) the drastically reduced computational time associated with the element-level model.

In addition, to the selection of the general model approach, the multi-girder modeling studies also provided insight into various implementation strategies for the element-level model. In particular, the following modeling strategies are recommended for the Phase II parametric study:

1) Shear deformation of the beam elements within the element-level models should be ignored to ensure proper convergence of results.
2) Boundary conditions that provide minimum restraint (such as those detailed in Section 3.5) should be used to minimize extraneous inputs associated with local, self-equilibrating forces.
3) Support reactions should be used to conservatively estimate the shear force in the girders, as the computed shear force in the beam elements is mesh dependent.
4) Deck stresses should be approximated by extrapolating the strain in the girders to the top of the deck to avoid local stress concentrations exist in the vicinity of rigid links.

3.7.2 Box Girder Bridges

Through a comparison of element-level, shell element, and solid element models, it was determined that a shell element model was adequate to simulate the response of box girder bridges to live load, dead load, and support movements. This conclusion is based upon the shell element model consistently producing results within 10% of the most refined model examined with a significant decrease in computational time.

4 Selection of Parameters (T1.3)

4.1 Task 1.3 Objectives

In order to properly plan for the multi-variate sensitivity study to be undertaken in Phase II, a smaller, single degree-of-freedom study was performed using the current bridge design, model development, and analysis software. Specifically, a set of bridge parameters were varied for a benchmark structure that consisted of a two-span continuous bridge. For each set of parameters, appropriate girder sizes were selected using the AASHTO specifications and an element-level FE model was created for each design (consistent with the modeling approach described in the previous section, Figure 4-1). The FE models were then subjected to a vertical support settlement of an abutment. Response values (such as various stresses and reaction forces) were extracted from the simulation results and compared to the bridge parameters to identify levels of sensitivity. The goals of this portion of the study were (1) to determine whether the performance indices of interest were sensitive to the chosen parameters and (2) to verify that the parameter ranges of interest were adequate for the Phase II study.

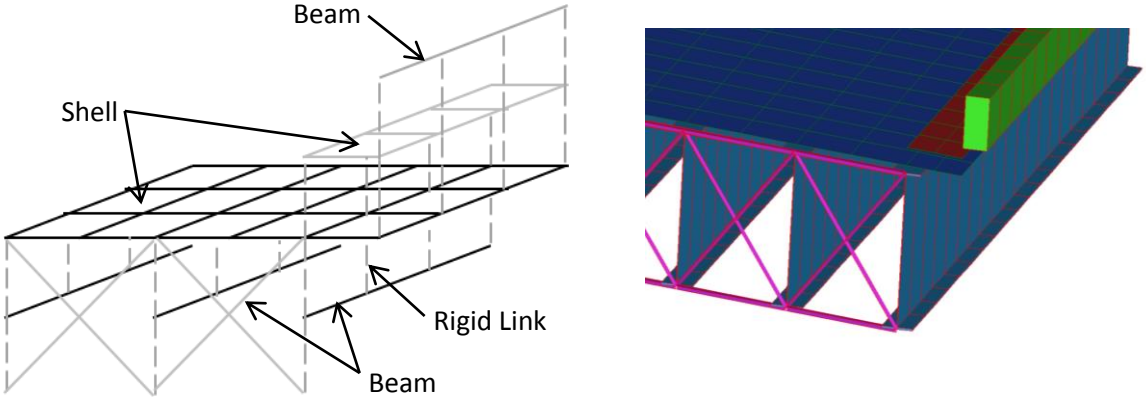

Figure 4-1 - Finite Element Bridge Models Developed with RAMPS

4.2 Responses of Interest

In order to simplify this process, only one type of demand input was studied: a 1 in. vertical settlement applied to one abutment of the two-span continuous benchmark structure (Figure 4-2). Three responses to this input were studied, namely, longitudinal stresses in the girders (termed total fiber stress), tensile stresses in the deck, and the reactions at the supports. Given the benchmark structure selected (2-span continuous bridge), the maximum value for each of

the three responses will be located over the interior support. Therefore, each of these responses were extracted above the interior support at three locations: at the exterior (or fascia) girder, at the 1st interior girder, and at the center interior girder.

Figure 4-2 – Schematic illustrating the support movement considered for the preliminary parametric study

4.3 Parameters of Interest

The study carried out under this task varied a series of parameters over a specific range one at a time while all other parameters were held constant at their "median" value. Table 4-1 provides the parameters included in this study, their ranges, and their median values.

Table 4-1 – Overview of Parameters

	Parameter	Values	Median Value
Varied Parameters	Span Length	40 ft to 160 ft	100 ft
	Bridge Width	36 ft. to 90 ft.	60 ft
	Girder Spacing	5 to 12 ft	7.5 ft
	Skew Angle	0^o to 60^o	0^o and 20^o degree skews were both used as median values.
	Material Properties (elastic modulus of concrete)	3000, 3500, 4000 ksi	3500 ksi
	Deck Thickness	7, 8, 9, 10 in	8 inches
	Span to Depth Ratio	L/20, L/22, L/25, L/28, L/30	L/25
	Stiffness of non-structural components (barriers and sidewalks)	Assumed fully active or ignored	N/A
Constant Parameters	"Primary" Bridge Types	*Not Varied*	Steel
	Design Method	*Not Varied*	Allowable Stress Design
	Superstructure Continuity	*Not Varied*	2-span continuous
	Shear deformation of members	*Not varied*	Off
	Overhang	*Dependent on other parameter*	½ of girder spacing
	Sidewalk Dimensions	*Not Varied*	10 in high x 48 in wide
	Barrier Dimensions	*Not Varied*	27 in high x 12 in wide

A few parameters, such as bridge type, design methodology, and superstructure continuity were not varied as they were either (1) deemed to be essential to the larger multi degree-of-freedom study and therefore sensitivity studies were unnecessary, or (2) not currently feasible due to the present state of development of the design and model building software. Steel multi-girder was chosen as the bridge type for this study as it is quite common and the current software iteration has the capability to both design and model such bridges. In addition, the Allowable Stress Design method was employed as the incorporation of the LRFD approach is not within the scope of Phase I.

Additional parameters that were held constant include the overhang dimension of the deck and the barrier and sidewalk dimensions. The overhang for each structure was kept to one half of the girder spacing. The sidewalks were modeled as 10 in. high by 48 in. wide while the barriers were modeled as 27 in. high by 12 in. wide. These values may be modified in later studies. Overhangs, sidewalks, and barriers dimensions were chosen as a generic average that would provide approximate loading effects to the exterior girders under dead load as well as stiffness (when required) during dead, live, and settlement loading.

To provide a more comprehensive study, two median values of skew were employed. Specifically, the median values of skew were taken as both zero degrees and 20 degrees, which results in two "parallel" single degree-of-freedom studies. Skew was also varied itself over a larger range (Table 4-1).

4.4 Sensitivity Study Results

Included in this chapter is a subset of the results obtained from the single degree-of-freedom sensitivity studies, which were selected to illustrate the key findings. The figures below show both 0^{o} and 20^{o} skew bridges on the same graph. All graphs shown below are for FE models with non-structural element stiffness turned on and shear deformation of all beam elements ignored. The complete set of results from this study can be found in Appendix D.

4.4.1 Total Composite Section Stress

Total composite section stress was calculated for the exterior, 1^{st} interior, and centerline girder over the central pier of a number of 2-span continuous bridges. Figure 4-3 through 4-7 detail the relationship between a subset of the parameters of interest and the total stress in the composite section. This stress was taken at the extreme bottom fiber of a two-node beam

element directly over the center support. The other parameters not shown did not exhibit a strong or unexpected relationship with total composite section stress; these results are included in Appendix D.

Figure 4-3 illustrates the relationship between girder spacing and total composite section stress over the center pier due to a 1 inch settlement at an exterior abutment. Stresses for most girders follow a slightly quadratic trend, however the exterior girder from the 0° skew bridge and 2nd girder from the 20° skew bridge diverge from the apparent trend. Although the cause of this apparent anomalous behavior is still in question, based on the interpretation conducted thus far, it appears to be due to the fact that girder spacing, bridge width, and overhang are all coupled parameters. Regardless, the influence of these parameters appears quite small compared with span length and skew angle (See Figures 4-5 and 4-6). Prior to initiating the larger parametric within Phase II additional investigation into the influence of girder spacing will be carried out.

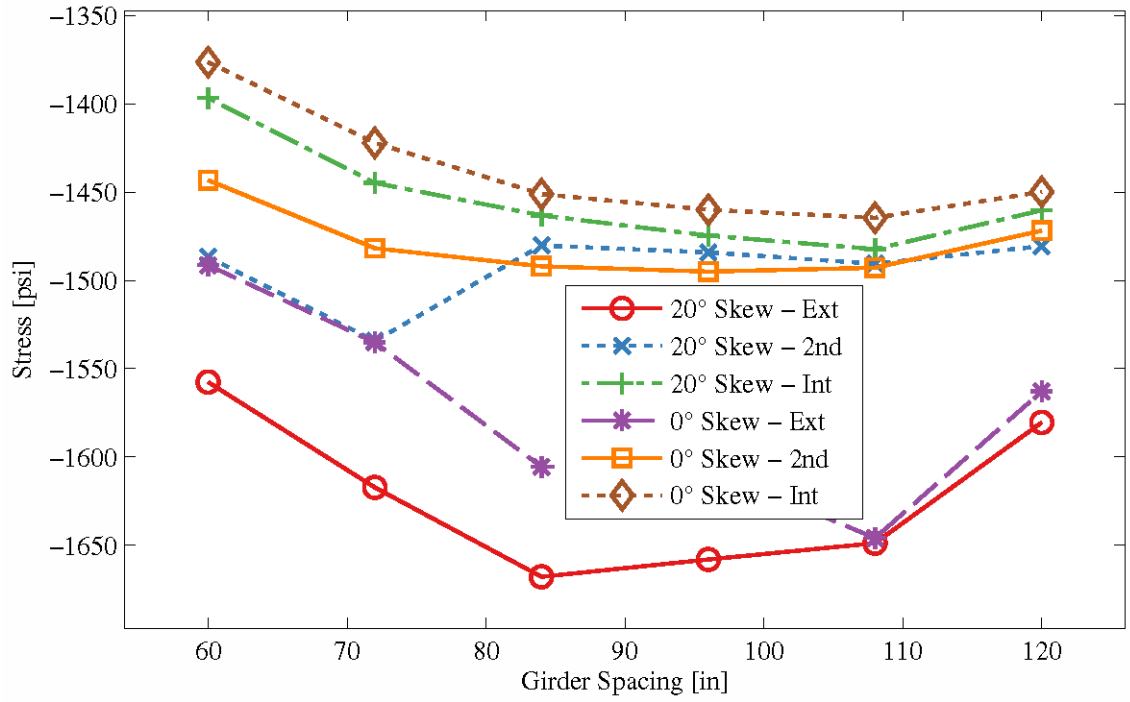

Figure 4-3 - Effect of Girder Spacing on Total Composite Section Stress with Non-structural Element Stiffness Included

Figures 4-4 and 4-5 show the influence of span length on total fiber stress both normalized by span length and non-normalized, respectively. As apparent from these figures, the relationship between girder stress and span length is nonlinear. In addition, span length has the largest

influence over girder stress due to support settlement, with stress varying over 800% for the 160 ft. to 40 ft. bridge spans examined.

Figure 4-6 shows the influence of skew on girder stress due to a support settlement, and indicates that the exterior girder stresses are quite sensitive to skew angle, while the interior girder stresses are not. Further, the influence of girder depth to span ratio is shown in Figure 4-7. Based on this figure it appears the relationship between girder depth to span ratio and stress is linear in nature.

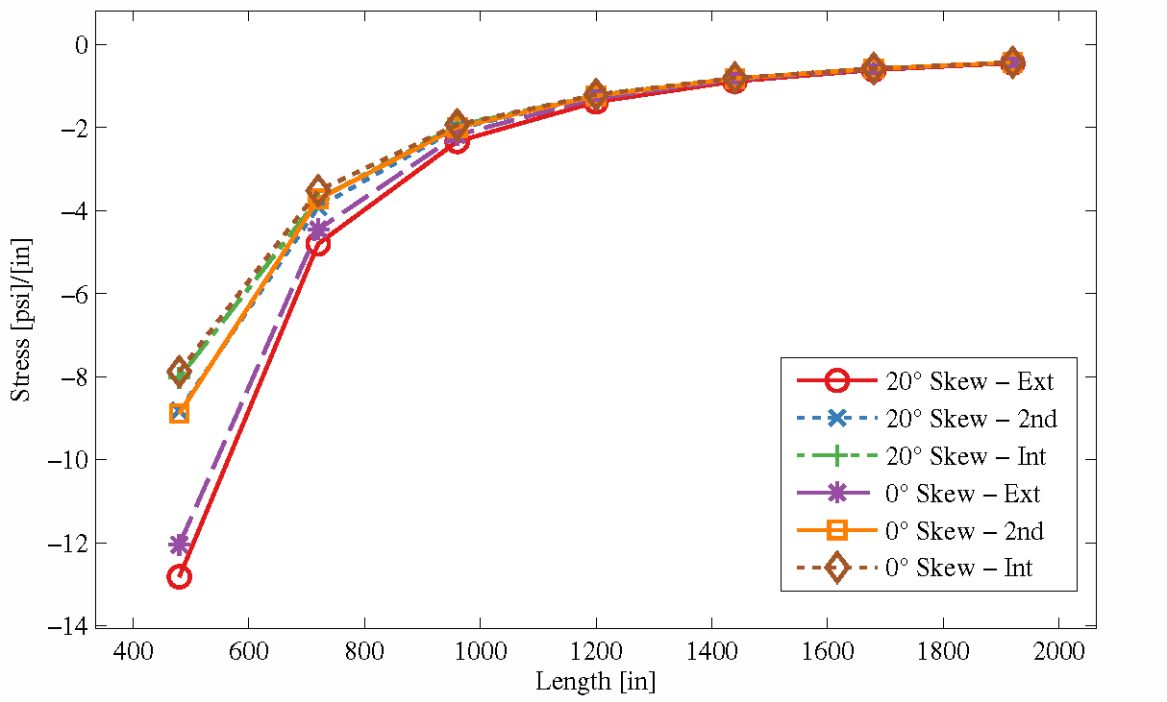

Figure 4-4 - Effect of Span Length Normalized by Length on Total Composite Section Stress

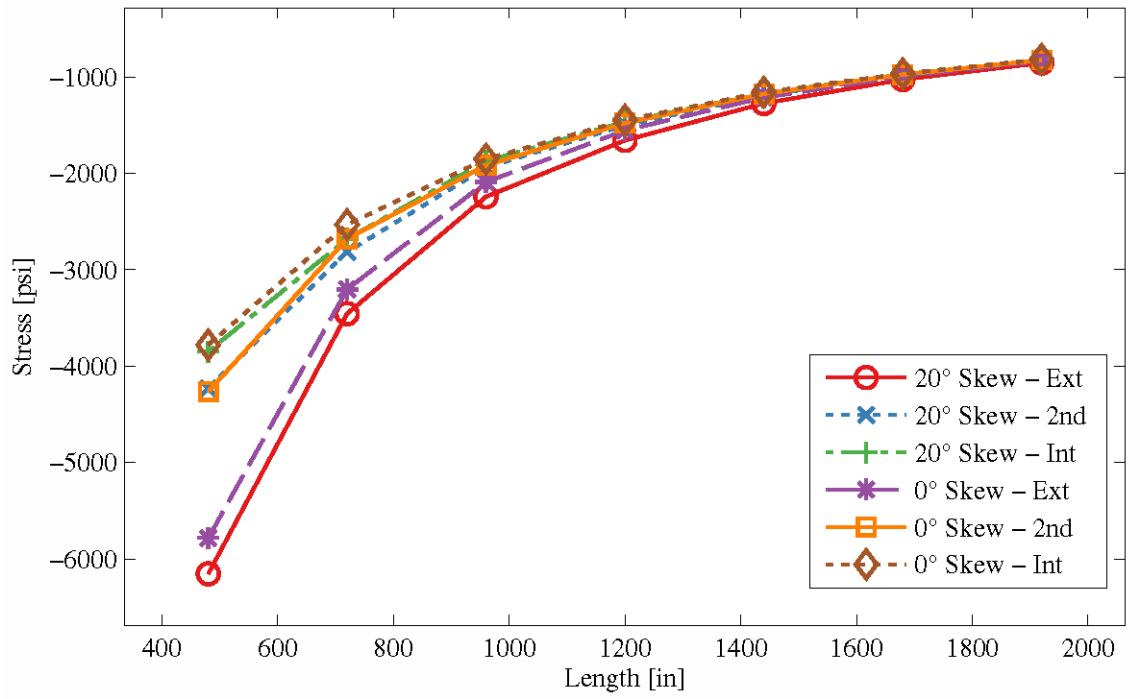

Figure 4-5 - Effect of Span Length on Total Composite Section Stress

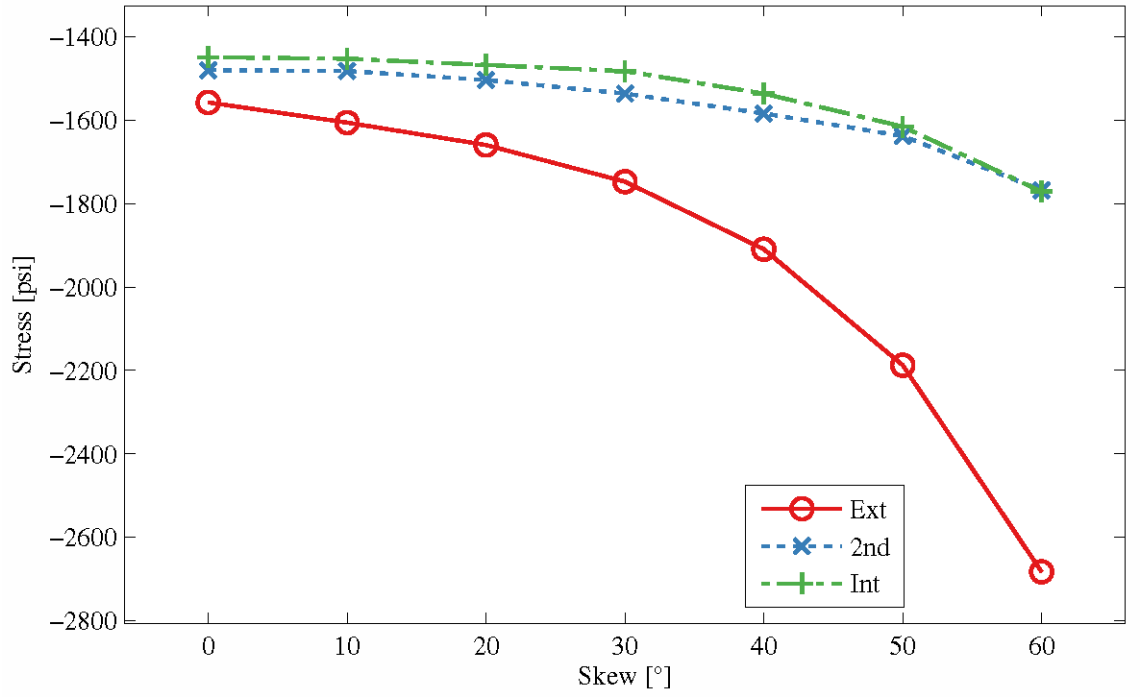

Figure 4-6 - Effect of Skew Angle on Total Composite Section Stress

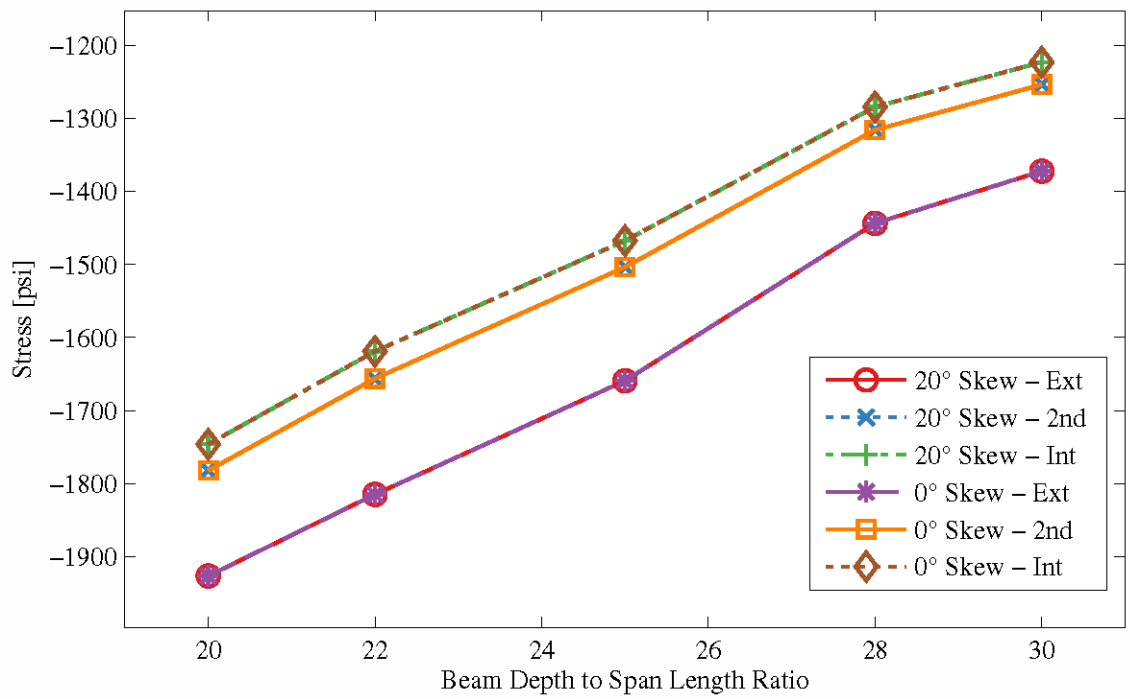

Figure 4-7 - Effect of Beam Depth on Total Composite Section Stress

4.4.2 Deck Stress

The influence of a number of parameters on the deck stress directly above the exterior, 1st interior, and centerline girder over the central pier of the benchmark structure was examined. Figures 4-8 through 4-12 detail the relationship between a subset of the parameters of interest and the stress in the topmost fiber of the deck at the centerline of each girder. A complete set of results can be found in Appendix D. The deck stresses shown in these plots were calculated using the procedure outlined in Section 3 of this report. As apparent from these figures, the same trends observed for girder stresses were also observed in the case of deck stresses.

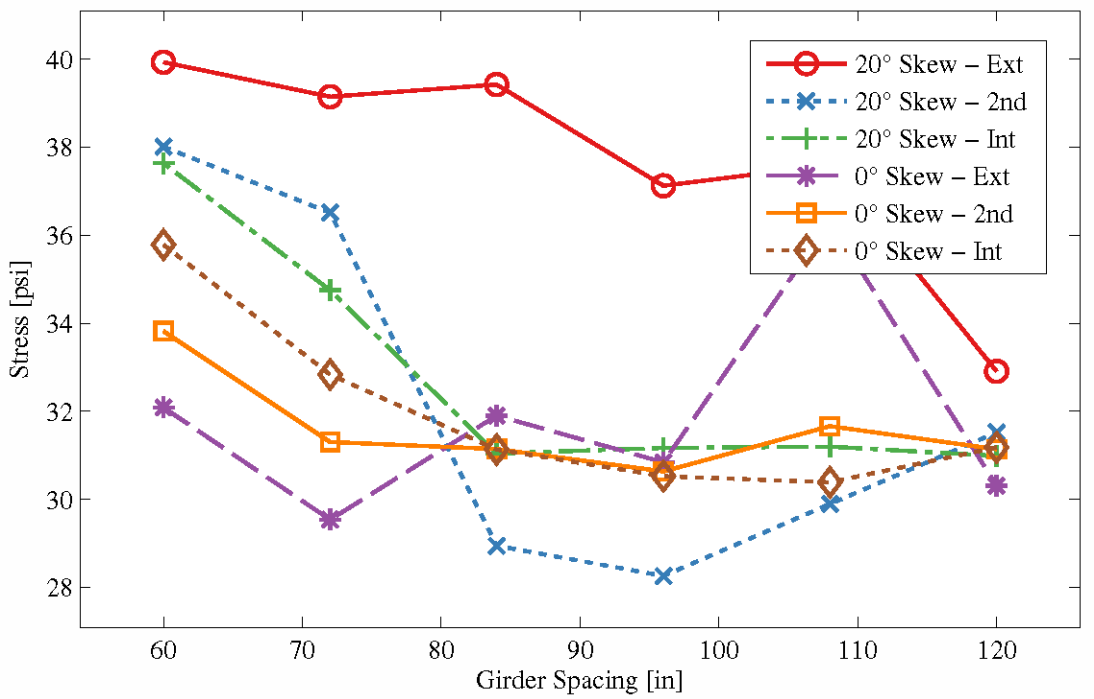

Figure 4-8 - Effect of Girder Spacing on Deck Stress

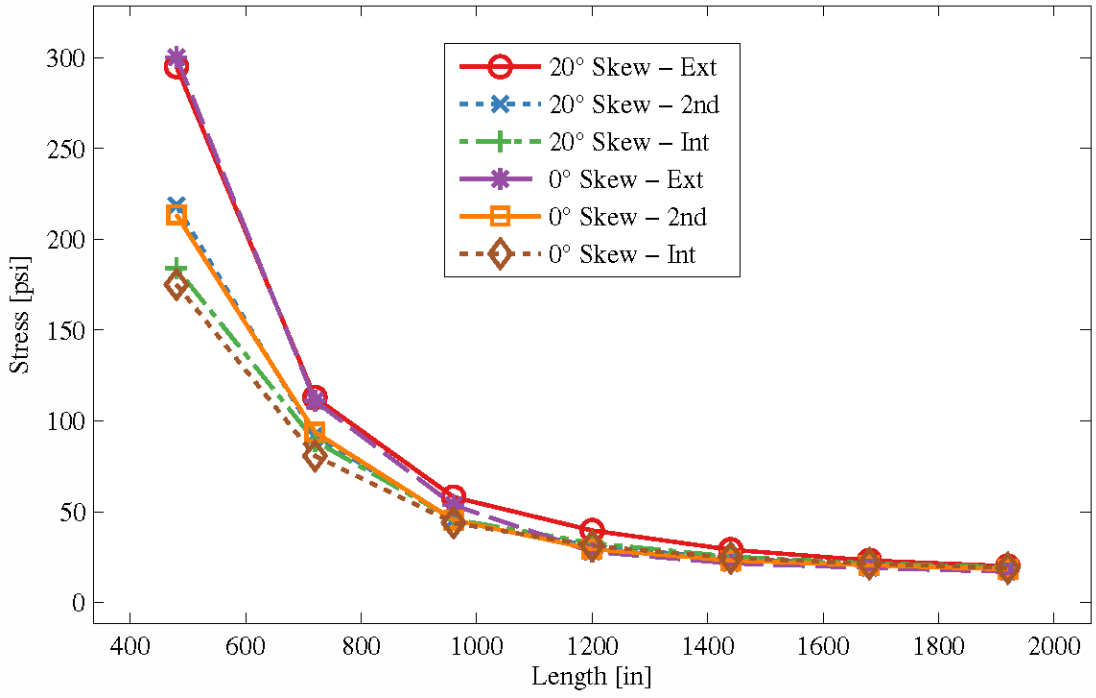

Figure 4-9 - Effect of Span Length Normalized by Length on Deck Stress

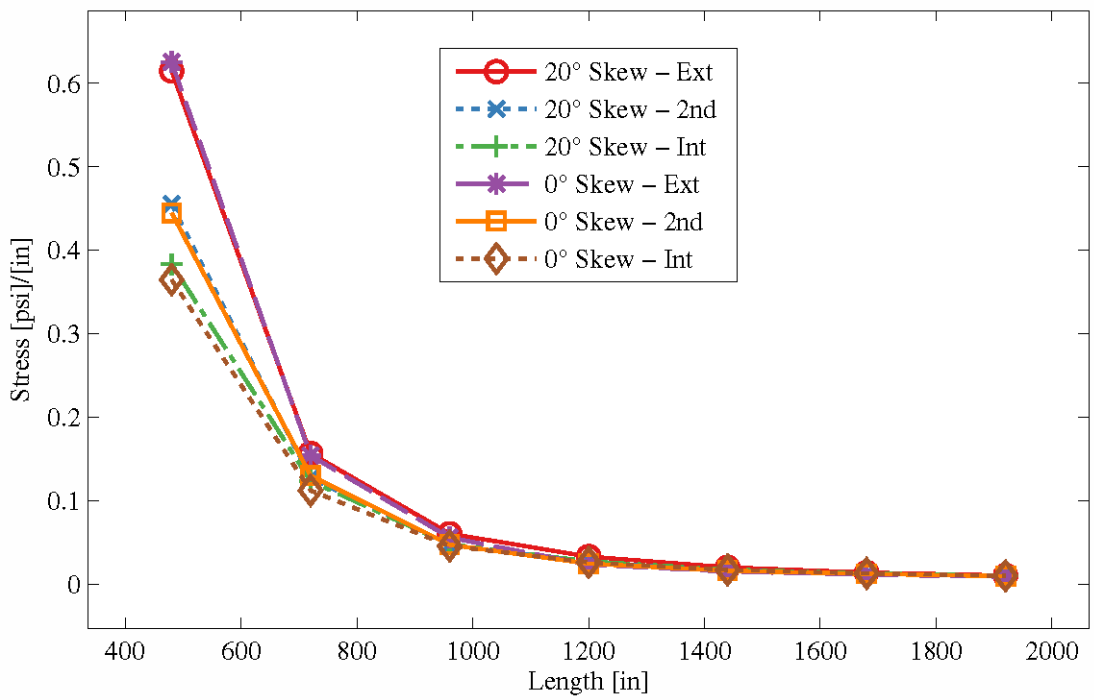

Figure 4-10 - Effect of Span Length on Deck Stress

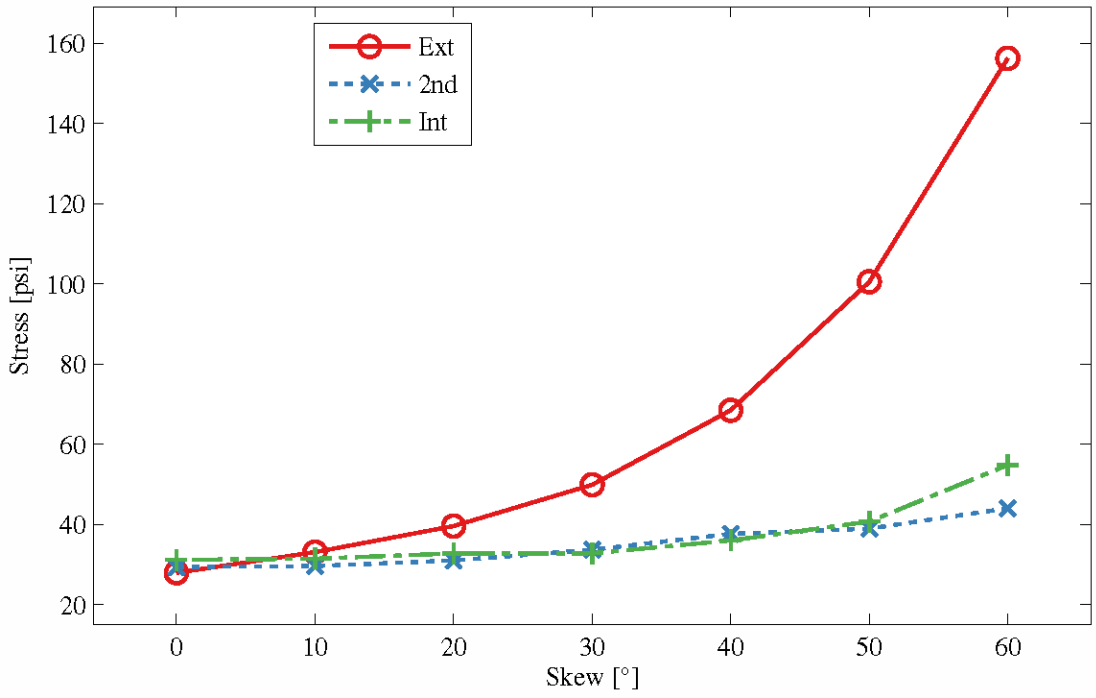

Figure 4-11 - Effect of Skew Angle on Deck Stress

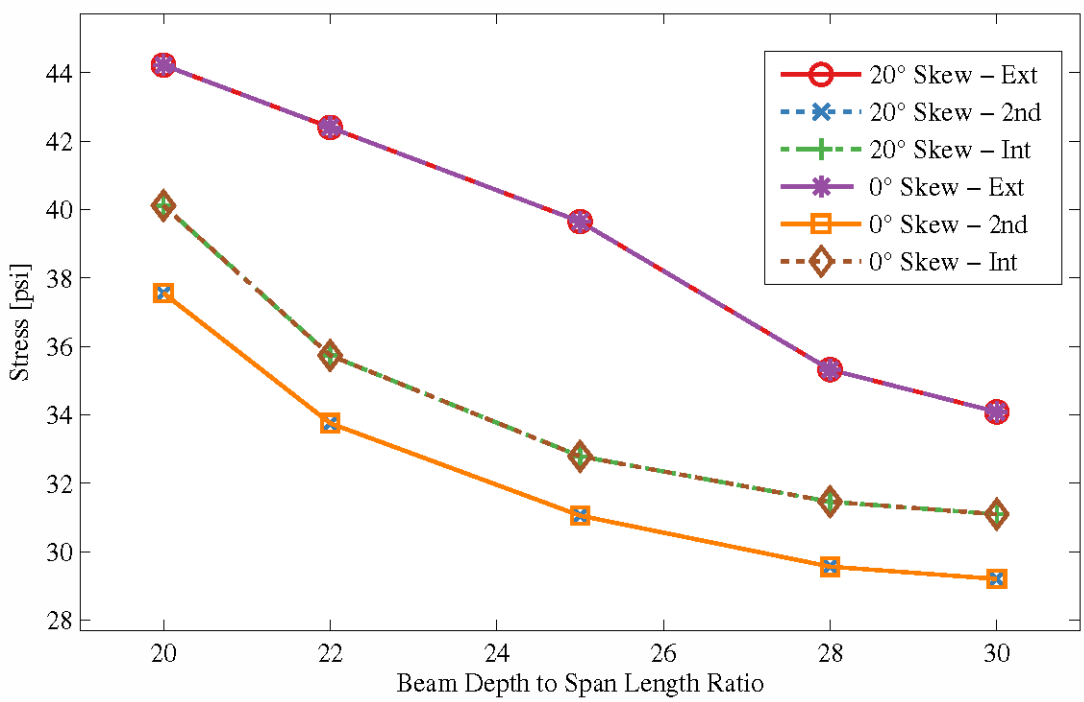

Figure 4-12 - Effect of Beam Depth on Deck Stress

4.4.3 Vertical Reaction at the Support

The influence of various parameters on the vertical reaction of the supports at the exterior, 1st interior, and centerline girders over the central pier of the benchmark structure was examined. Figures 4-13 through 4-17 show the relationship between a subset of the parameters of interest and these boundary reactions. A full set of results can be found in Appendix D.

As apparent from these plots, similar trends observed for both total fiber stress in the girders and deck stresses were also observed in the case of boundary reactions. Some notable exceptions include more consistent trends related to girder spacing, opposite trends between exterior and interior reactions relative to skew, and a nonlinear relationship with girder depth to span length ratio.

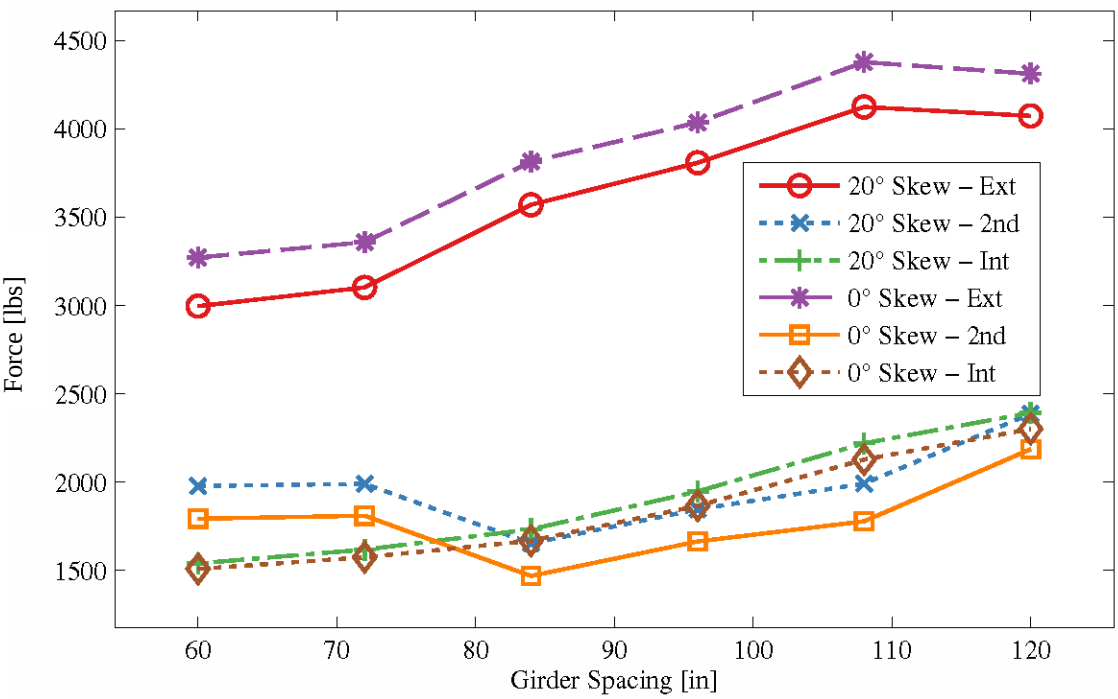

Figure 4-13 - Effect of Girder Spacing on Vertical Reaction at the Support

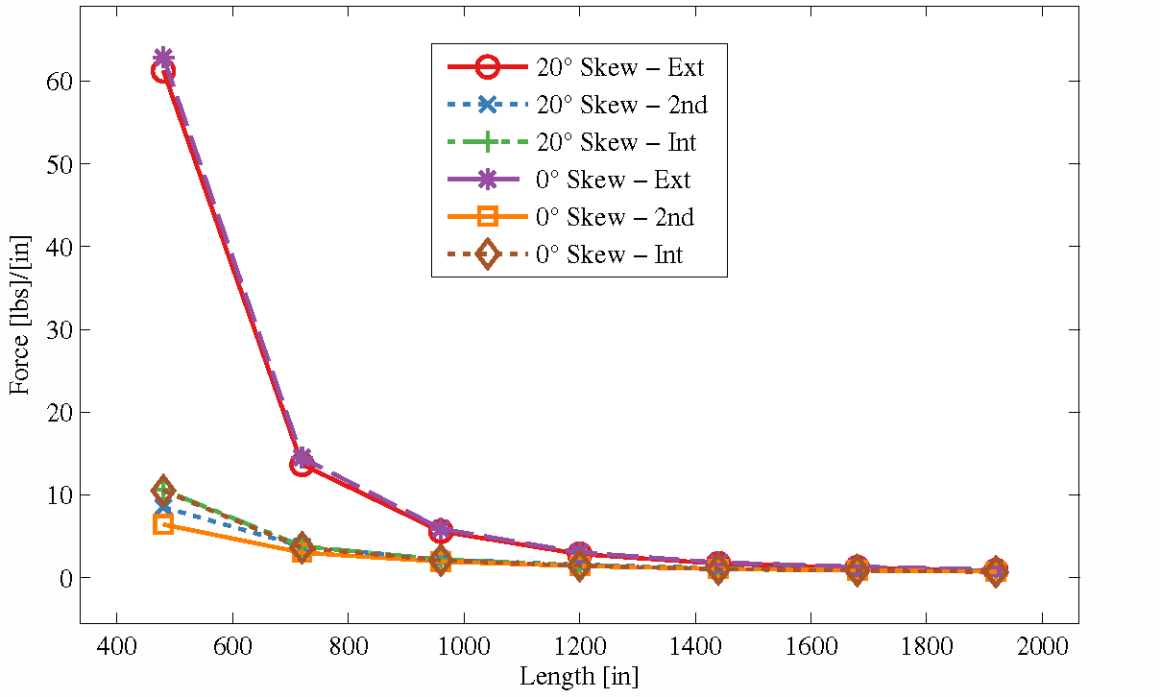

Figure 4-14 - Effect of Span Length Normalized by Span Length on Vertical Reaction at the Support

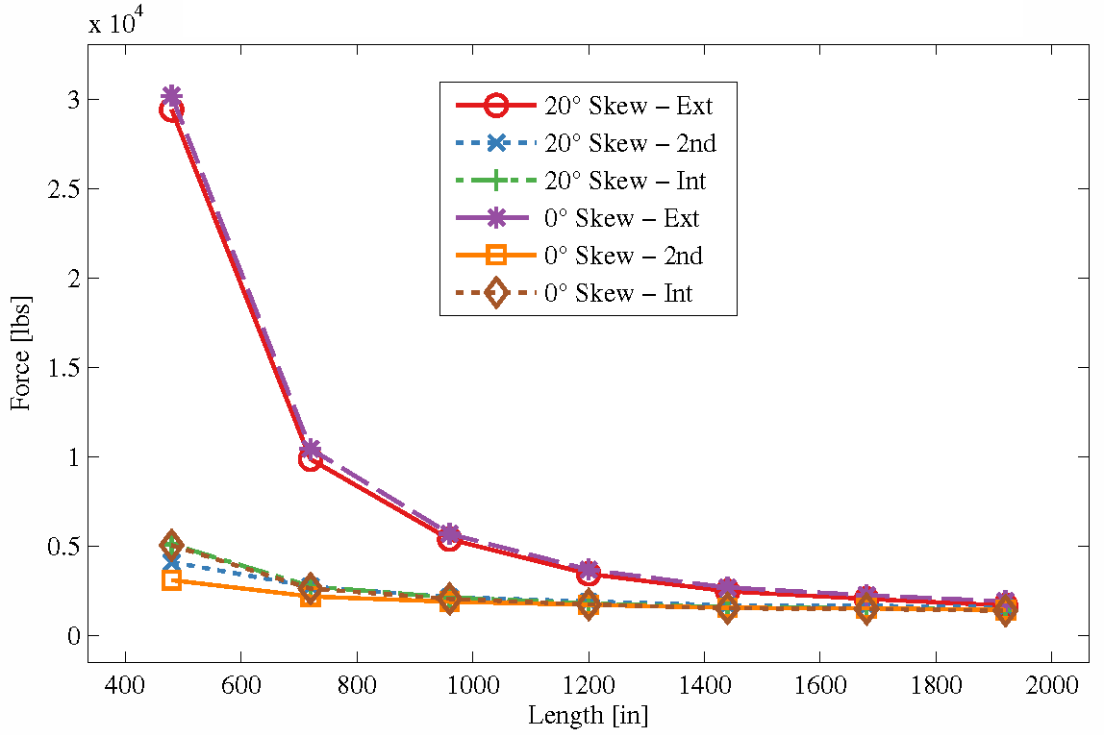

Figure 4-15 - Effect of Span Length on Vertical Reaction at the Support

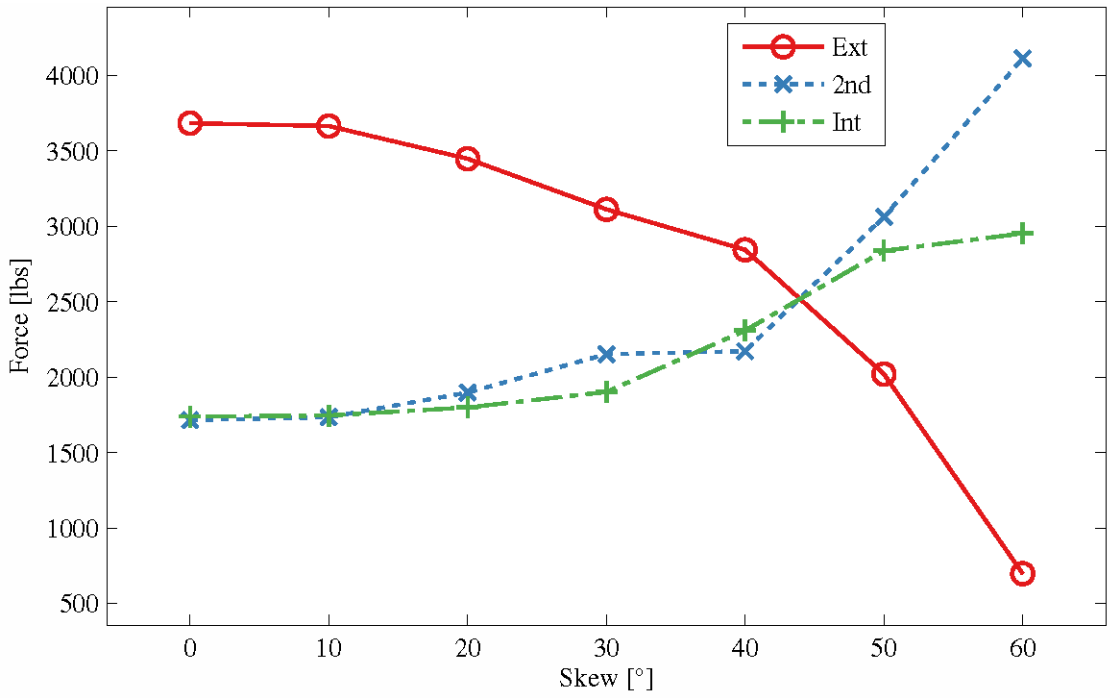

Figure 4-16 - Effect of Skew Angle on Vertical Reaction at the Support

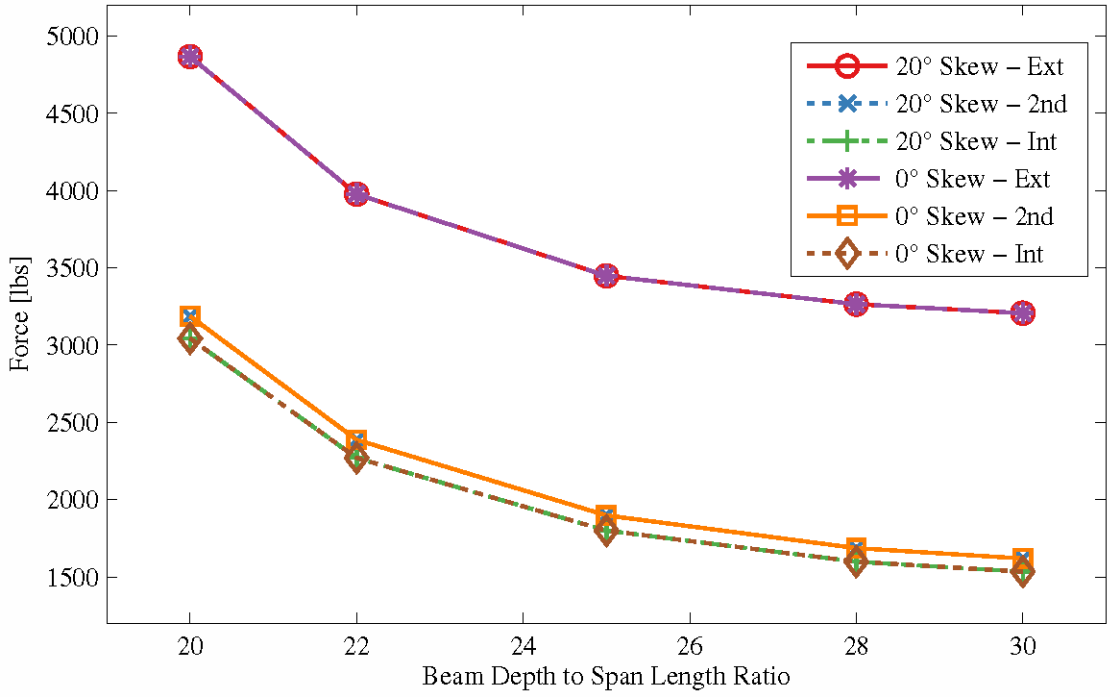

Figure 4-17 - Effect of Beam Depth on Vertical Reaction at the Support

4.5 Task 1.3 Conclusions

The goals of this task were (1) to determine whether the performance indices of interest were sensitive to the chosen parameters and (2) to verify that the parameter ranges of interest were adequate for the Phase II study. To satisfy these objectives a series of single degree of freedom parametric studies were carried out on a set of two-span continuous, steel multi-girder benchmark bridges. Based on the results of this study, the following conclusions were drawn.

1) The parameters that exert the most significant influence on the responses due to support movements are Span Length, Skew Angle, and Girder Depth-to-Span Ratio. While Span Length and Skew Angle had nonlinear influences over all responses examined, Girder Depth to Span showed a linear influence over stresses and slightly nonlinear influence over support reactions.
2) Parameters such as Girder Spacing, Bridge Width, Barrier/Sidewalk Participation, Elastic Modulus of Concrete, and Deck Thickness have significantly less influence on the responses induced by vertical support settlement.

3) While several parameters showed relatively small influence over responses to support movement, such parameters have been shown (through past studies by the investigators) to have influence over both live and dead load demand calculations. As such, in order to reliably identify tolerable support movements for the Limit State outlined in Section 5, such parameters must be included within Phase II.
4) The results of this initial study indicated that the initially proposed parameters and bounds are appropriate for Phase II. Table 4-2 provides a summary of these parameters.

Table 4-2 – Bridge Configuration Parameters

	Parameter	Bounds, Limits	Notes
Discrete	"Primary" Bridge Types	Steel Multi-Girder and PS Concrete Multi-Girder	These bridge types were selected as they represent the most likely bridges to be designed/ constructed in the future
	Superstructure Continuity	Simple, 2-span Continuous, and 3-Span Continuous	These levels of superstructure continuity allow for spans with no continuity, continuity at one end, and continuity at both ends
	Superstructure-to-Substructure Continuity	Fixed-expansion bearings and integral abutments	Allows the investigation of the influence of different support restraints
	Girder Spacing	5 ft. to 12 ft.	These nominal girder spacings will be adjusted (rounded) based on bridge width to define the number of girders
	Stiffness of non-structural components (barriers and sidewalks)	Assumed fully active or ignored	Since these items increase the superstructure stiffness, ignoring them is not necessarily conservative in the case of support movements
Continuous	Span Length	20 ft. to 160 ft.	Typical span-length bounds for multi-girder bridges
	Bridge Width	36 ft. to 72 ft.	Approximately 2 to 4 lanes
	Skew Angle	0^o to 60^o	Larger skew angles will require using advanced analysis methods
	Span to Depth Ratio	L/20 to L/30	These represent typical bounds on girder depth and also govern the relationship between girder strength and stiffness
	Material Properties (elastic modulus of concrete)	3,500 ksi to 8,000 ksi	Elastic modulus of concrete has significant influence on superstructure and deck stiffness and has a high variability (compared with steel)

5 Revised Phase II Work Plan (T1.4)

As described in the Amplified Work Plan, the approach proposed to satisfy the objectives of Phase II (outlined above) will focus on developing a set of "deemed to comply" (also often referred to as "deemed to satisfy") levels of support movement for various bridge configurations. Note that herein the terms "support" and "foundation" are used interchangeably for movements that can affect the performance of the bridge superstructure. In general, the term "support" can include the movement of the foundation as well as the substructure.

Although it may be possible to re-calibrate the probabilistic limit states within the AASHTO LRFD Specifications to include support movements, this approach is not proposed for two reasons. First, in the estimation of the authors, to do this properly, such an approach may require a change in the basic limit states currently identified in AASHTO, and the intent of the current project is to work within the existing AASHTO framework. Second, given the inherent conservatism build into the structural analysis models relied upon to calibrate the AASHTO LRFD Specifications (see Section 3), there may be sufficient margins in current designs to accommodate reasonable levels of support movement without any explicit changes to the probability-based limit states. That is, the structural analysis models used for the design of common bridges inherently provide a level of conservatism (related to dead load and live load actions) that may render common levels of support movement tolerable.

As a result, the proposed approach aims to identify the level of support movement that the inherent conservatism in current design methods may accommodate. For cases where such tolerable support movements are easily achievable by current practice, guidance to designers in the form of "deemed to comply" limitations will be provided. In cases where tolerable support movements are sufficiently small as to warrant design modifications, recommendations for future work related to the incorporation of support movements within the probabilistic LRFD limit states will be provided.

Developing such "deemed to comply" limitations require a large of number of variables to be examined, and the most appropriate approach to do so is through the use of a multivariate parametric study. To ensure that the resulting work plan is realistic in light of the time and budgetary constraints, it is first necessary to clearly define the extent (or scope) of the parametric study. The most important decisions in this regard are related to (1) the set of limit states that will explicitly be addressed, (2) the set of parameters that will define which bridge

configurations will be examined, and (3) the specific modeling approaches that will be employed to examine (1) and (2). These three decisions directly influence the cost and time requirements of the study as they define the type and number of models required as well as the specific simulations that must be carried out.

A list of proposed limit states, bridge parameters (see Section 4), and modeling approaches to be included in the study are shown in Tables 5-1, 5-2 (repeated from Section 4 for convenience), and 5-3, respectively. These were developed in an attempt to address the most common and relevant issues while also ensuring the scope is realistic considering the time and budget provided.

Table 5-1 – Summary of Proposed Limit States for Study

	Name	Description	Criteria for Tolerable Support Movement
Existing Limit States	Strength I	Basic load combination related to normal vehicle use of the bridge	Eqn 1.3.2.1-1 (AASHTO LRFD 2012)
	Strength II	Load combination related to owner-specified or permit vehicles	Eqn 1.3.2.1-1 (AASHTO LRFD 2012)
	Service I	Load combination related to estimation of foundation movements	Article 10.5.2.2 and C10.5.2.2 (AASHTO LRFD 2012)
	Service II	Load combination intended to control yielding of steel structures	Eqn 1.3.2.1-1 (AASHTO LRFD 2012)
	Service III	Load combination for the analysis of longitudinal tension in prestressed concrete superstructures	Eqn 1.3.2.1-1 (AASHTO LRFD 2012)
Supplementary Limit States	Service A	Limit state intended to avoid transverse cracking of reinforced concrete decks due to differential support movements	Deck stress induced by support settlement plus Service I load combination is less than the tensile strength of concrete
	Service B	Limit state intended to avoid joint performance problems due to differential support movements	Based on the results of Phase I, tolerable displacements and rotations will be identified for several joint types (such as poured seal, compression seal, strip seal, and modular)
	Service C	Limit state intended to avoid bearing performance problems due to differential support movements	Based on the results of Phase I, tolerable displacements and rotations will be identified for several bearing types (such as elastomeric, pot, and integral abutment)
	Service D	Limit state intended to avoid damage to utilities due to differential support movements	Based on the results of Phase I, tolerable displacements and rotations will be identified for several utility conduits carried by bridges

Table 5-2– Primary Bridge Configuration Parameters

	Parameter	Bounds, Limits	Notes
Discrete	"Primary" Bridge Types	Steel Multi-Girder and PS Concrete Multi-Girder	These bridge types were selected as they represent the most likely bridges to be designed/ constructed in the future
	Superstructure Continuity	Simple, 2-span Continuous, and 3-Span Continuous	These levels of superstructure continuity allow for spans with no continuity, continuity at one end, and continuity at both ends
	Superstructure-to-Substructure Continuity	Fixed-expansion bearings and integral abutments	Allows the investigation of the influence of different support restraints
	Girder Spacing	5 ft. to 12 ft.	These nominal girder spacings will be adjusted (rounded) based on bridge width to define the number of girders
	Stiffness of non-structural components (barriers and sidewalks)	Assumed fully active or ignored	Since these items increase the superstructure stiffness, ignoring them is not necessarily conservative in the case of support movements
Continuous	Span Length	20 ft. to 160 ft.	Typical span-length bounds for multi-girder bridges
	Bridge Width	36 ft. to 72 ft.	Approximately 2 to 4 lanes
	Skew Angle	0^o to 60^o	Larger skew angles will require using advanced analysis methods
	Span to Depth Ratio	L/20 to L/30	These represent typical bounds on girder depth and also govern the relationship between girder strength and stiffness
	Material Properties (elastic modulus of concrete)	3,500 ksi to 8,000 ksi	Elastic modulus of concrete has significant influence on superstructure and deck stiffness and has a high variability (compared with steel)

In addition to the "primary" bridge types listed in Table 5.2, a secondary study will be carried out to "spot check" the trends and level of tolerable support movement for the other common superstructure types listed in the *AASHTO LRFD Bridge Specifications, Table 4.6.2.2.1-1 – Common Deck Superstructures Covered in Articles 4.6.2.2.2 and 4.6.2.2.3*. Specifically, the bridge types to be incorporated in this study will include:

- Closed Steel or Prestressed Concrete Boxes
- Open Steel or Precast Concrete Boxes
- Cast-in-Place Concrete Tee Beams
- Precast Concrete Channel Sections with Shear Keys
- Precast Concrete Double Tee Sections with Shear Keys
- Precast Concrete Tee Sections with Shear Keys
- Wood Beams
- Cast-in-place Concrete Multicell Box
- Precast Solid, Voided or Cellular Concrete Boxes with Shear Keys with Cast-in-Place Concrete Overlay
- Precast Solid, Voided, or Cellular Concrete Boxes with an Integral Concrete Deck

Table 5.3 – Proposed Modeling Approaches

Bridge Configuration	Modeling Approach	Support Movements Considered	Computed Responses
Simple Spans – For support movements that do not give rise to forces	3D Geometric model to capture rigid-body movements	• Longitudinal translation • Vertical translation • Longitudinal rotation (about an axis transverse to the bridge)	Various translations and rotations
Simple Spans – For support movements that induce forces	3D FE model composed of 1D elements, 2D elements, and links/offsets to preserve actual geometry	• Transverse rotation (about an axis longitudinal to the bridge)	Member actions (axial, moment, shear), member stresses, reaction forces, and various deflections
Continuous Spans – For all support movements	3D FE model composed of 1D elements, 2D elements, and links/offsets to preserve actual geometry	• Longitudinal translation • Vertical translation • Longitudinal rotation (about an axis transverse to the bridge) • Transverse rotation (about an axis longitudinal to the bridge)	Member actions (axial, moment, shear), member stresses, reaction forces, and various translations and rotations

Considering the time and budget constraints, it is not feasible to perform the comprehensive parametric study outlined above for each of these bridge types. However, following the execution and interpretation of the results associated with the two primary bridge types, a series of secondary analyses that focus on the bridge types listed above will be carried out as an additional activity within Task 2.3. The aim of this study will be to identify any differences in either the observed trends or levels of tolerable support movements through a series of "spot checks" that examine the governing sets of bridge configuration parameters.

For the multi-girder type bridges listed, the element-level modeling approach outlined in Section 3 will be employed with modifications related to both the geometric shape of the girders and material properties. For the non-multi-girder type bridges listed, the modeling approach evaluated and selected in Section 3 for box-girder bridges will be employed.

5.1 Summary of Research Plan

Figure 5-1 provides a flow chart representation of the key action items within the research plan. This representation is cross-referenced to the lists of tasks provided for Phase II in Figure 1-1.

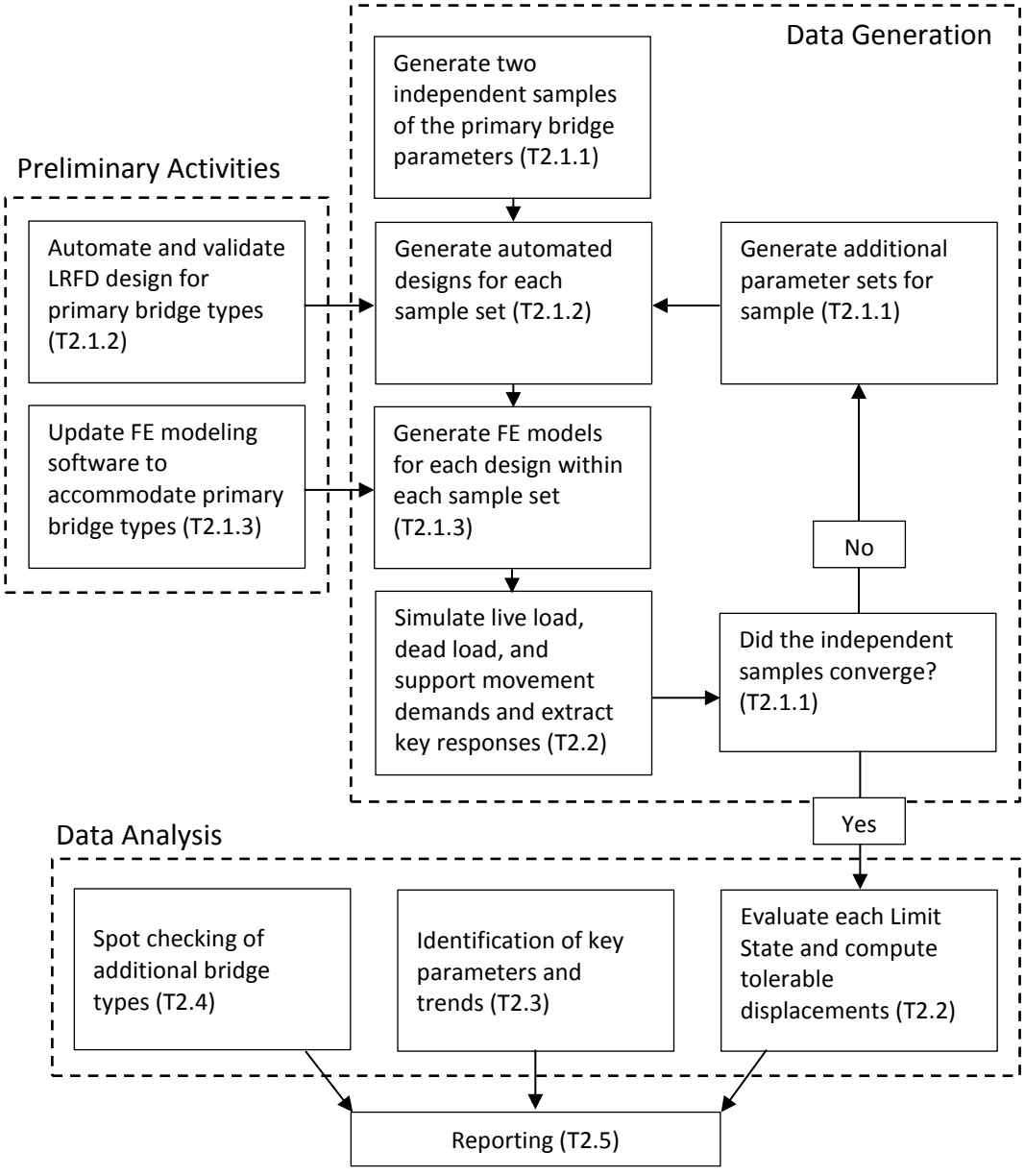

Figure 5-1 – Flow chart representation of the Phase II work plan

5.2 Detailed Description of Tasks

The following sections provide detailed descriptions of the tasks identified for Phase II of the project (Figure 1-1). The specific objectives identified for each phase are summarized in Table 1-2 and the overarching objectives of the study are provided in Section 1.1.

5.2.1 T2.1 – Definition and Construction of 3D FE Bridge Models

5.2.1.1 T2.1.1 – Sampling of Parameters to Develop a Bridge Suite (Moon)

Once the final set of parameters (and their ranges) have been identified, it is necessary to sample them to develop a representative "bridge suite" (or sample of bridges) to allow the impact of differential support movements to be examined. The goal of this sampling is to effectively and efficiently cover the parameter space (as defined in Section 4, Table 5-2). To satisfy this objective a hybrid sampling method is proposed that utilizes a statistical sampling approach known at Latin Hypercube Sampling (LHS) for the continuous parameters, and a Design of Experiments (DoE) approach for discrete parameters (Figure 5-2).

As shown in Figure 5-2, the proposed sampling methodology uncouples the discrete parameters from the continuous parameters. This is done since the discrete parameters assume such a small number of values that a full-factorial approach (i.e. every possible combination of these parameters) only produces 48 samples.

Due to the large number of values that continuous parameters may assume, such a simple sampling approach cannot efficiently cover their space. In these cases, random sampling approaches are generally used. For the task at hand, the LHS sampling approach is proposed (see Figure 5-2 for a step by step description of this approach). Although conventional Monte Carlo (MC) sampling is also possible, the LHS method generally covers a multi-dimensional continuous parameter space with fewer samples. This increased efficiency is primarily due to the stratification of the parameter space that does not permit the clustering of samples that MC approaches are susceptible to (Smith and Saitta, 2008).

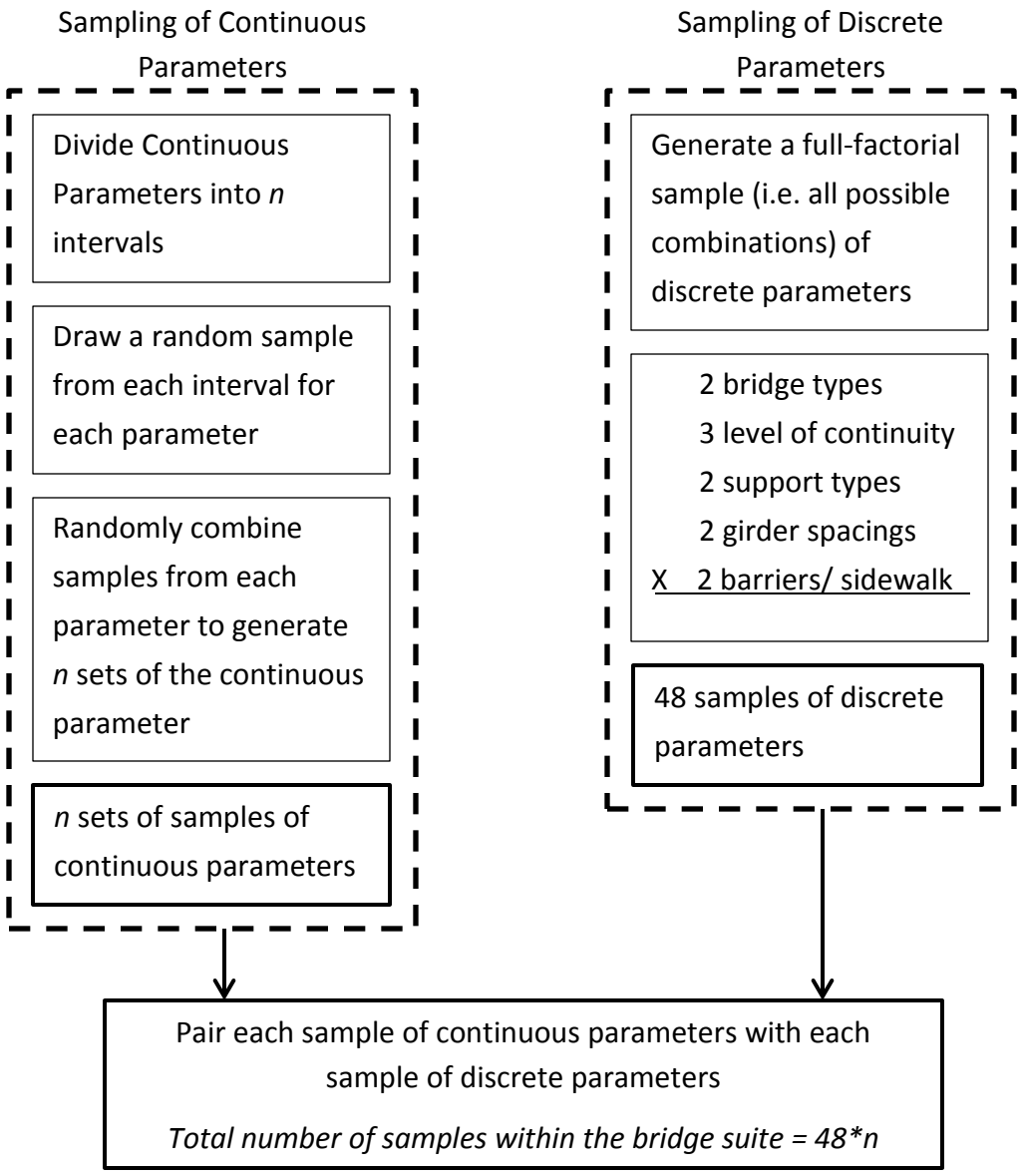

Figure 5-2 – Schematic illustrating the proposed sampling methodology

As with any sampling approach, it is critical that a criteria and strategy be defined to ensure that the sample is representative of the population from which it is drawn. Towards that end, it is proposed that the sampling and analysis be carried out multiple times until the results (i.e. the computed tolerable support movement distributions) converge. The logic behind this approach is that if two independent samples show the same results, then the results are likely representative of the population from which they are drawn (and independent of the specific samples).

To allow for this convergence check, it is anticipated that the original sampling runs will generate 100 samples from the continuous parameters, which will produce 4,800 bridge configurations. If the two independent samples produce results that are significantly different, then each population will be increased in increments of 4,800 until convergence is realized. To assess convergence, the z-test will be employed, which measures the difference between two distributions (Eqn 1).

$$z = \frac{\mu_1 - \mu_2}{\sqrt{\sigma_1^2 + \sigma_2^2}} \quad (1)$$

Where μ_1 and μ_2 are the means of sample 1 and 2, and σ_1 and σ_2 are the standard deviations of sample 1 and 2. Mathematically, the *z* statistic is the same as the safety (reliability) index, β. In the case of structural reliability it is desirable for the distribution of resistance to be significantly different (e.g. larger mean) than the distribution of demand, thus a large *z* (or β) is considered desirable. Conversely, for this task a *z* value of zero is desirable since this would indicate that the two independent samples provide the same results. The specific criteria for convergence will be set once the characteristics of the distributions are better known, but something on the order of 0.1 or less is anticipated. It should be noted that this approach assumes normal distributions; if such an assumption proves inappropriate, an additional metric will be defined.

5.2.1.2 T2.1.2 – Automated LRFD Design of Bridge Suite (Moon and Mertz)

The goal of this task is to develop member designs (e.g. steel girder dimensions, prestressing force/eccentricity, etc.) for each bridge configuration produced in Task 2.1.1. To ensure the relevancy of the overall study, it is imperative that the designs produced in this task are representative of the ones produced by designers following the AASHTO LRFD Specifications and common conventions based on heuristics (e.g. sizing increments for webs, flanges, etc.).

Given the size of the sample needed to investigate all of the potentially influential parameters identified, automation of the member sizing/prestressing processes will be required. Through a past research grant, the PI has developed an open-source Matlab program that performs the design of simply-supported and continuous multi-girder steel bridges (using both rolled sections and plate girders) using the allowable stress design methodology. To investigate the ability of this software to produce designs consistent with practice, three bridges that were recently load-tested by the PI were designed "blindly" by the automated software. Table 5-4 provides a

comparison of the actual member properties with the ones estimated using the automated design tool.

Table 5-4 – Comparison of Actual and Estimated Member Properties

	Pennsuaken Creek		NJ TPK (MP28.9)		US202/NJ23	
	Actual	Automated (% diff)	Actual	Automated (% diff)	Actual	Automated (% diff)
Flange Area (in^2)	22	22 (-)	106	71 (33)	101	88 (13)
Total Area (in^2)	38	41 (8)	128	116 (9)	123	112 (9)
Girder Depth (in)	31	33 (6)	66	91 (38)	65	72 (11)
Girder Moment of Inertia (in^4)	5761	7450 (29)	$10.7x10^4$	$17.4x10^4$ (63)	$9.4x10^4$	$11.1x10^4$ (18)
Girder Section Modulus (in^3)	428	477 (11)	3,880	3,810 (2)	2,900	3,100 (7)
Composite Moment of Inertia (in^4)	$1.5x10^4$	$2.0x10^4$ (31)	$20.7x10^5$	$31.3x10^4$ (51)	$15.9x10^4$	$20.0x10^4$ (26)
Composite Section Modulus (in^3)	646	659 (2)	4,800	4,520 (6)	3,440	3,620 (5)

Examining Table 5-4 the following observations can be made that illustrate both the nature of automated member sizing and the need for some of the parameters shown in Table 5-2.

- Automating the member sizing process will generally produce very similar results for the governing limit state, but may vary for other limit states. For the examples shown, the governing limit state was related to strength and thus the composite section moduli had relatively low discrepancies (less than 10%). Conversely, the discrepancies in moments of inertia were relatively large, since the deflection criteria did not govern the design.
- The somewhat arbitrary selection of girder span-to-depth ratio has significant influence over the relative levels of strength (section moduli) and stiffness (moment of inertia). For these designs a span-to-depth ratio of L/25 was assumed when the actual ratios for the NJTPK and US202 bridges were closer to L/35 (which is unusually shallow) and L/30, respectively. The result of assuming deeper girders was that the automated design approach produced lighter (less total area) and stiffer girders (but with the same section moduli). Since several different span-to-depth ratios are possible, the proposed approach will vary this parameter to "cover" the design space.
- In addition to girder depth, incremental sizing rules are also somewhat arbitrary and influence the balance between conservatism and efficiency. For example, if flange

dimensions/girder widths were treated as continuous variables, a truly "optimum" and unique solution to the design problem is possible. In reality however, plate sizes/thicknesses are typically defined in increments and thus minimum dimensions are rounded up resulting in additional strength/stiffness. The current sizing rules were based on discussions with designers and will be verified through Phase I of this research project.

As part of this research it is proposed that this software be expanded to include (1) member design based on the AASHTO LRFD Specifications, and (2) prestressed concrete multi-girder bridges. Although these modifications may appear significant, the original program was designed from the outset to accommodate them. Specifically, all the demand calculations were indexed separately to seamlessly accommodate unique factoring.

To accommodate the design of prestressed concrete girders two additional modifications will be required. First, for demand calculations it will be necessary to compute dead load actions in a simply-supported conditions and super-imposed dead load and live load in the continuous condition (for continuous configurations). Second, the optimization of resistance needs to be extended to allow the selection of common prestressed concrete girder forms (AASHTO girders, bulb tees) and the computation of prestress force and eccentricity using various criteria.

5.2.1.3 T2.1.3 – Automated 3D FE Modeling of Bridge Suite (Moon)

A unique aspect of the proposed research approach is the use of an automated tool to create 3D FE models of multi-girder bridges. This approach makes use of a commercially-available FE simulation software (Strand7, www.strand7.com) that provides a seamless interface with Matlab through an API. The API allows Matlab to drive the model construction and results extraction activities that are normally done through tedious manual interaction. In the proposed approach, all manual interaction with the simulation software is eliminated and replaced by an automated interaction via Matlab.

To generate a 3D FE model of a bridge, the software requires that a number of parameters and common practices be explicitly defined. Specifically, the required information can be grouped into three categories based on how it will be obtained:

1) Bridge configuration (achieved through sampling the parameters shown in Table 5-2 to be carried out under T2.1.1)

2) Member sizes (achieved through automation of the bridge design specifications to be carried out under T2.1.2)
3) Common details of secondary elements (e.g. barrier and sidewalk sizes, diaphragm type and spacing, deck thickness, etc. defined using heuristics)

Once defined, the automation of the FE model construction and results extraction process proceeds in systematic manner as show in Figure 5-3.

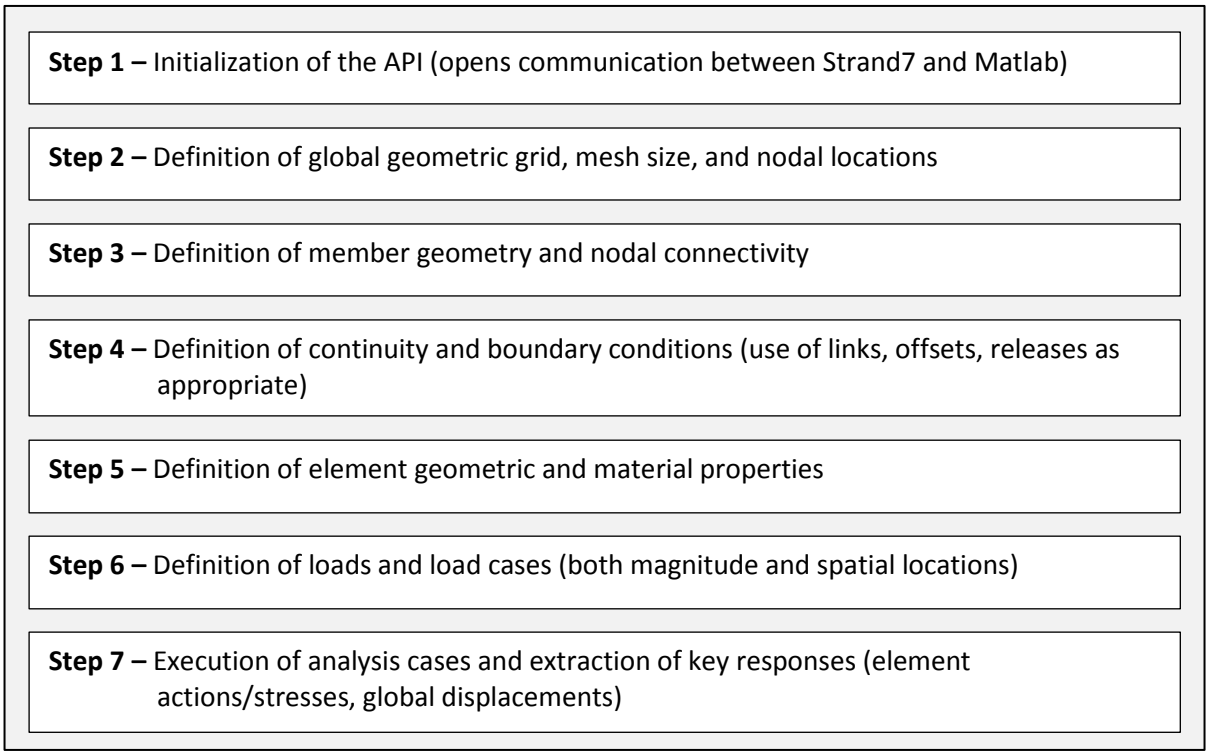

Figure 5-3 – Summary of Automated FE Modeling Procedure

Under this task, the automated FE modeling approach will be used to generate 3D FE models for the entire bridge suite (defined through T2.1.1 and T2.1.2). In addition to generating the FE models, this task will also implement two minor modifications to the current software to allow for the full set of bridge configurations shown in Table 5-2 to be examined. These include modifications (1) to allow live load-only continuity for prestressed concrete multi-girder bridges to be simulated, and (2) to allow the partial restraint provided by integral abutments to be simulated.

5.2.2 T2.2 – Estimation of Maximum Tolerable Support Movement (Moon and Mertz)

The goal of this task is to identify the levels of support movement associated with each of the limit states defined by Table 5-1 for every bridge defined and modeled in Task 2.1. The first step in this process will be to compute the responses of each model to the demands associated with the Strength I, Strength II, Service I, Service II, and Service III load combinations (without any assumed support settlement). For the supplementary limit states outlined in Table 5-1 there are currently no accepted load combinations. However, since they are all related to serviceability concerns, they will be evaluated by employing the existing service load combinations.

This analysis will require the explicit consideration of common construction practices and their influence on the resulting member-level (moments, shears, etc.) and material-level (stresses) demands. For example, the standard approaches to applying dead load, super-imposed dead load, and live load demands to models that represent the state of the bridge during the corresponding construction stage will be followed.

The second step in this process will be to impose unit support movements (vertical, horizontal and/or rotational) to each model and compute the resulting member-level and material-level demands. As discussed previously, the support movements will correspond to those occurring after the superstructure erection begins, and will be conservatively assumed to act on the complete superstructure. The use of a unit support movement will allow the resulting responses to be included within the various limit state equations as shown in Eqn. 2.

$$S_s = (S_1)(\Delta_{tol}) \tag{2}$$

Where, S_s is the member- or material-level demand included in the limit state equations (Table 5-1); S_1 is the member- or material-level demand due to a unit support movement; and Δ_{tol} is the associated tolerable support movement. Following this approach, the equations associated with each limit state can be formed with the only unknown being the tolerable support movement (Δ_{tol}). For example, Table 5-5 provides examples for both the Strength I and Service I limit states.

Finally, to populate the equations associated with the identified limit states, the relevant member- and material-level demands must be clearly defined so they can be extracted from

the FE analysis results in an automated manner. The following list provides a summary of the demand quantities that will be extracted separately for all load cases (e.g. LL, DC, DW, SE, etc.):

- Moments and axial forces within girders at mid-span of simple spans and interior continuous spans, 0.4L of exterior continuous spans, and over interior supports of continuous spans.
- Shear forces within girders at supports
- Deck stresses over interior supports within continuous bridges
- Bearing forces (x, y, and z directions)
- Bearing displacements (all six components)
- Joint displacements (displacements along the end of the deck)

Table 5-5 – Example Computation of Tolerable Support Movements

Limit State	Numerical Expression	Δ_{tol}
Strength I	$1.0R_n = 1.75(1 + 0.33)(S_{LL}) + 1.25(S_{DL})+(S_1)(\Delta_{tol})$	7.4 in
	$50ksi = 1.75(1.33)(6ksi) + 1.25(20ksi)+(1.5ksi)(\Delta_{tol})$	
Service I (Deck Cracking)	$0.9R_n = 1.0(1 + 0.33)(S_{LL}) + 1.0(S_{DL})+(S_1)(\Delta_{tol})$	5.1 in
	$0.9(0.45ksi) = 1.0(1 + 0.33)(0.15ksi) + 1.0(0ksi)+(0.04ksi)(\Delta_{tol})$	

5.2.3 T2.3 – Identification of parameters that govern the presence and extent of performance problems due to Support Movements (Moon and Mertz)

The goal of this task is to mine the large amount of data generated in T2.2 above to identify the parameters or combinations of parameters that have the largest influence over tolerable support movements. Once identified, these relationships between bridge parameters and tolerance to support movements will inform the structuring of the recommendations to the AASHTO LRFD Specifications.

Given the number of parameters included in Table 5-2, it is expected that 10,000 to 50,000 FE models may be required to estimate tolerable support settlements for at least the nine limit states in Table 5-1. The field of data mining, which aims to identify patterns within large data sets (typically classified as association rules, correlations, sequences, classifiers, and clusters), is ideally suited to guide the interpretation of this dataset (Wang and Ghosn 2006).

To identify correlations between tolerable support movements and bridge parameters, Principal Component Analysis (PCA) will be used. Since its development by Pearson in 1901, PCA has proven highly effective at identifying correlations within multidimensional data sets to

reduce the data set to lower dimensions. This is accomplished by identifying linear combinations of dimensions that best characterize the data. By reducing the dimensionality of the data set, conventional 2D or 3D data visualization techniques may be used to further enhance interpretation. In addition to PCA, a technique known as k-means (MacQueen 1967) has been shown quite effective at reducing large and disparate data sets to relatively small set of clusters. This approach aims to develop k clusters of the data such that the variance associated with each cluster is minimized.

To help guide the interpretation of the large parameter study, these two data mining methods will be combined using the approach outlined by Smith and Siatta (2008). Specifically, the data that defines the relationship between bridge parameters and tolerable support movement will first be subjected to a PCA to reduce its dimensionality and then clustered using the k-means method. Once completed, the resulting clusters will be used to structure the recommendations to the AASHTO LRFD Specifications.

5.2.4 T2.4 – Spot Checking Additional Bridge Types

To identify the relevance of the trends and levels of tolerable support movements to other common bridge types, a secondary study will be carried out to "spot check" the following common superstructure types:

- Closed Steel or Prestressed Concrete Boxes
- Open Steel or Precast Concrete Boxes
- Cast-in-Place Concrete Tee Beams
- Precast Concrete Channel Sections with Shear Keys
- Precast Concrete Double Tee Sections with Shear Keys
- Precast Concrete Tee Sections with Shear Keys
- Wood Beams
- Cast-in-place Concrete Multicell Box
- Precast Solid, Voided or Cellular Concrete Boxes with Shear Keys with Cast-in-Place Concrete Overlay
- Precast Solid, Voided, or Cellular Concrete Boxes with an Integral Concrete Deck

Taken together with the two primary bridge types examined, these ten bridge types cover all those addressed within the AASHTO LRFD Bridge Specifications, Table 4.6.2.2.1-1 – Common Deck Superstructures.

5.2.5 T2.5 – Reporting (All)

The Interim Report No. 2 documenting Tasks 2.1 through 2.4 will be prepared and submitted no later than 18 months after the project start date. After a 1-month review period, the research team will meet with the NCHRP 12-103 Panel to discuss their assessment, comments, and recommendations. Based on this feedback and after receiving authorization, Phase III of the project will begin.

6 Identification of Design Provisions that may be Revised (T1.5)

The research will result in guidance to bridge designers as to what constitutes tolerable differential support movements for various types/configurations of typical highway bridges. This guidance will consider the strength and service limit states of the LRFD Specifications as well as distress to joints, bearings, utilities, ride quality, deck drainage, and bridge aesthetics.

In line with this guidance, revisions, additions and/or deletions to the LRFD Specifications will be recommended. In *AASHTO LRFD* (2012), Article 10.5.2 ("Service Limit States") in Section 10 ("Foundations") is the primary article that provides guidance for service limit state design for bridge foundations in terms of tolerable movements. The results of this research program will be used primarily to revise this article. Article 10.5.2 is referenced in other articles as indicated in Table 7-1 and therefore these additional articles may also require revision.

Table 6-1 – Summary of Relevant Articles in *AASHTO LRFD* for Foundation Deformations

Article (See Note)	Title	Relates to
10.6.2.2	Tolerable Movements	Spread footings
10.6.2.5	Overall Stability	Spread footings
10.7.2.2	Tolerable Movements	Driven piles
10.7.2.4	Horizontal Pile Foundation Movement	Driven piles
C10.7.2.5	Commentary to "Settlement due to Downdrag"	Driven piles
10.8.2.1	Service Limit State	Drilled shafts
10.8.2.2.1	General	Drilled shafts
10.8.2.3	Horizontal Movements of Shafts and Shaft Groups	Drilled shafts
10.9.2.2	Tolerable Movements	Micropiles
10.9.2.4	Horizontal Micropile Foundation Movement	Micropiles
C11.10.11	Commentary to "MSE Abutments"	MSE Walls
14.5.2.1	Number of Joints	Joints and Bearings
Note: Article 10.5.2 or its sub-articles is frequently referenced in the articles noted in the first column and their corresponding commentary portion. In this table, the article number is based on the first occurrence of the reference to Article 10.5.2.		

References

AASHTO LRFD (2012) "AASHTO LRFD Bridge Design Specifications," Customary U.S. Units, 6th Edition, American Association of State Highway Transportation Officials, Washington, DC

ASCE (2013) "Structural Identification of Constructed Systems Approaches: Methods, and Technologies for Effective Practice of St-Id," ASCE Report, Edited by F.N. Çatbas, T. Kijewski-Correa, and A.E. Aktan, Reston, VA

Arizona Department of Transportation (ADOT) Bridge Design Guidelines (2009): http://www.azdot.gov/Highways/bridge/Guidelines/DesignGuidelines/index.asp

Strand7 Pty Ltd. (2012). Using Strand 7 - Introduction to the Strand7 Finite Element Analysis System. Edition 4, Australia.

MacQueen, J.B. (1967) "Some methods for classification and analysis of multivariate observations," Proceedings of 5-th Berkeley Symposium on Mathematical Statistics and Probability, Berkeley, University of California Press, pp 281-297

Moulton, L. K., GangaRao, H. V. S. and G. T. Halvorsen (1985). *Tolerable Movement Criteria for Highway Bridges,* Report No. FHWA RD-85-107, Federal Highway Administration, U.S. Department of Transportation, Washington, D.C.

NCHRP (1983). *Shallow Foundations for Highway Structures - NCHRP Report 107*, Author: H. E. Wahls, Transportation Research Board, National Research Council, Washington, D.C.

Samtani, N.C, and Nowatzi, E.A. (2006). *Soils and Foundations – Volumes I and II*, Report No., FHWA-NHI-06-088 and FHWA-NHI-06-089, Federal Highway Administration, U.S. Department of Transportation, Washington, D.C.

Samtani, N. C., Nowatzki, E. A. and D. R. Mertz (2010). "*Selection of Spread Footings on Soils to Support Highway Bridge Structures*." Publication No. FHWA RC/TD-10-001, Federal Highway Administration – Resource Center, Matteson, IL.

Smith, I.F.C., and Saitta, S. (2008). "Improving Knowledge of Structural System Behavior through Multiple Models." Journal of Structural Engineering, 134(4), 553-561.

Wang, J. and M. Ghosn (2006) “Hybrid Data Mining/Genetic Shredding Algorithm for Reliability Assessment of Structural Systems,” ASCE Journal of Structural Engineering, Vol. 132, No. 9

WSDOT (2010). Geotechnical Design Manual M 46-3.07. Chapter 8, Table 8-4, http://www.wsdot.wa.gov/Publications/Manuals/M46-03.htm

White, D.W., D. Coletti, B.W. Chavel, A. Sanchez, C. Ozgur, J. Chong, R.T. Leon, R. Medlock, R. Cisneros, T. Galambos, J. Yadlosky, W. Gatti, and G. Kowatch (2012) “Guidelines for Analytical Methods and Erection Engineering of Curved and Skewed Steel Deck-Girder Bridges,” Final Report, NCHRP Project 12-79

AASHTO LRFD Bridge Design Specifications, Customary U.S. Units (6th Edition) with 2012 and 2013 Interim Revisions; and 2012 Errata. American Association of State Highway and Transportation Officials (AASHTO), Washington, D.C.

Grant, R., Christian, J. T., and Vanmarcke, R. H. “Differential Settlement of Buildings”, Journal of Geotechnical Division, ASCE, Vol. 100, No. GT9, 1974, pp. 973-991.

Moulton, L. K., GangaRao, H. V. S. and G. T. Halvorsen (1985). Tolerable Movement Criteria for Highway Bridges, Report No. FHWA RD-85-107, Federal Highway Administration, U.S. Department of Transportation, Washington, D.C.

NCHRP (1983). Shallow Foundations for Highway Structures - NCHRP Report 107, Author: H. E. Wahls, Transportation Research Board, National Research Council, Washington, D.C.

Pennsylvania Department of Transportation (PennDOT) Structures Design Manual (2012): ftp://ftp.dot.state.pa.us/public/PubsForms/Publications/PUB%2015M.pdf

Samtani, N.C, and Nowatzi, E.A. (2006). Soils and Foundations – Volumes I and II, Report No., FHWA-NHI-06-088 and FHWA-NHI-06-089, Federal Highway Administration, U.S. Department of Transportation, Washington, D.C.

Samtani, N. C., Nowatzki, E. A. and D. R. Mertz (2010). “Selection of Spread Footings on Soils to Support Highway Bridge Structures.” Publication No. FHWA RC/TD-10-001, Federal Highway Administration – Resource Center, Matteson, IL.

Skempton, A. W., and MacDonald, D. H. (1956). “Allowable Settlement of Buildings,” Proceedings, Institution of Civil Engineers, Part III, Col 5, London, U.K., 1956

Appendices

A Model Discretization

A.1 Model Forms

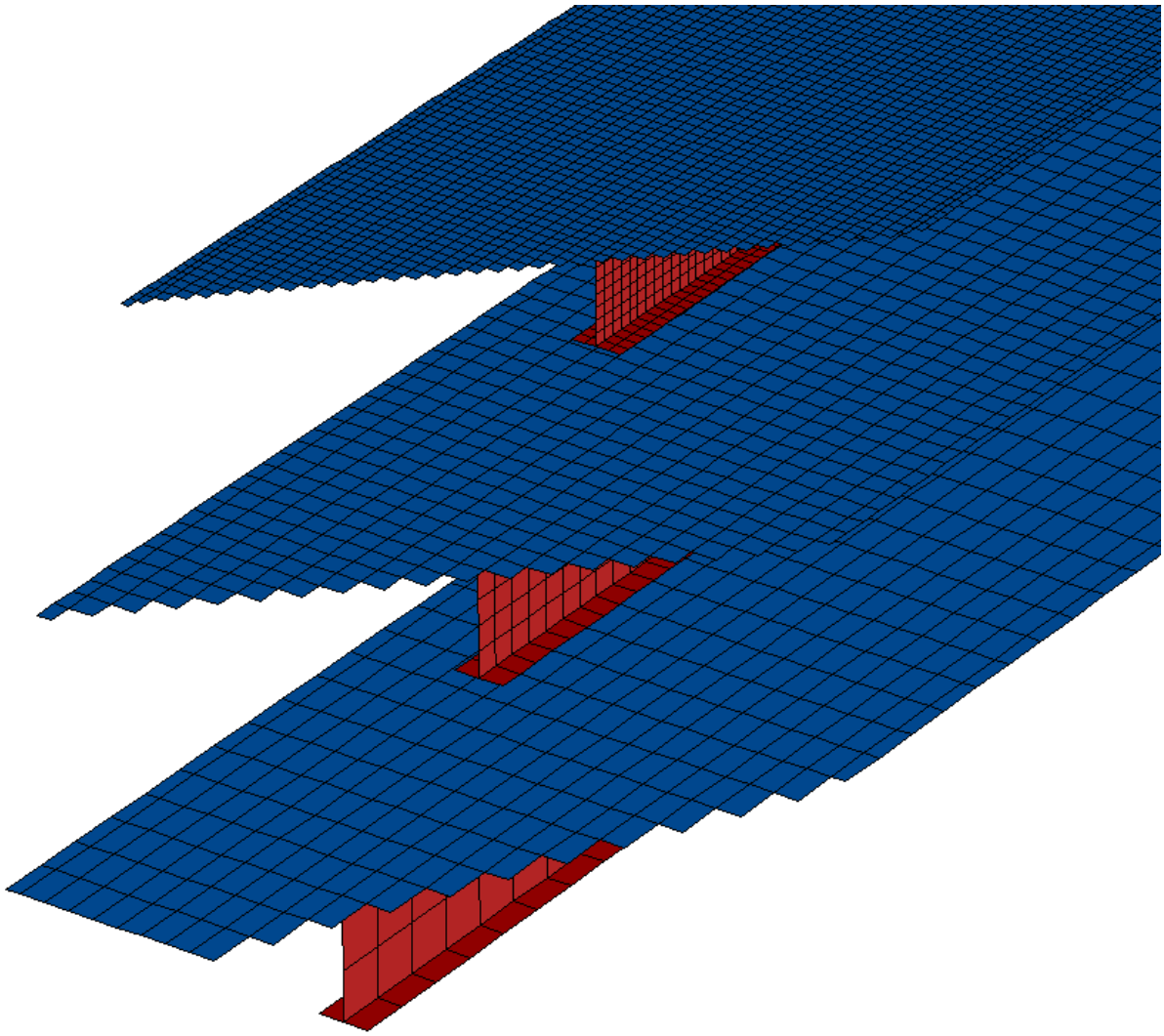

Figure A-1. Shell Element Discretization for Single Girder Model

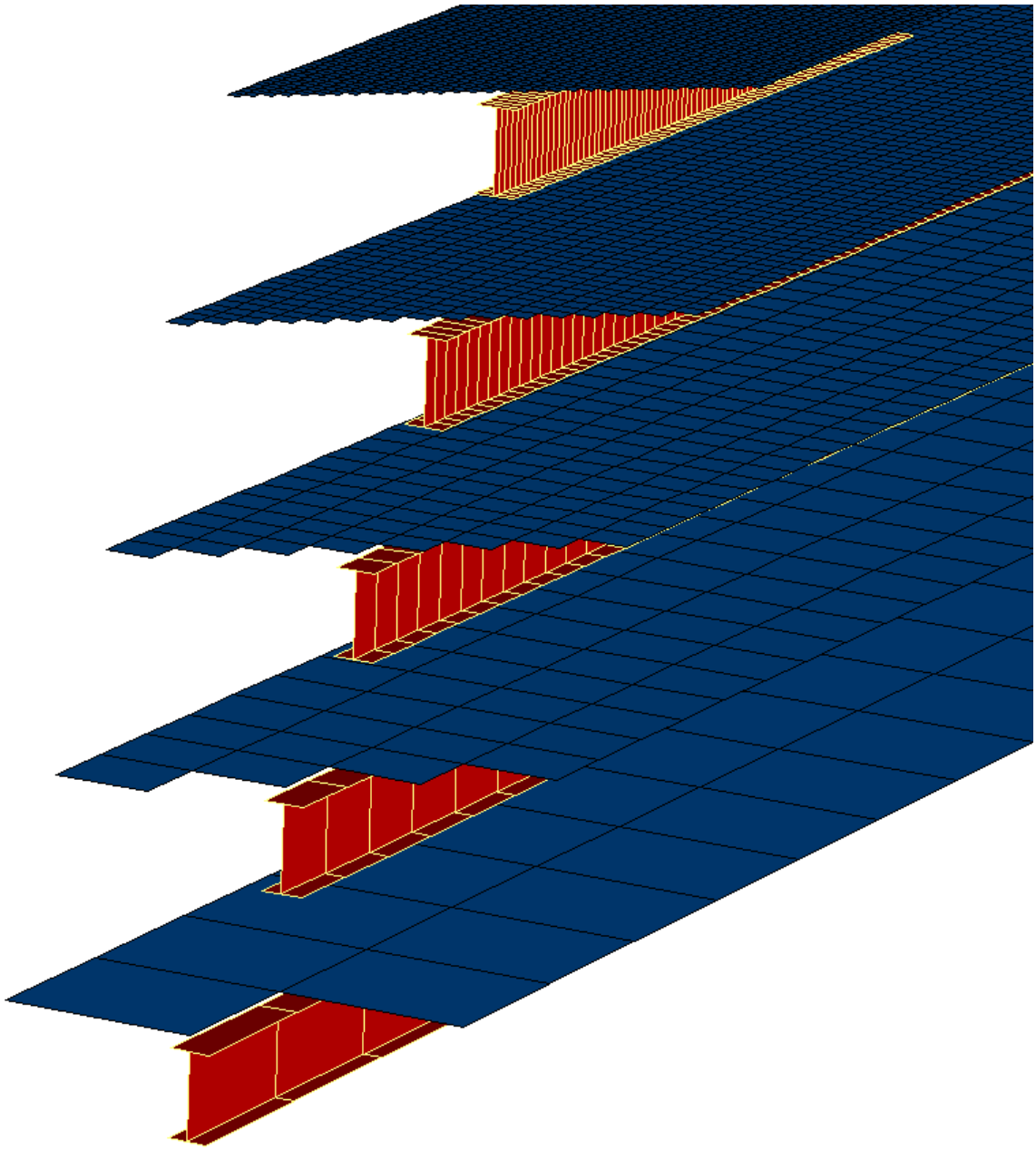

Figure A-2 - Beam Element Discretization for Dingle Girder Model

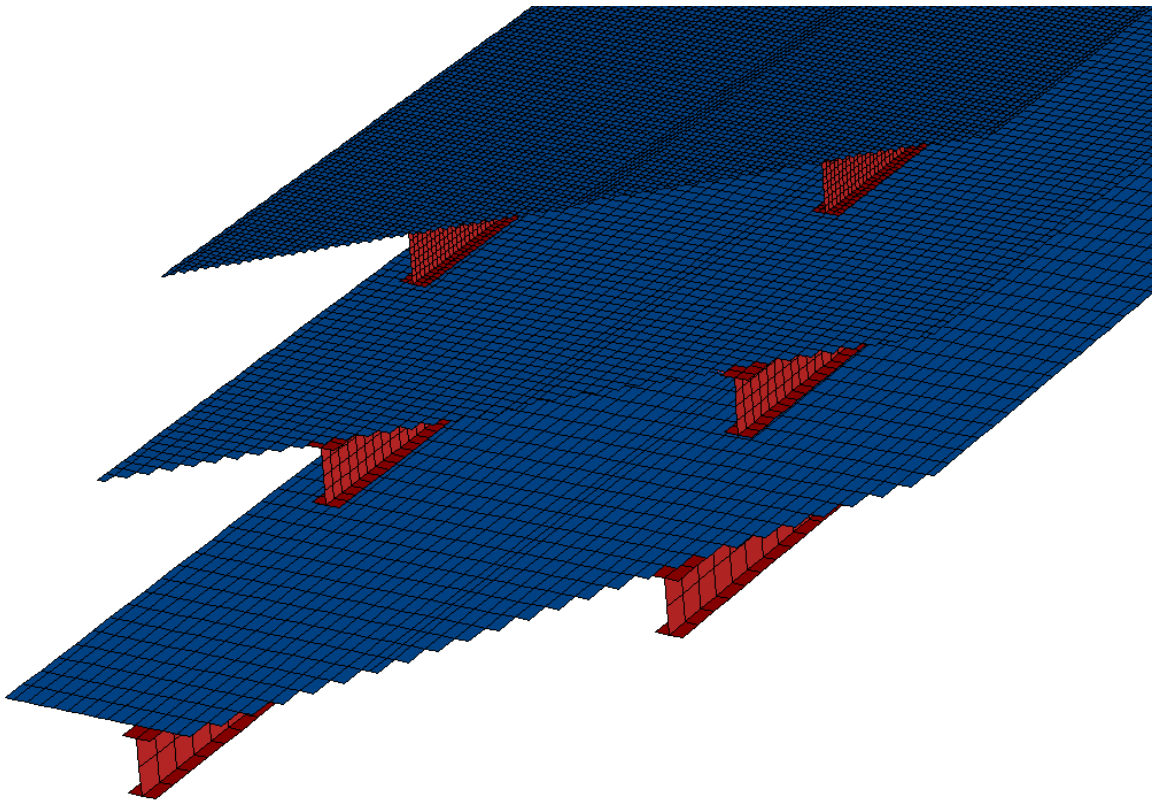

Figure A-3 - Shell Element Discretization for Two Girder Model

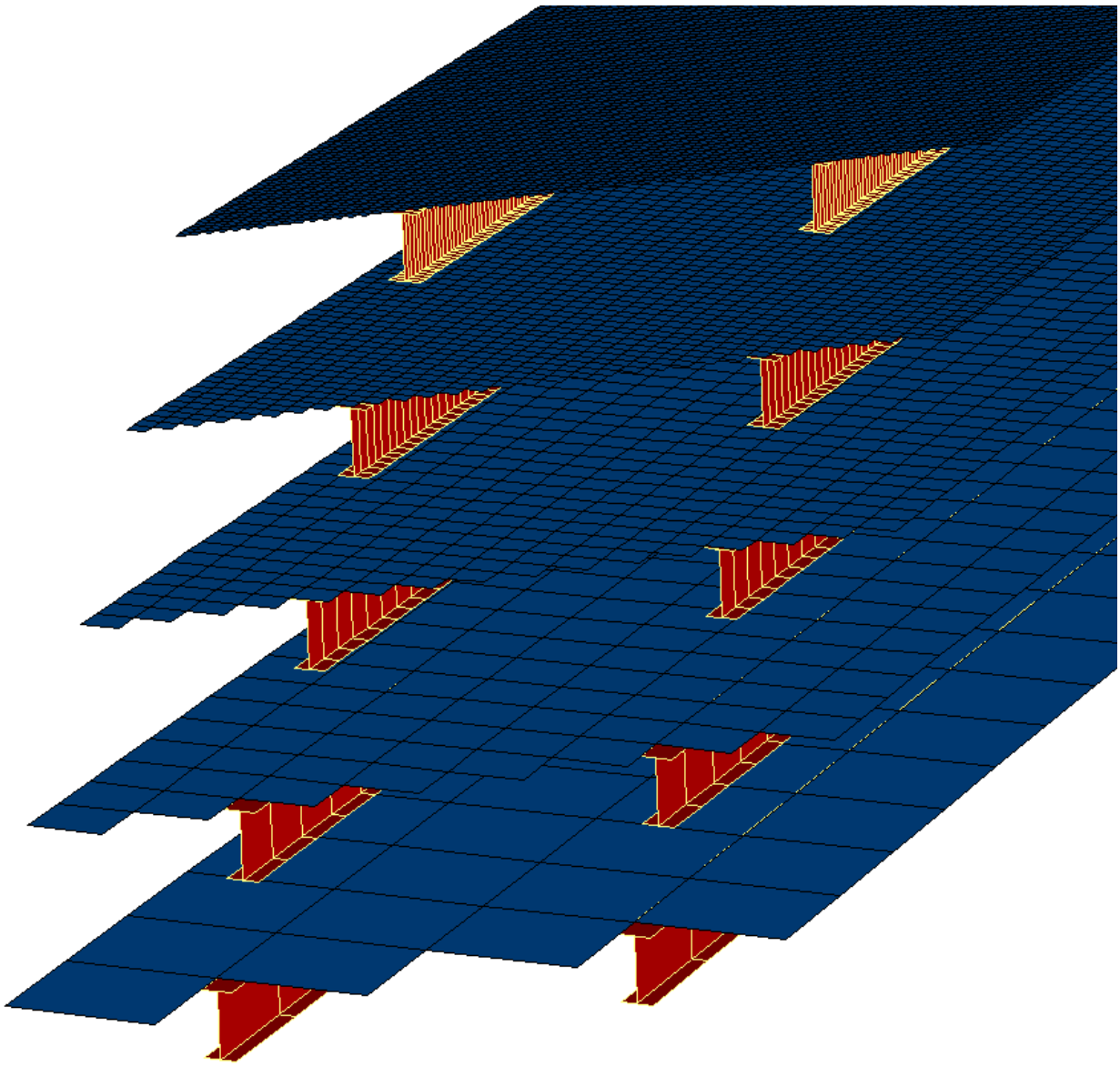

Figure A-4 - Beam Element Discretization for Two Girder Model

A.2 Shear and Mesh Size Dependency

A.2.1 Member Actions

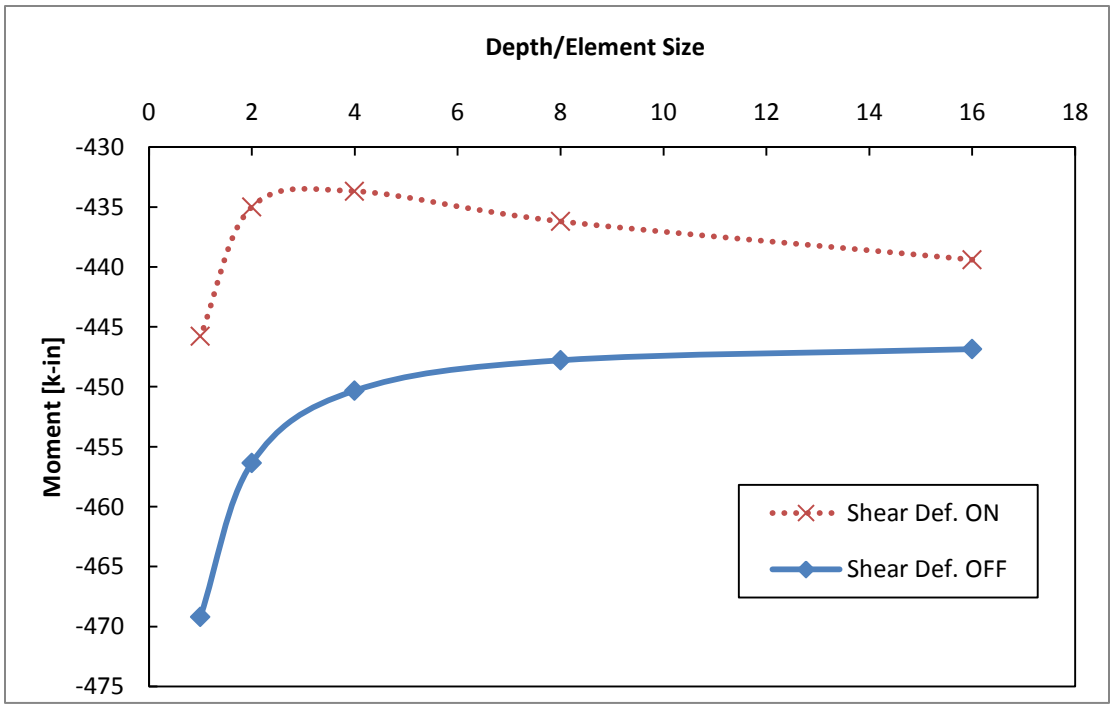

Figure A-5 - Effect of Element Size on Maximum Bending Moment under a Vertical Settlement in Single Girder Beam Element Model

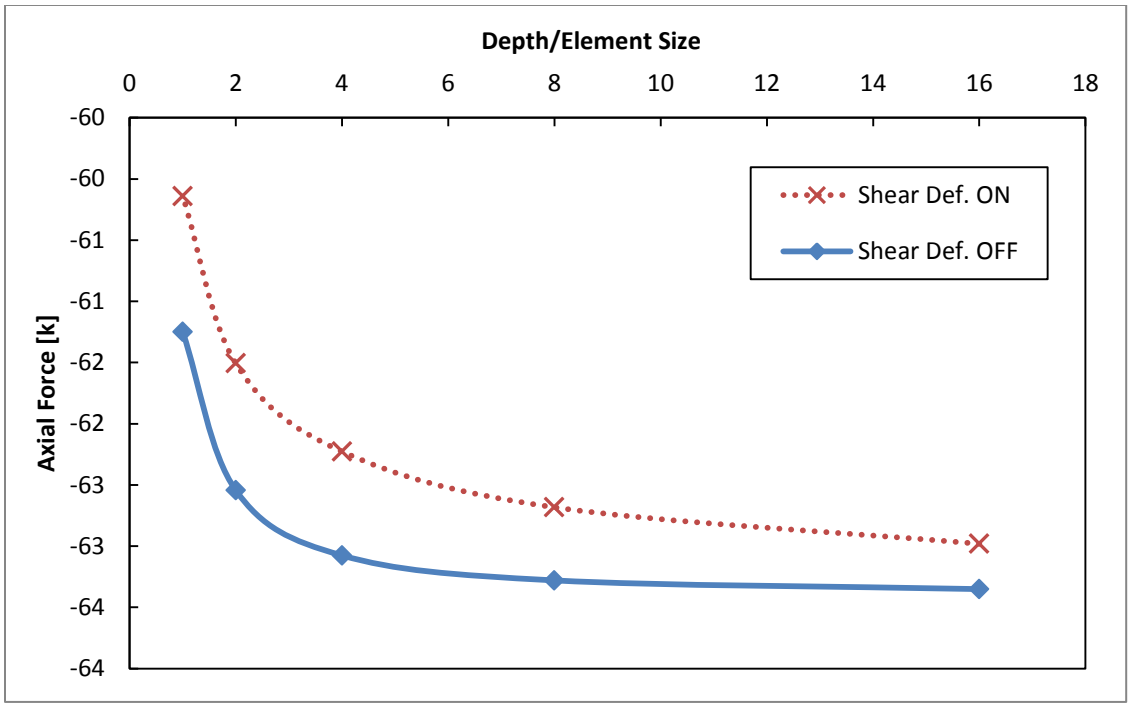

Figure A-6 - Effect of Element Size on Maximum Axial Force under a Vertical Settlement in Single Girder Beam Element Model

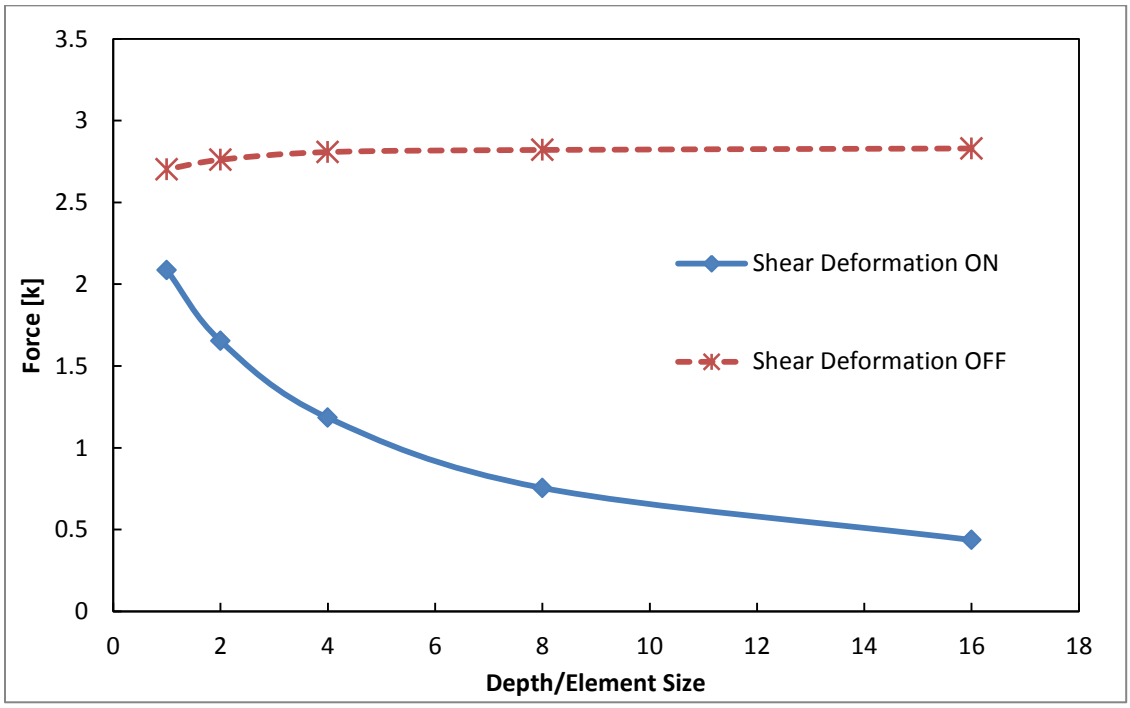

Figure A-7 - Effect of Element Size on Shear under a Vertical Settlement in Two Girder Beam Element Model

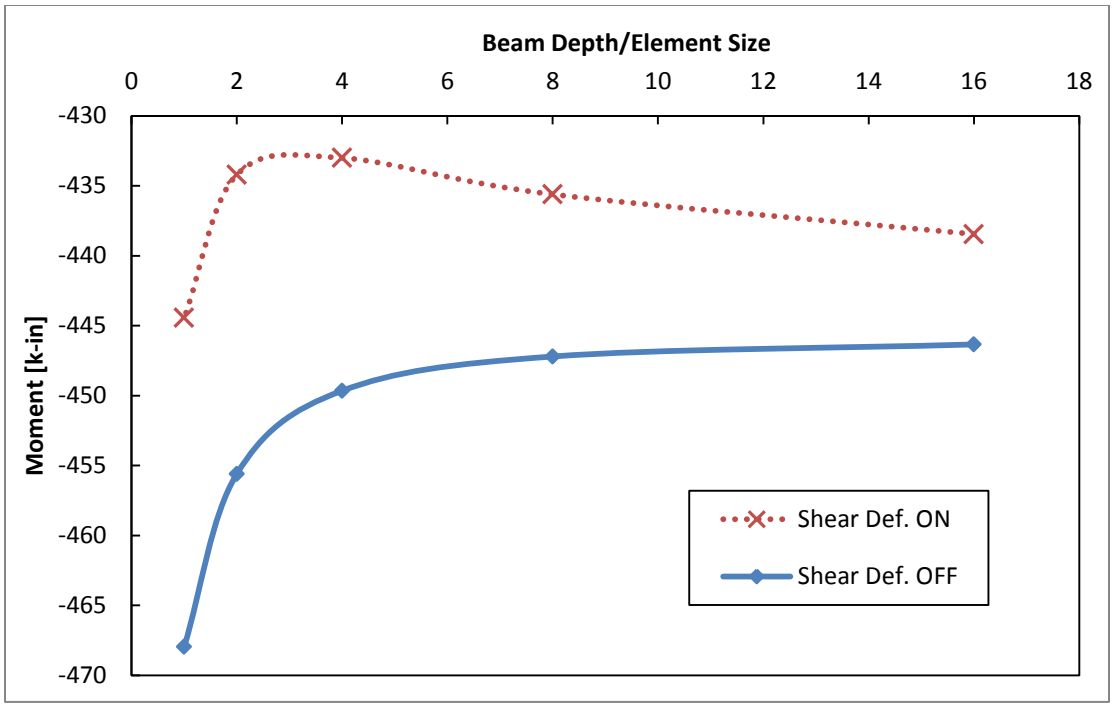

Figure A-8 - Effect of Element Size on Maximum Bending Moment under a Vertical Settlement in Two-Girder Beam Element Model

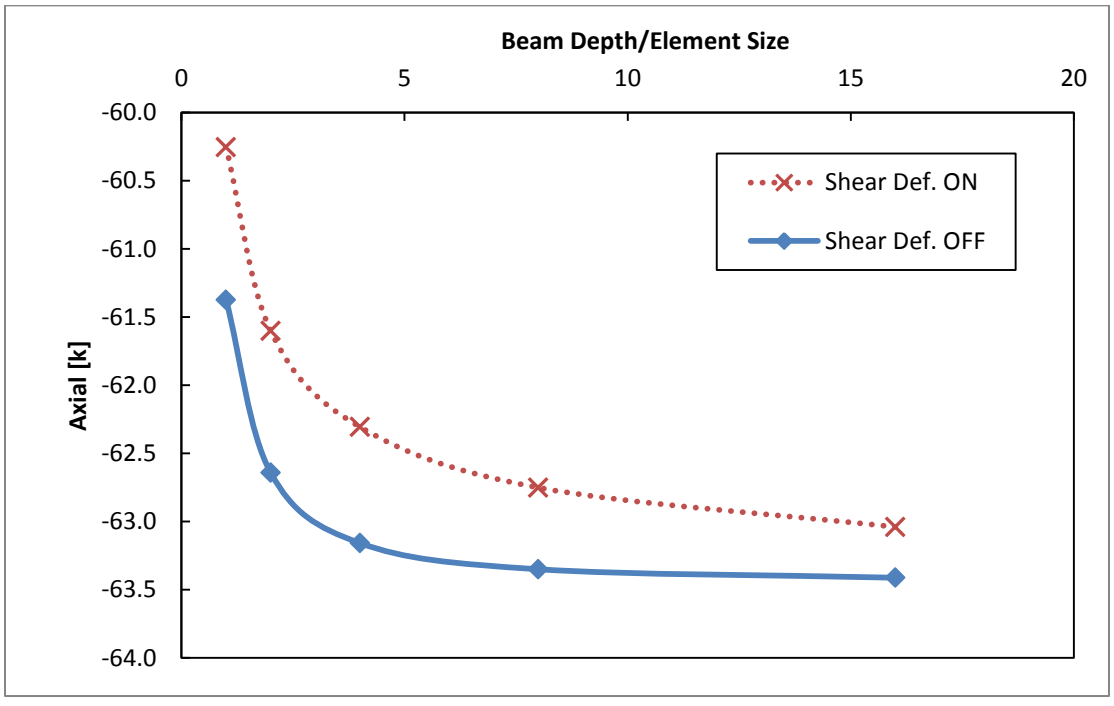

Figure A-9 - Effect of Element Size on Maximum Axial Force under a Vertical Settlement in Two-Girder Beam Element Model

A.2.2 Total Fiber Stress

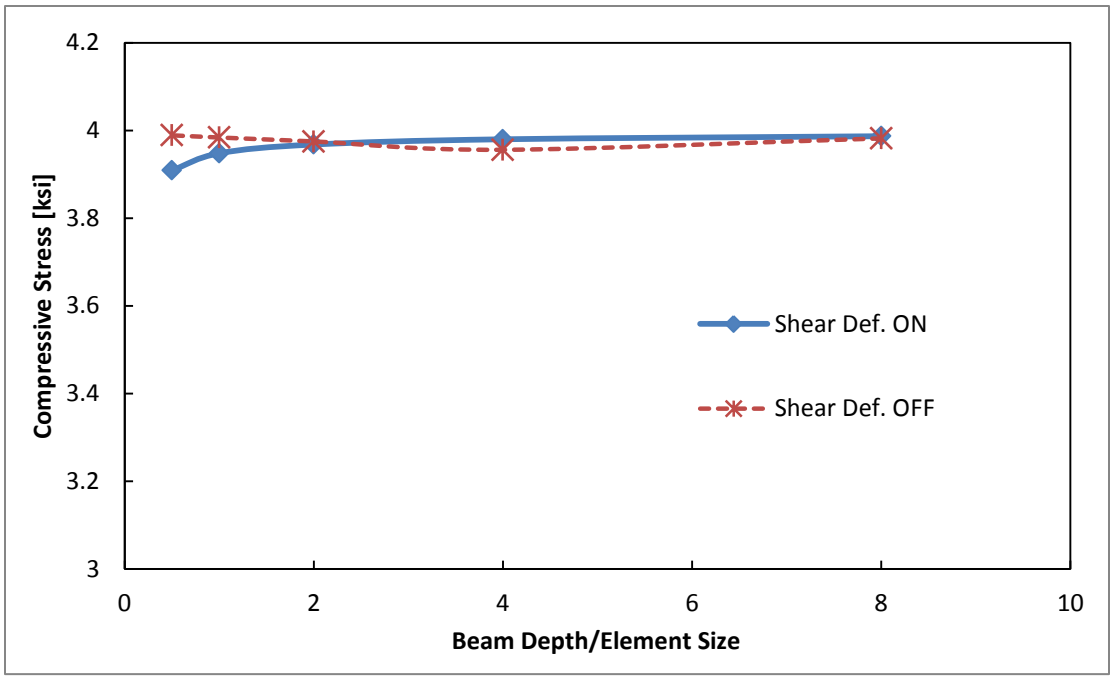

Figure A-10 - Effect of Element Size on Maximum Total Fiber Stress in Compression under a Vertical Settlement in Single Girder Beam Element Model

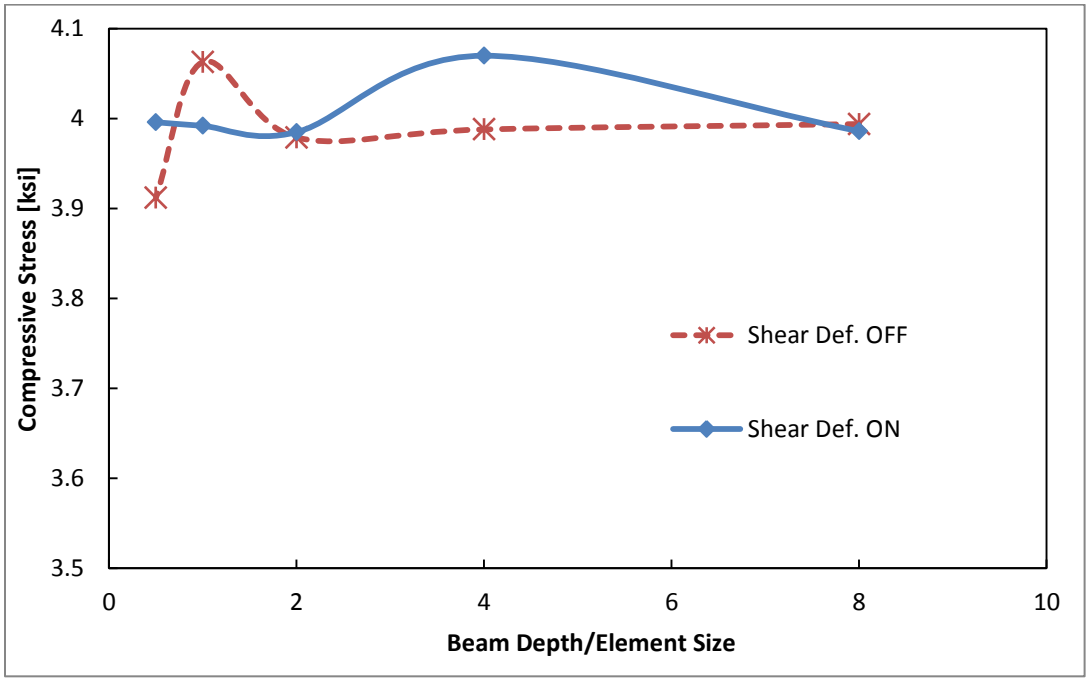

Figure A-11 - Effect of Element Size on Maximum Total Fiber Stress in Compression under a Vertical Settlement in Two Girder Beam Element Model

A.2.3 Support Reaction

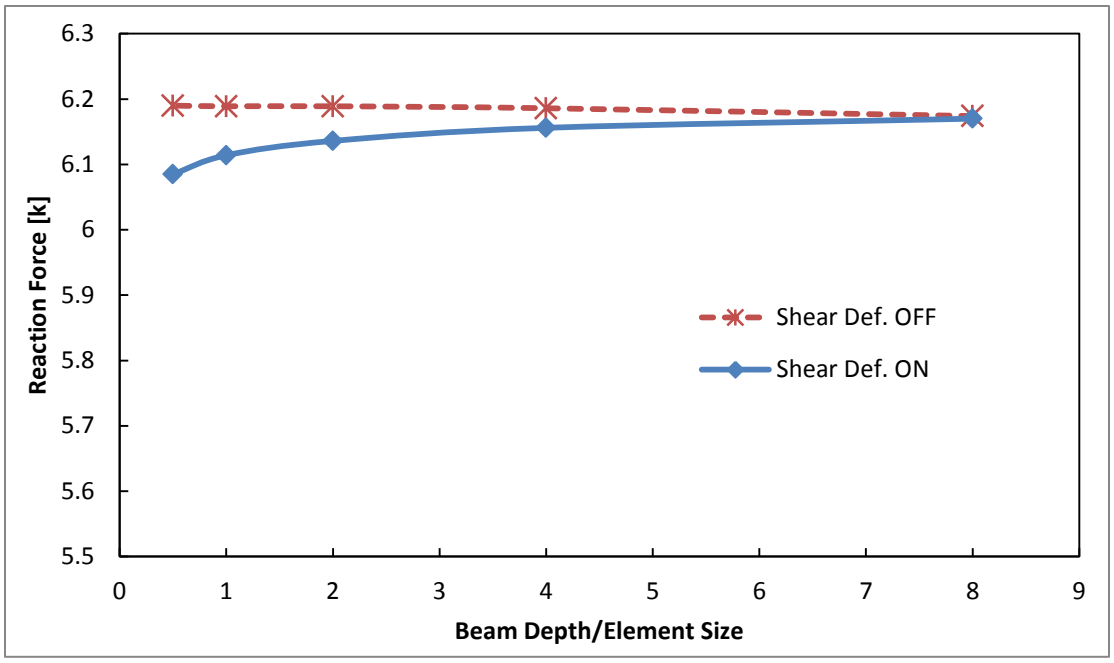

Figure A-12 - Effect of Element Size on Maximum Reaction under a Vertical Settlement in Single Girder Beam Element Model

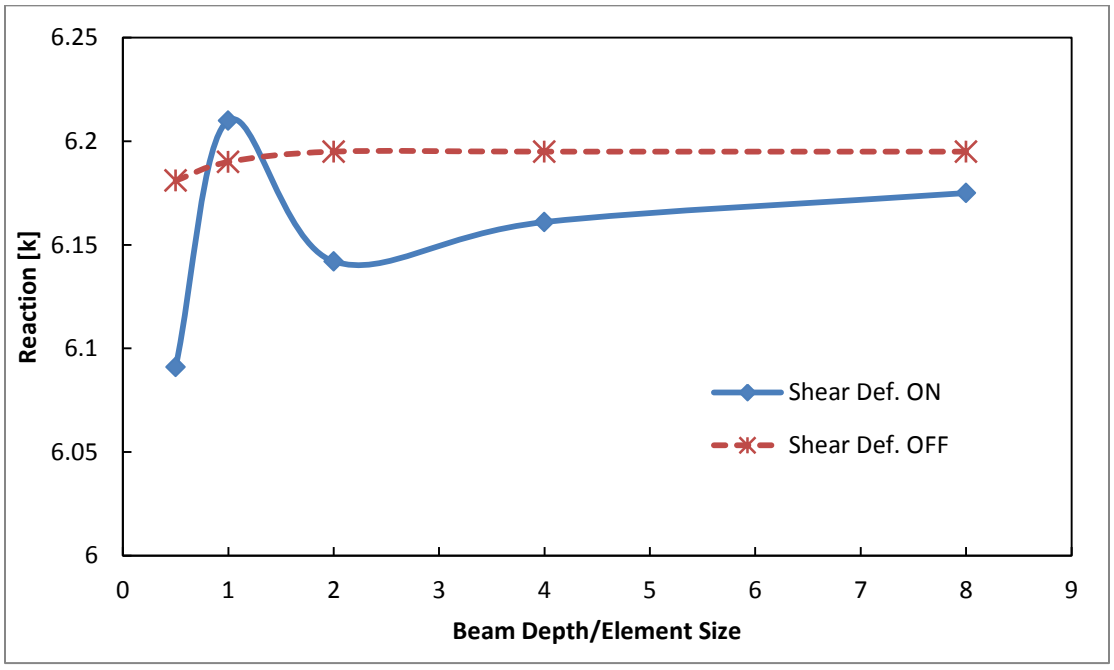

Figure A-13 - Effect of Element Size on Maximum Reaction under a Vertical Settlement in Two Girder Beam Element Model

A.2.4 Vertical Displacement

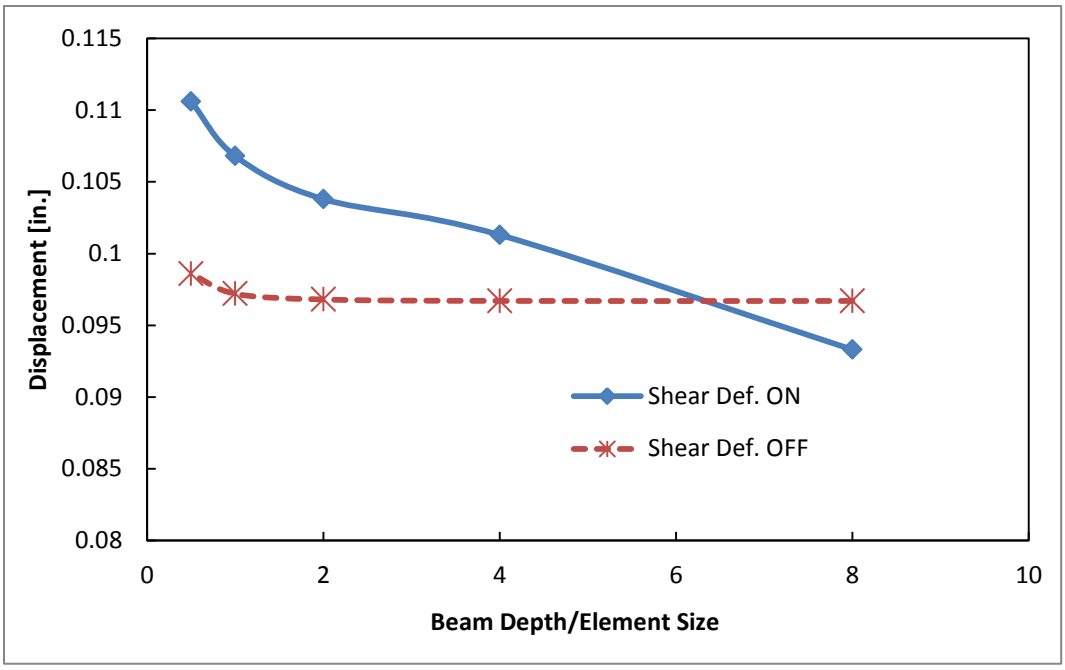

Figure A-14 - Effect of Element Size on Maximum Vertical Displacement in Single Girder Beam Element Model under Dead Load

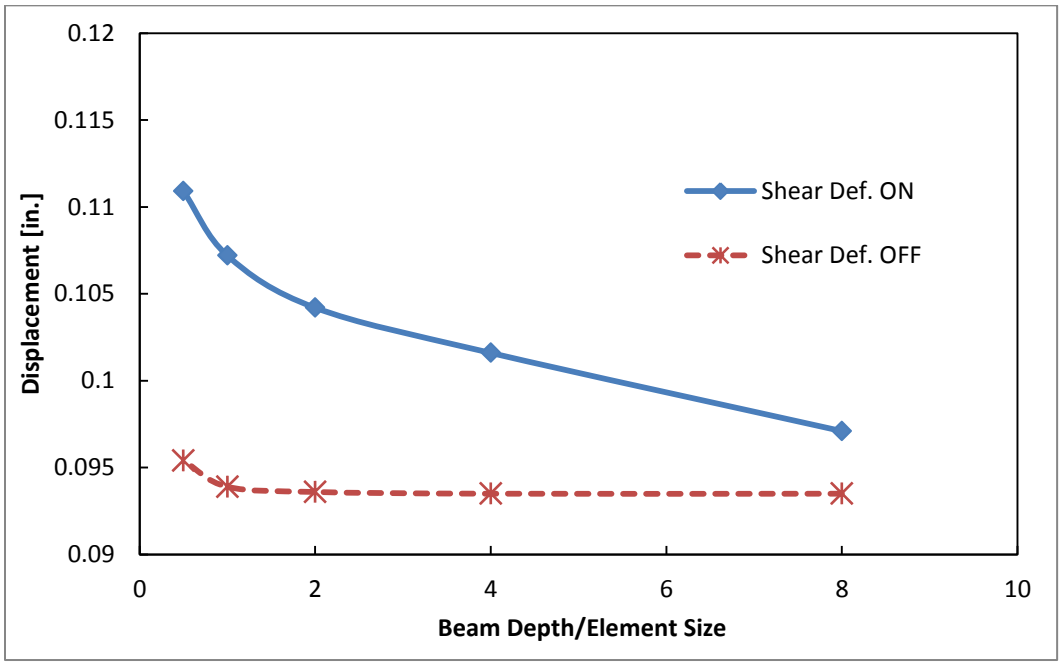

Figure A-15 - Effect of Element Size on Maximum Vertical Displacement under Dead Load in Two Girder Beam Element Model

A.2.5 Deck Stress

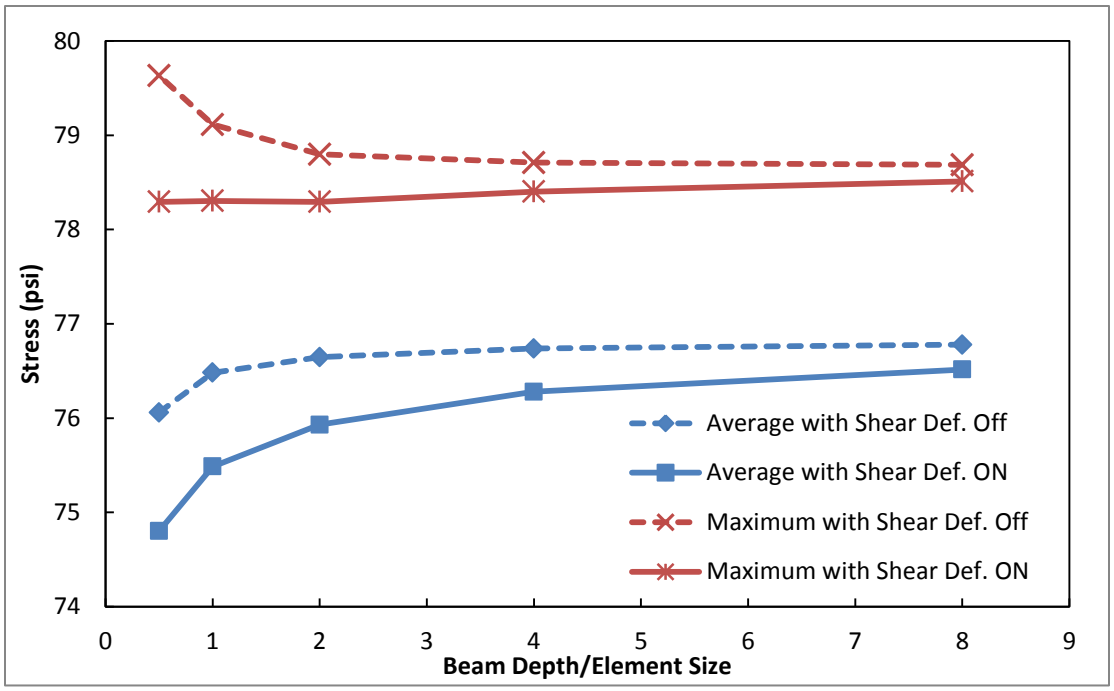

Figure A-16 - Effect of Element Size on Deck Stress under a Vertical Settlement in Two Girder Beam Element Model

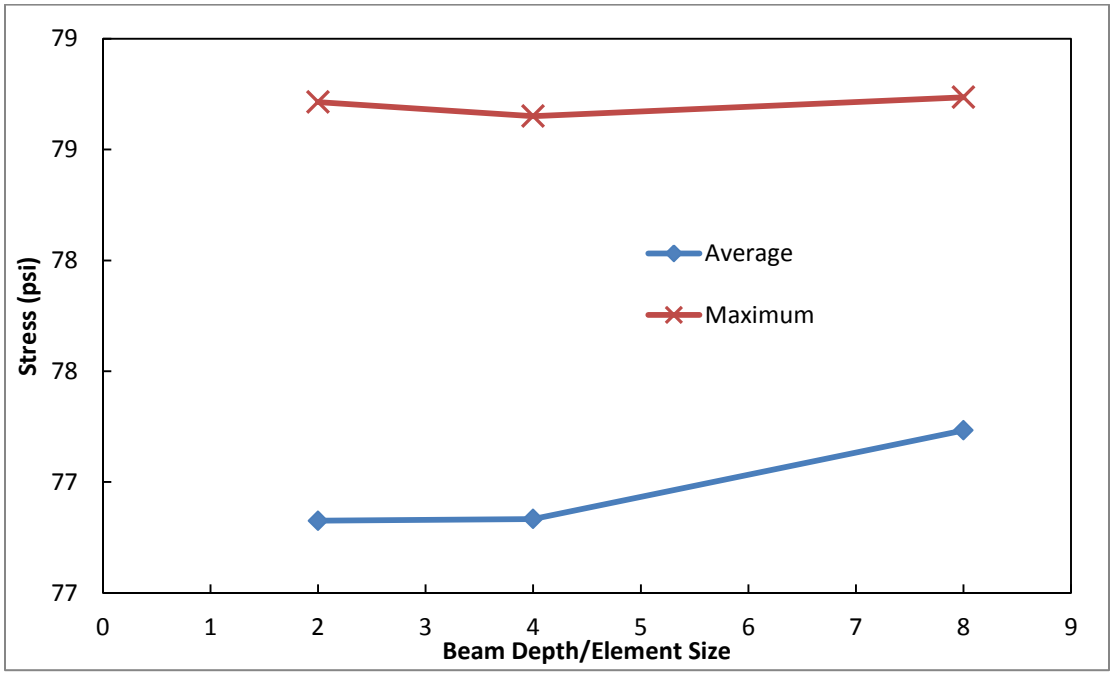

Figure A-17 - Effect of Element Size on Deck Stress under a Vertical Settlement in Two Girder Shell Element Model

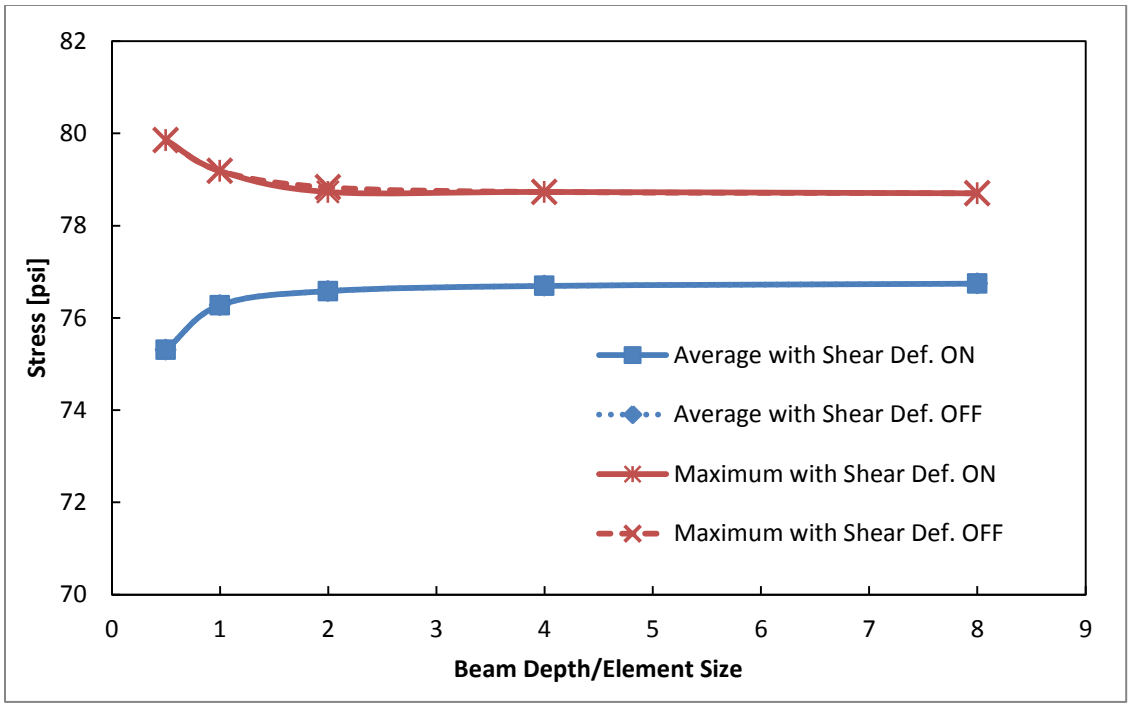

Figure A-18 - Effect of Element Size on Deck Stress under a Vertical Settlement in Single Girder Beam Element Model

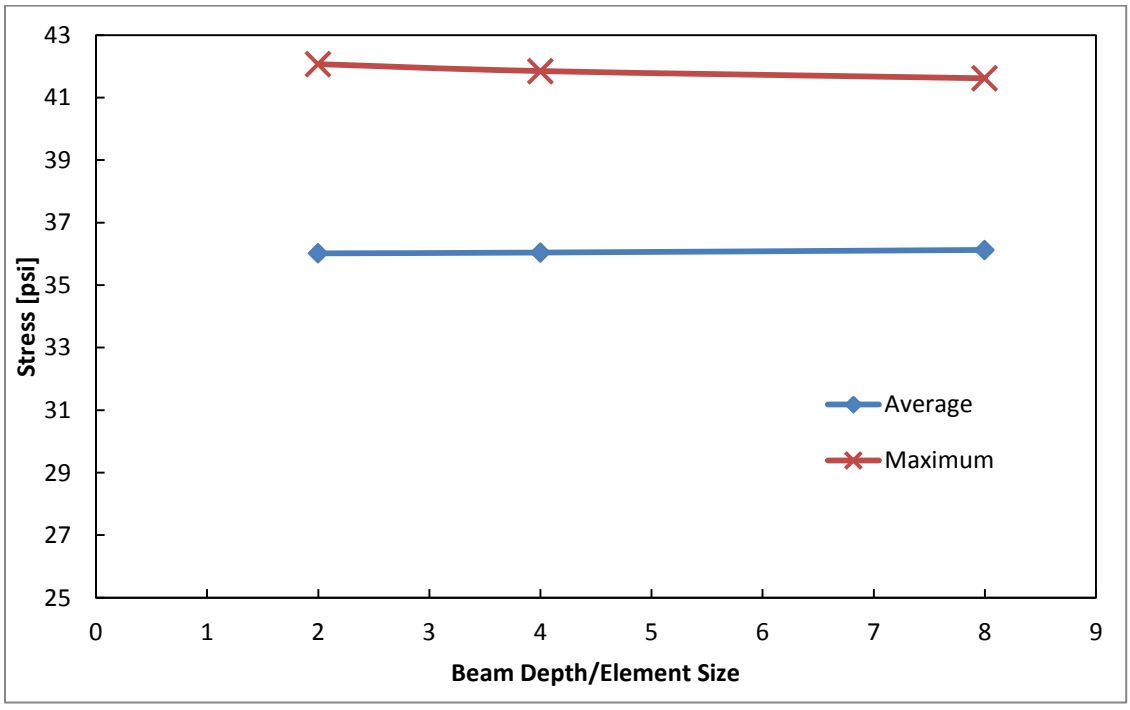

Figure A-19 - Effect of Element Size on Deck Stress under a Vertical Settlement in Single Girder Shell Element Model

B Full Scale Bridge Model Discretization Study

B.1 Dead Load Reponses

B.1.1 Moment Over Center Pier

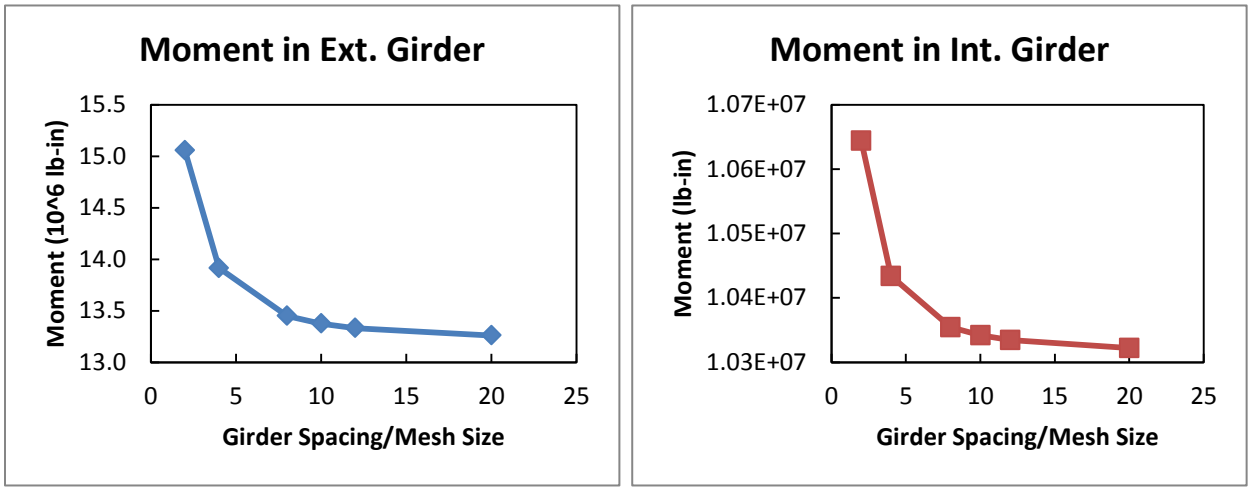

Figure B-1 – Effect of Mesh Size on Moment

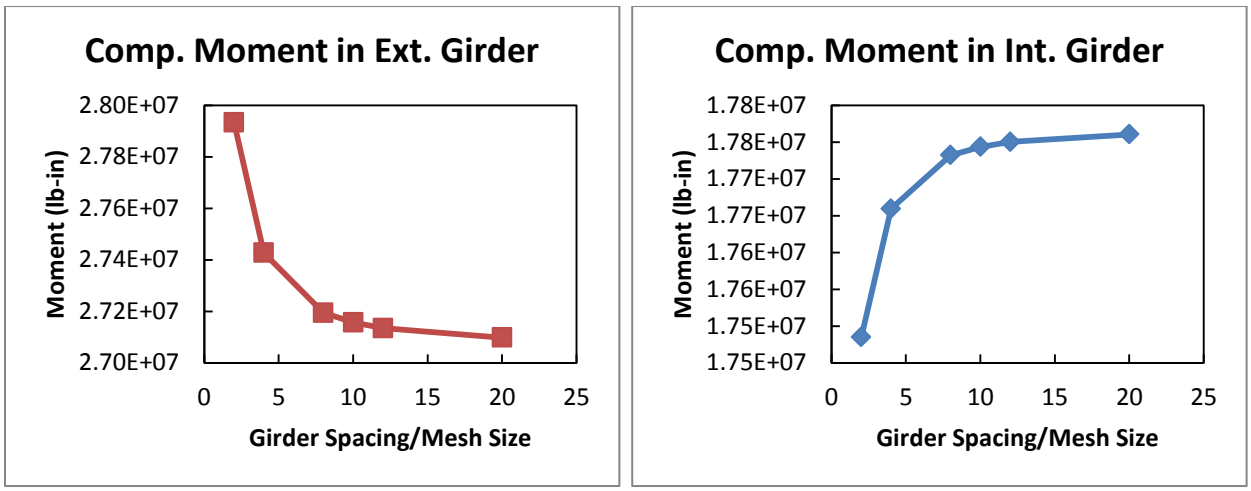

Figure B-2 - Effect of Mesh Size on Composite Moment

B.1.2 Axial Force over Center Pier

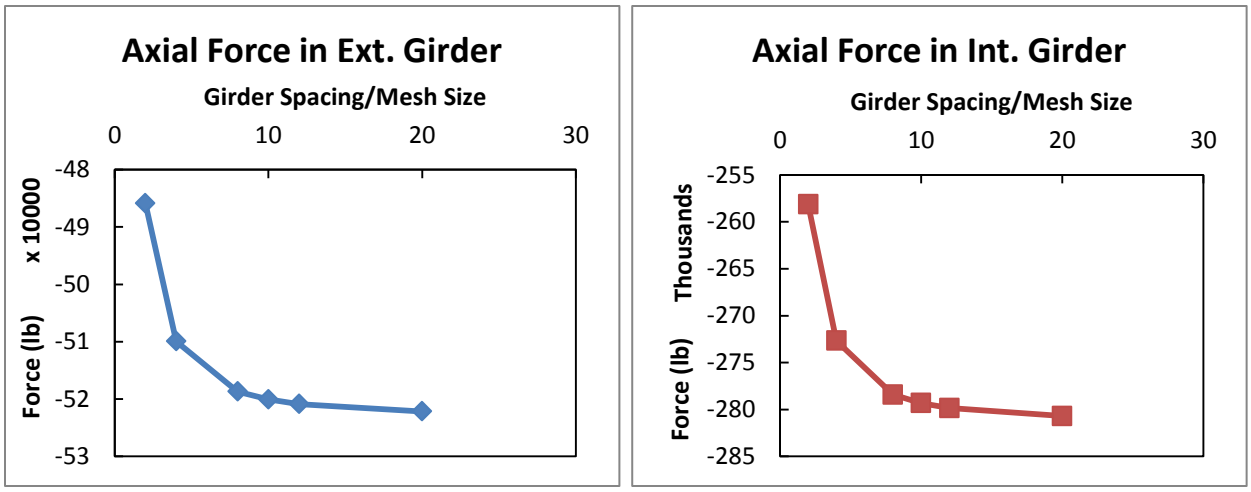

Figure B-3 - Effect of Mesh Size on Axial Force

B.1.3 Reaction at Abutment for Specified Girders

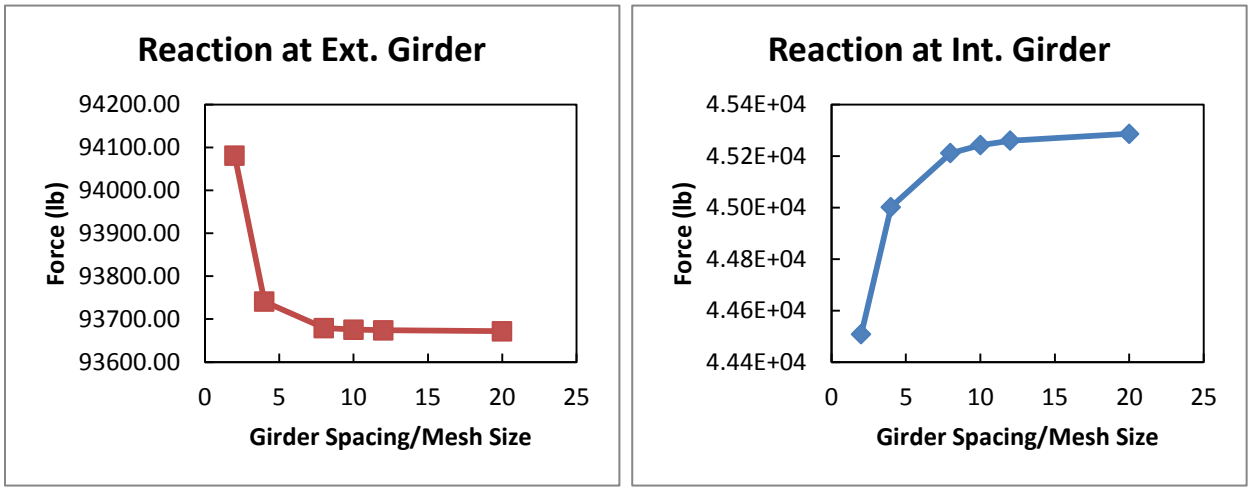

Figure B-4 - Effect of Mesh Size on Vertical Reactions

B.2 Point Load Responses

B.2.1 Moment at Applied Point Load

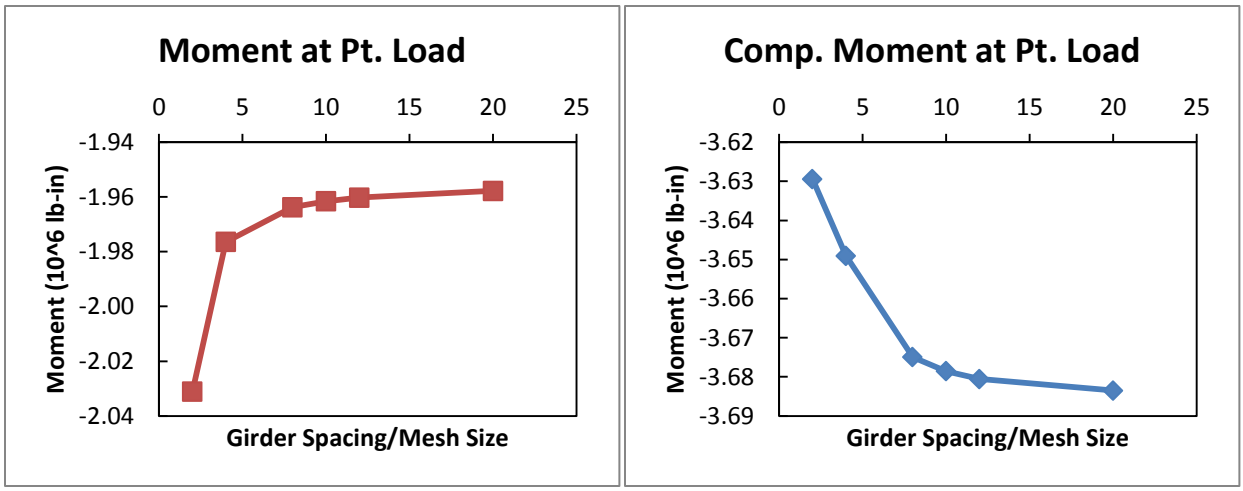

Figure B-5 - Effect of Mesh Size on Moment

B.2.2 Axial Force at Applied Point Load

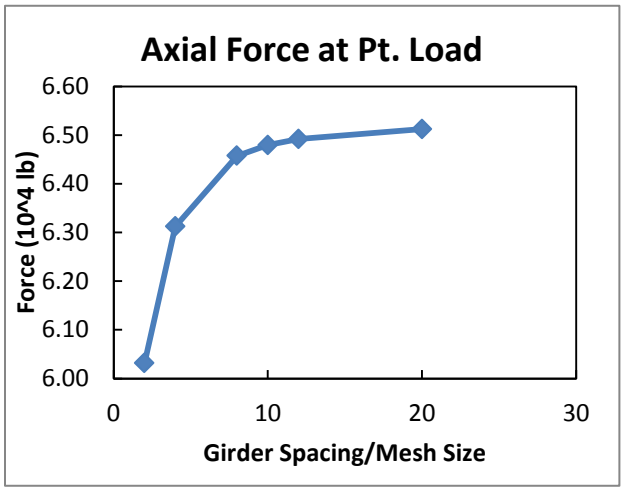

Figure B-6 - Effect of Mesh Size on Axial Force

B.2.3 Reaction at Abutment for Girder on which Point Load Was Applied

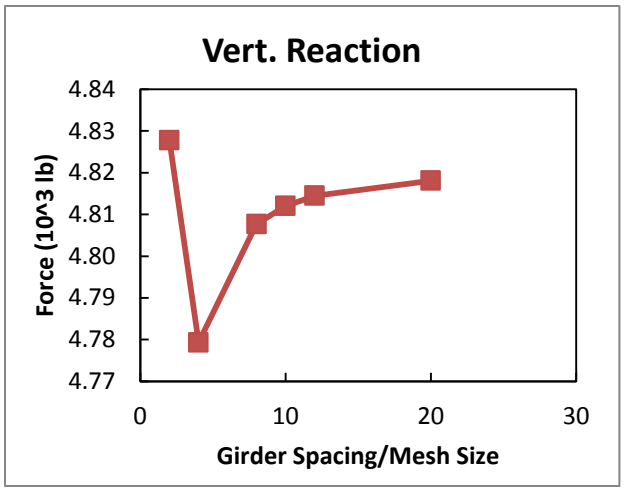

Figure B-7 - Effect of Mesh Size on Vertical Reaction

B.3 Settlement Response

B.3.1 Moment Over Center Pier

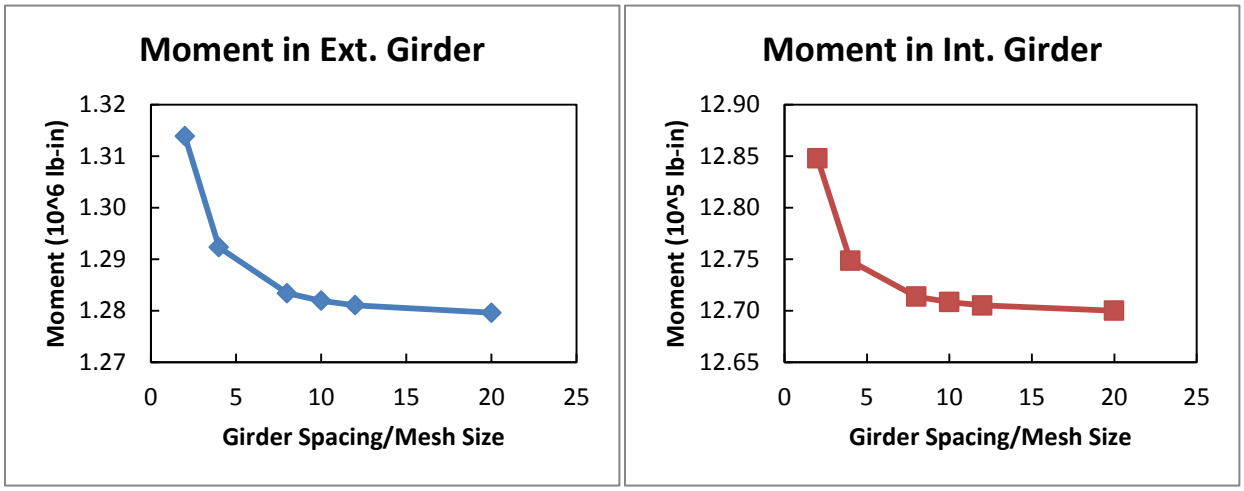

Figure B-8 - Effect of Mesh Size on Moment

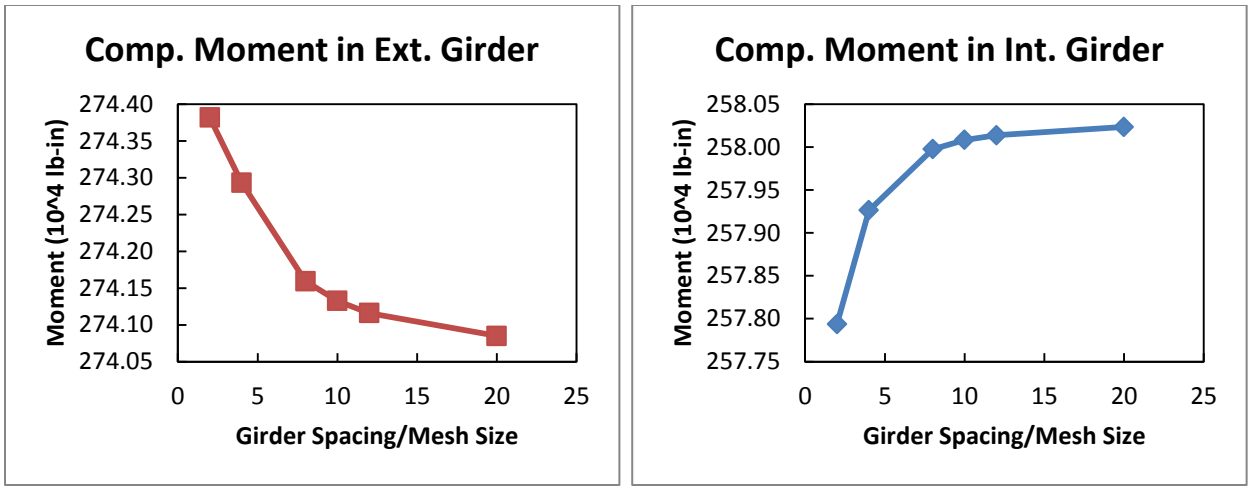

Figure B-9 - Effect of Mesh Size on Composite Moment

B.3.2 Axial Force Over Center Pier

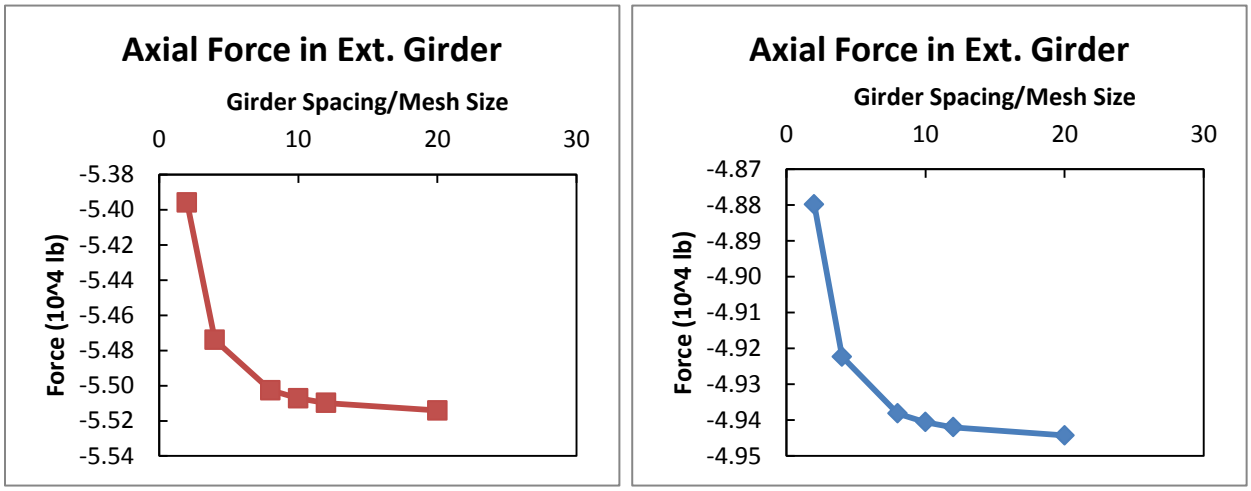

Figure B-10 - Effect of Mesh Size on Axial Force

B.3.3 Vertical Reaction at Abutment for Specified Girders

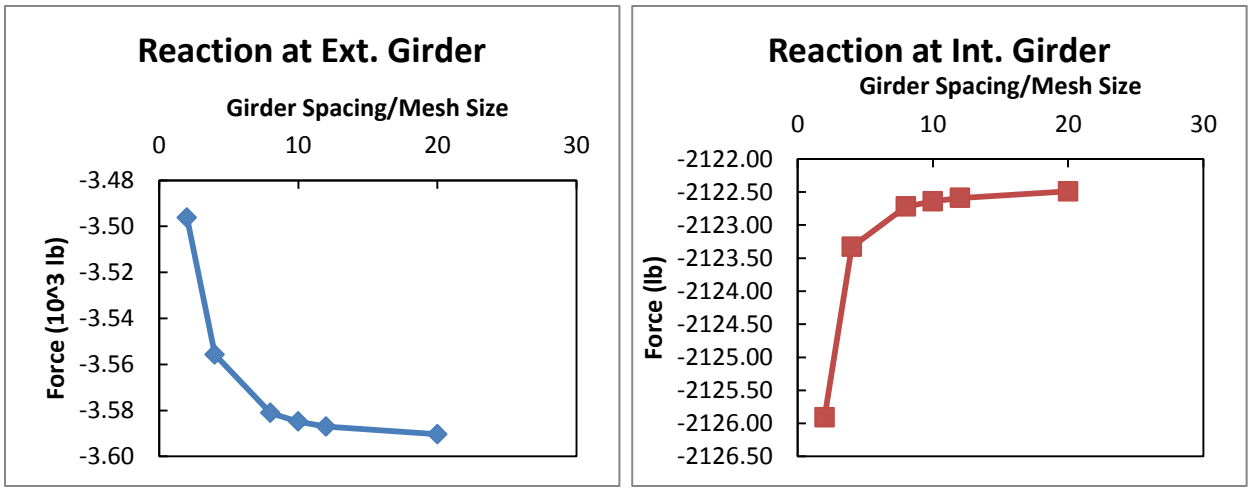

Figure B-11 - Effect of Mesh Size on Vertical Reactions

C Box Girder Study

C.1 Vertical Reactions

C.1.1 Reaction Forces across Bridge Width for all Models

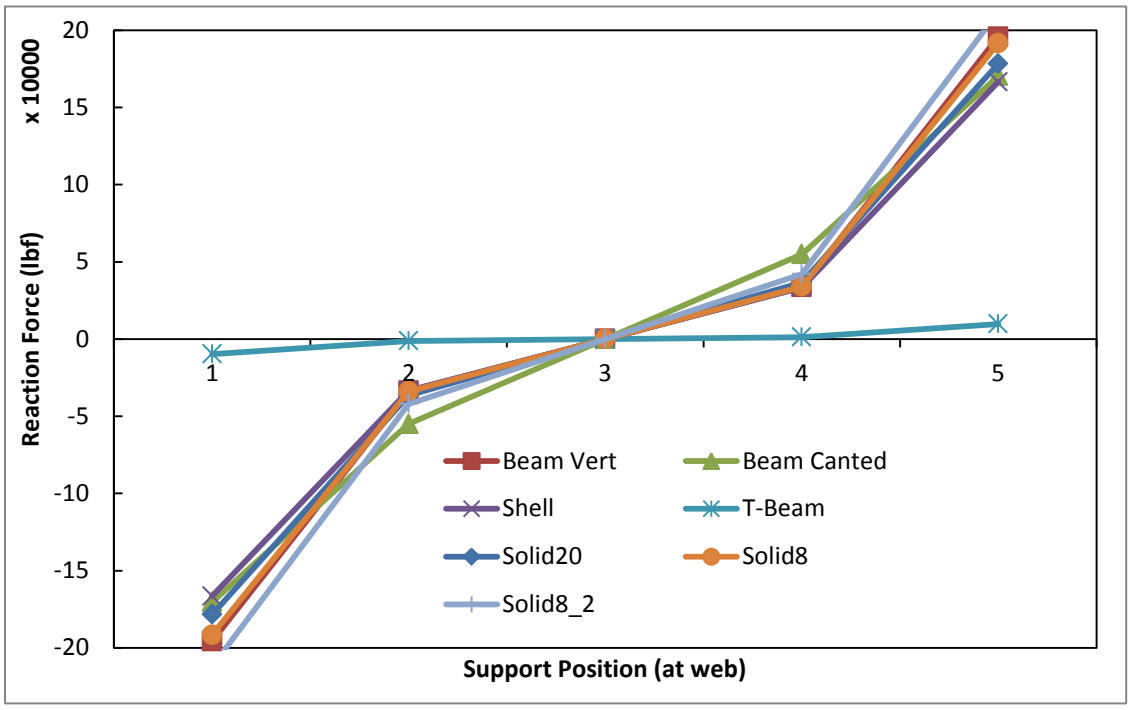

Figure C-1 – Effect of FE Model Type on Reactions

D Single Degree-of-Freedom Study

D.1 Total Composite Section Stress

D.1.1 Non-Structural Element Stiffness On

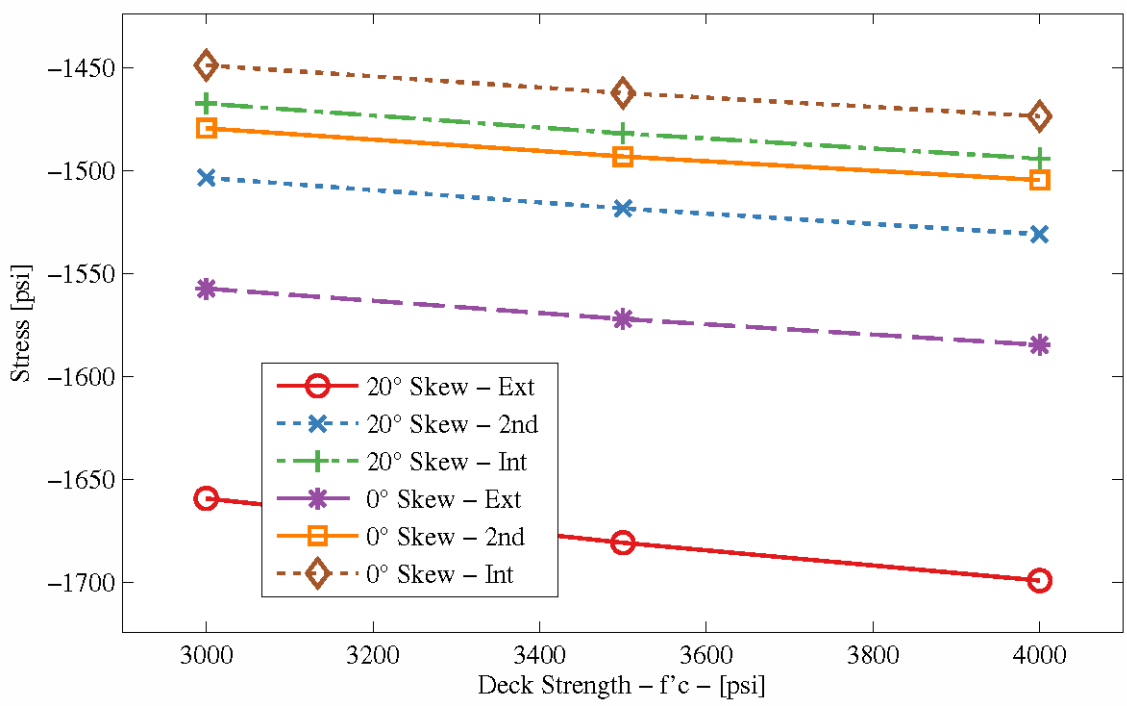

Figure D-1 - Effect of Deck Strength on Total Composite Section Stress

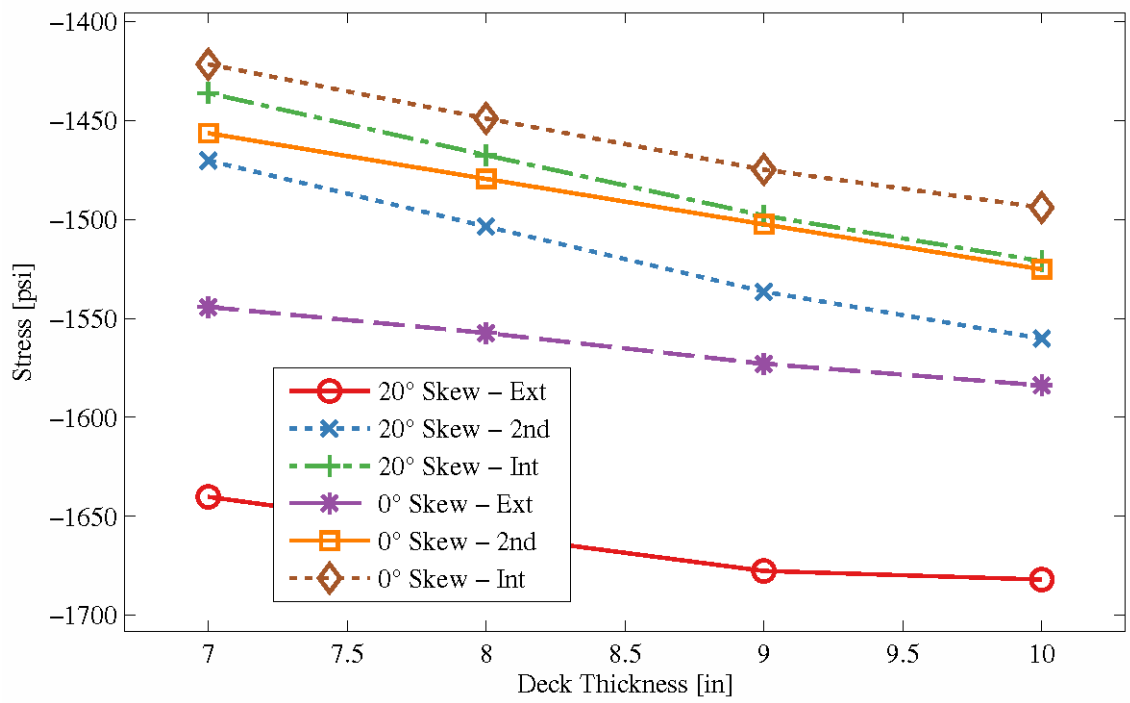

Figure D-2 - Effect of Deck Thickness on Total Composite Section Stress

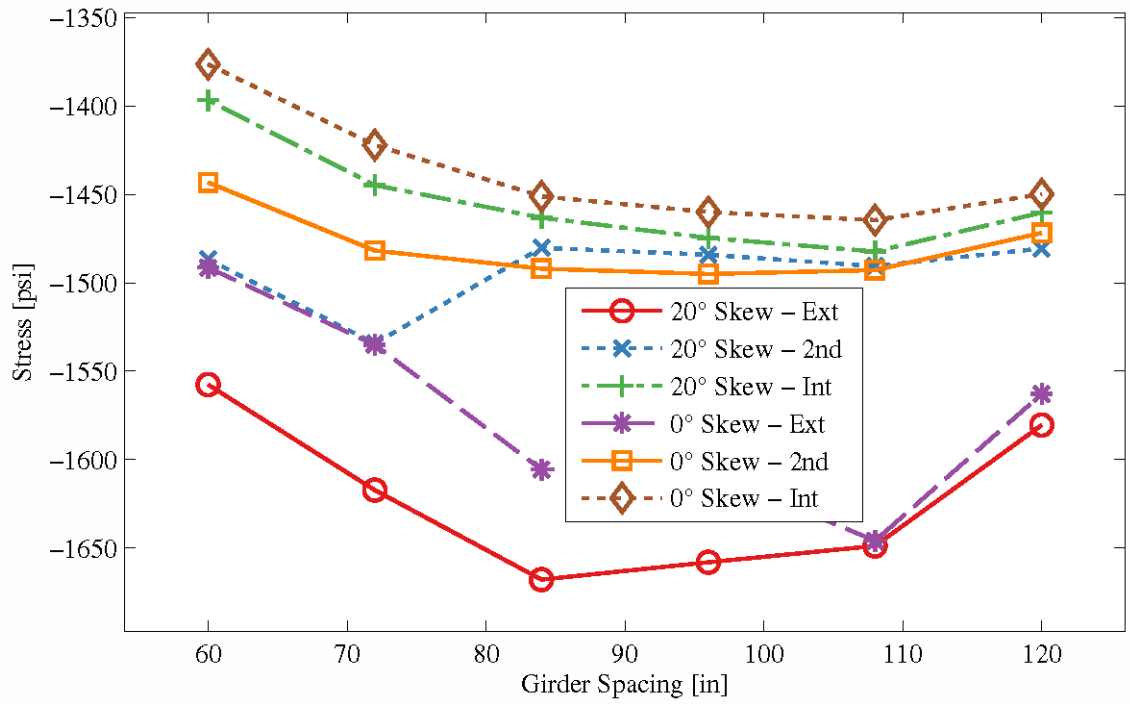

Figure D-3 - Effect of Girder Spacing on Total Composite Section Stress

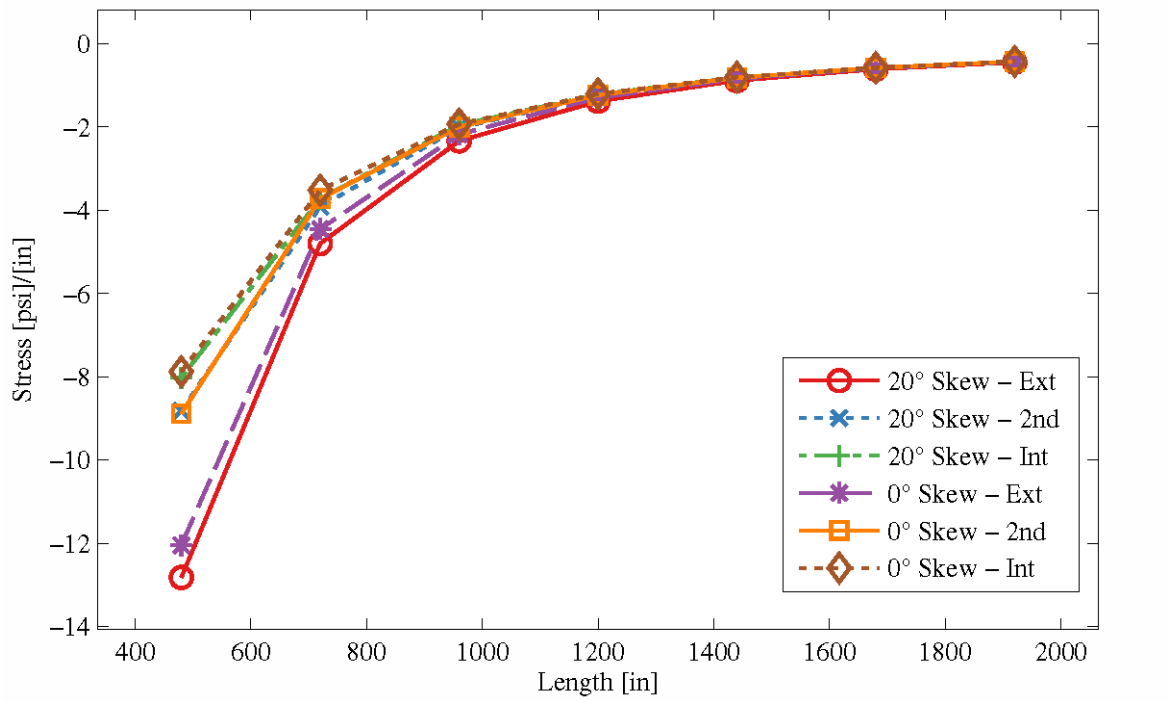

Figure D-4 - Effect of Span Length Normalized by Length on Total Composite Section Stress

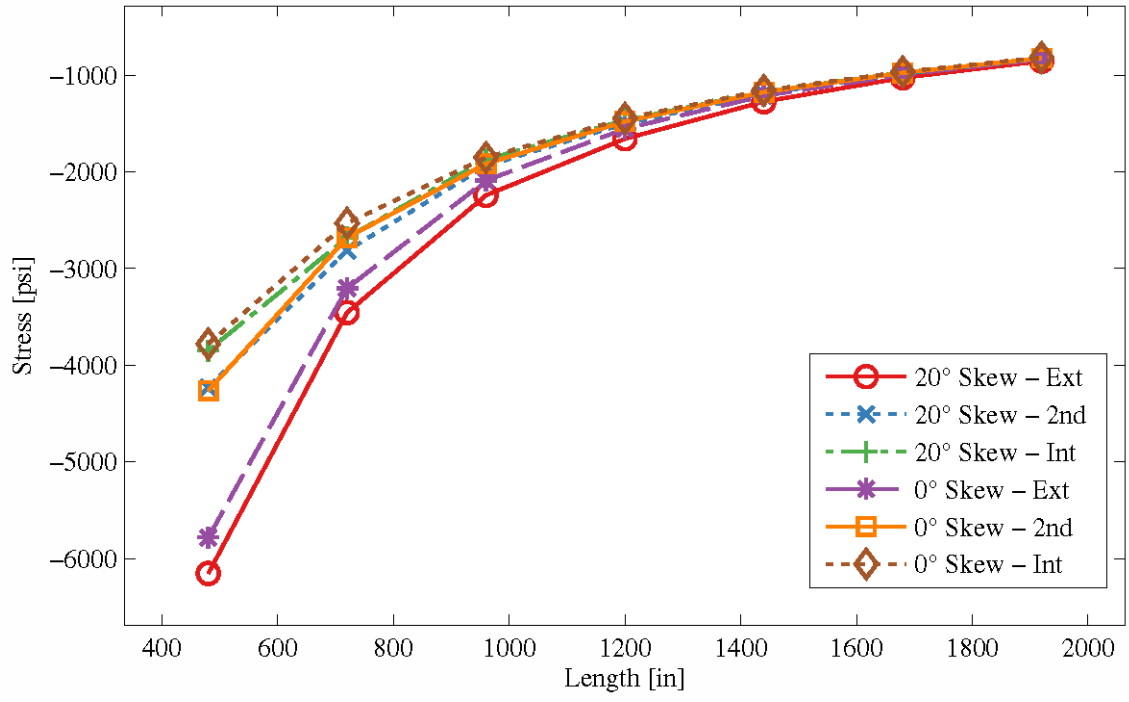

Figure D-5 - Effect of Span Length on Total Composite Section Stress

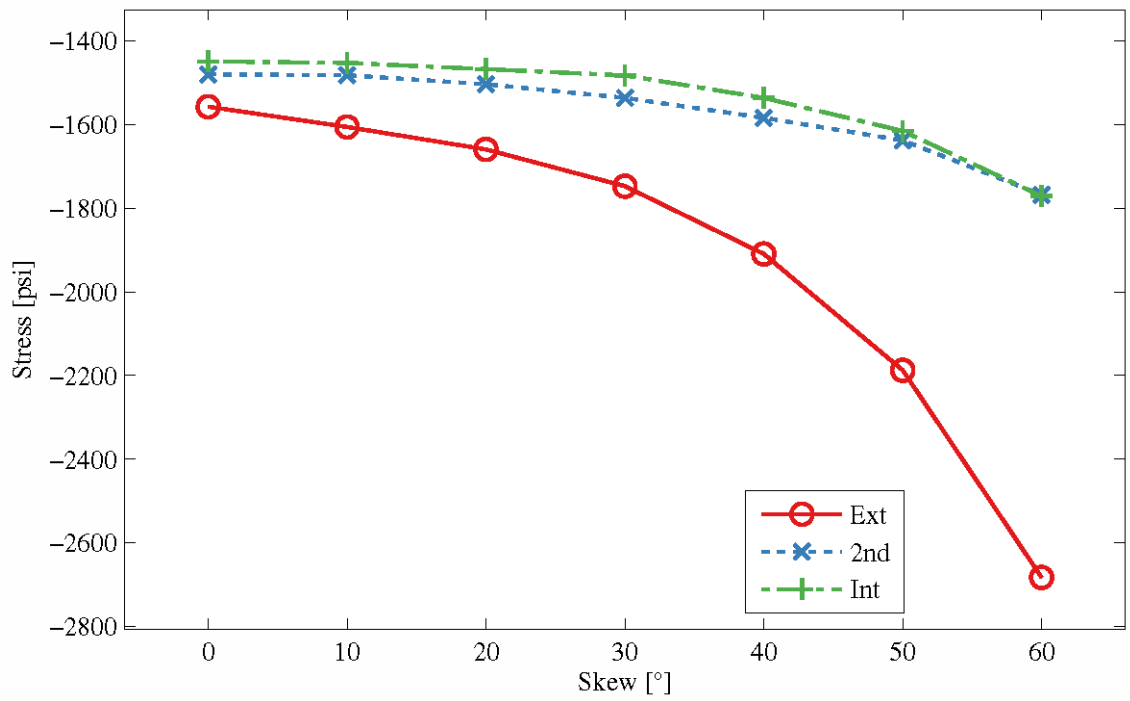

Figure D-6 - Effect of Skew Angle on Total Composite Section Stress

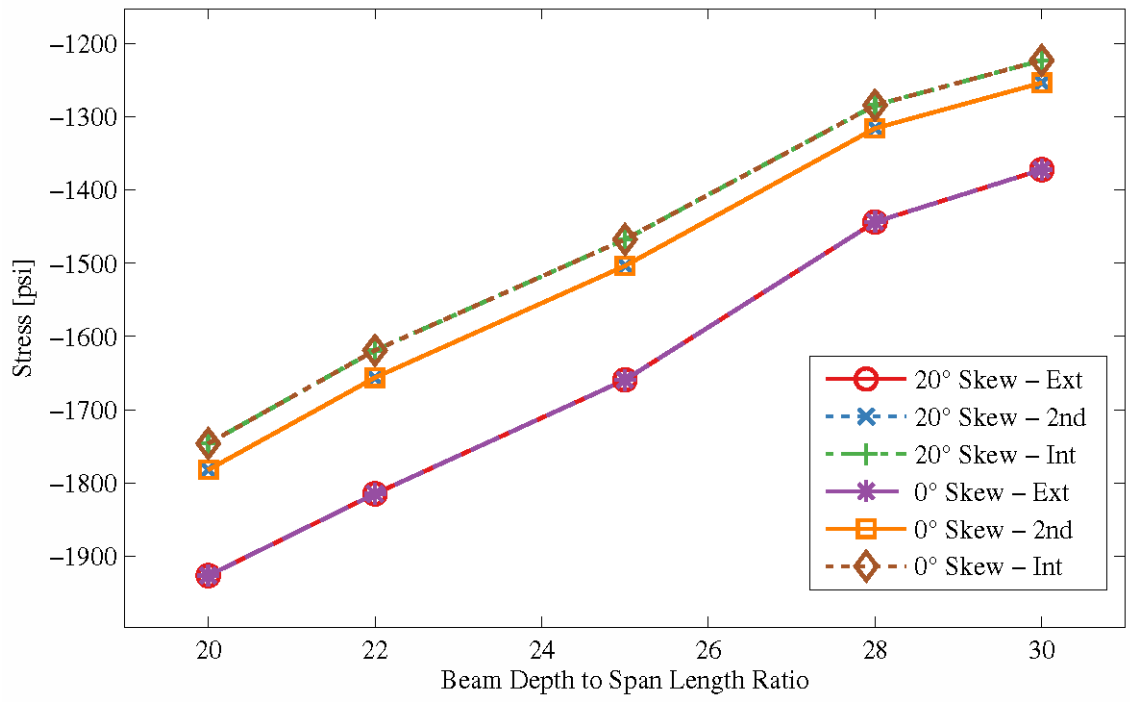

Figure D-7 - Effect of Beam Spacing on Total Composite Section Stress

D.1.2 Non-Structural Element Stiffness Off

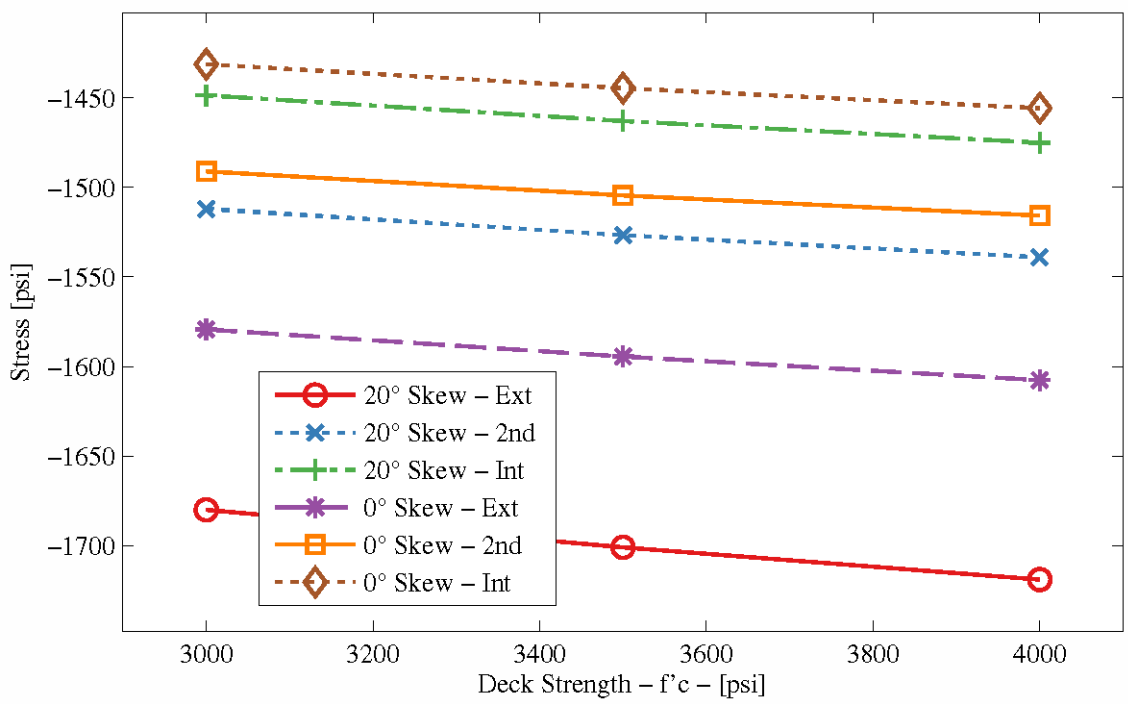

Figure D-8 - Effect of Deck Strength on Total Composite Section Stress

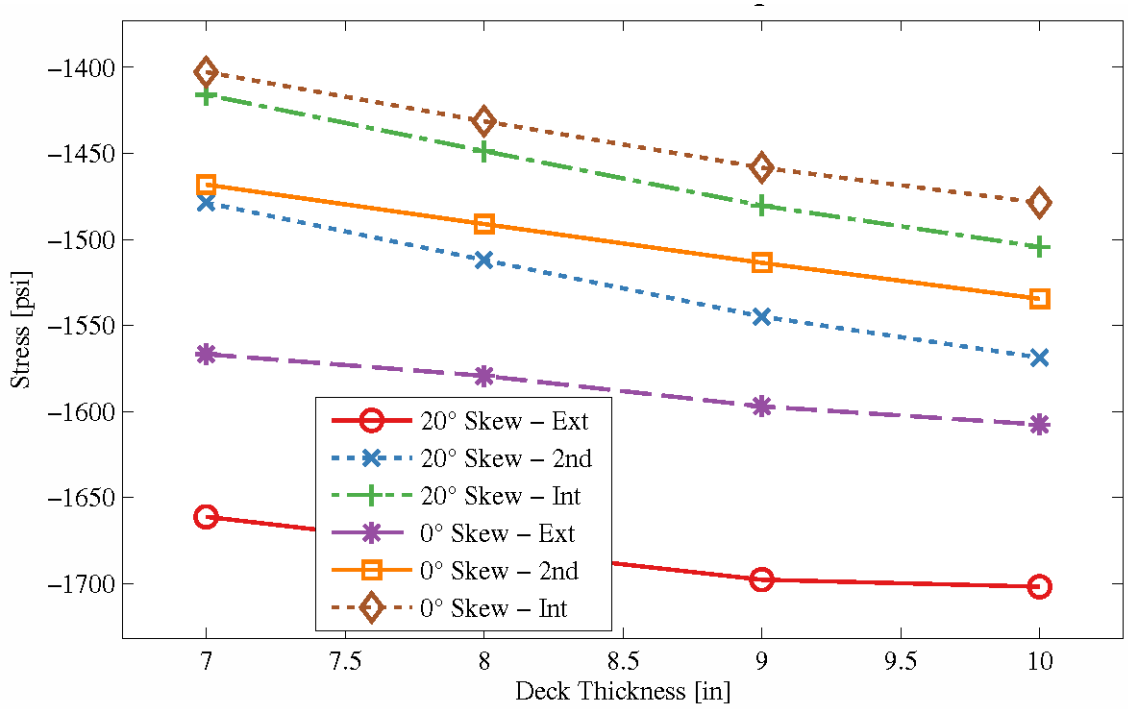

Figure D-9 - Effect of Deck Thickness on Total Composite Section Stress

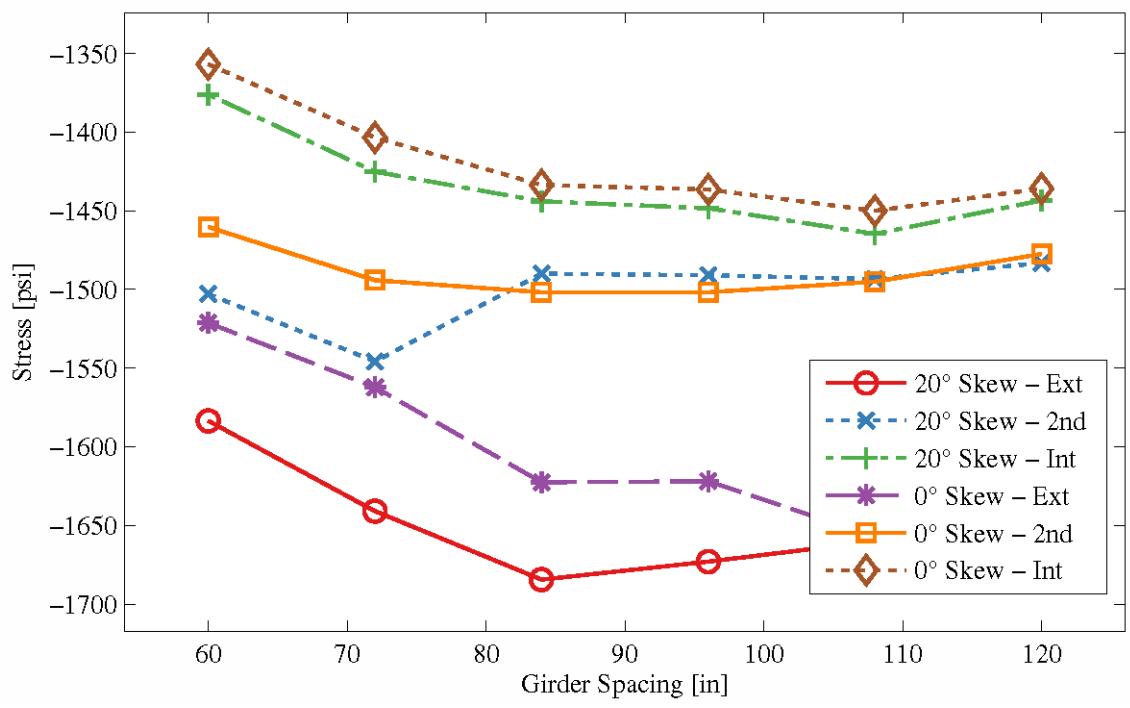

Figure D-10 - Effect of Girder Spacing on Total Composite Section Stress

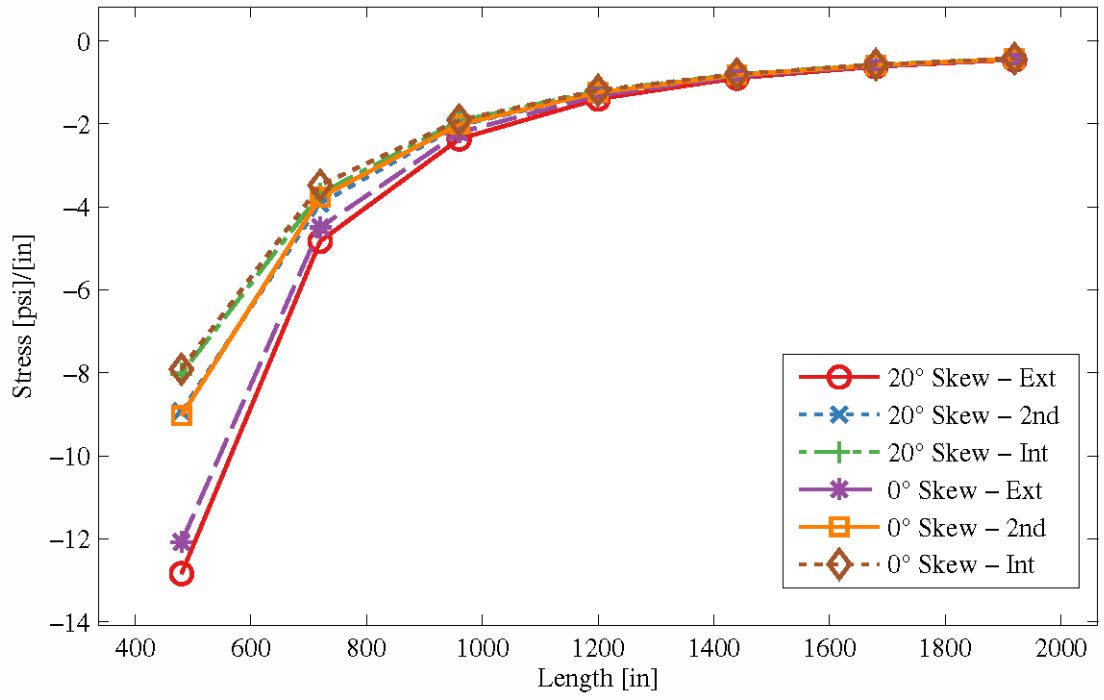

Figure D-11 - Effect of Span Length Normalized by Length on Total Composite Section Stress

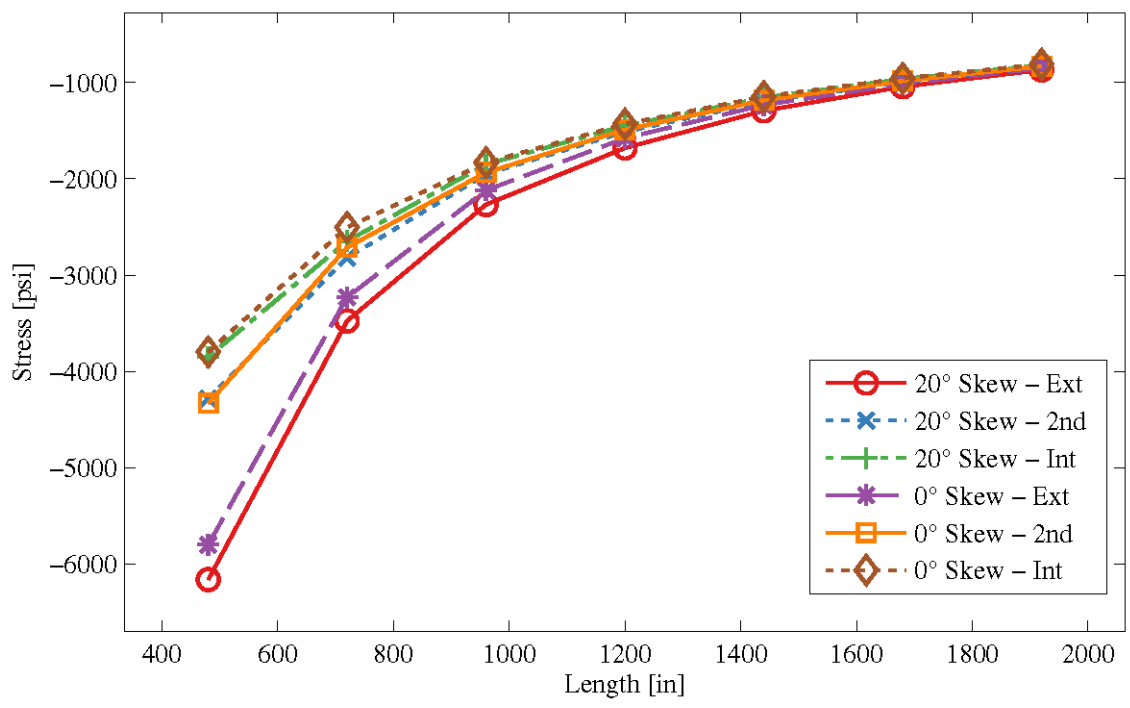

Figure D-12 - Effect of Span Length on Total Composite Section Stress

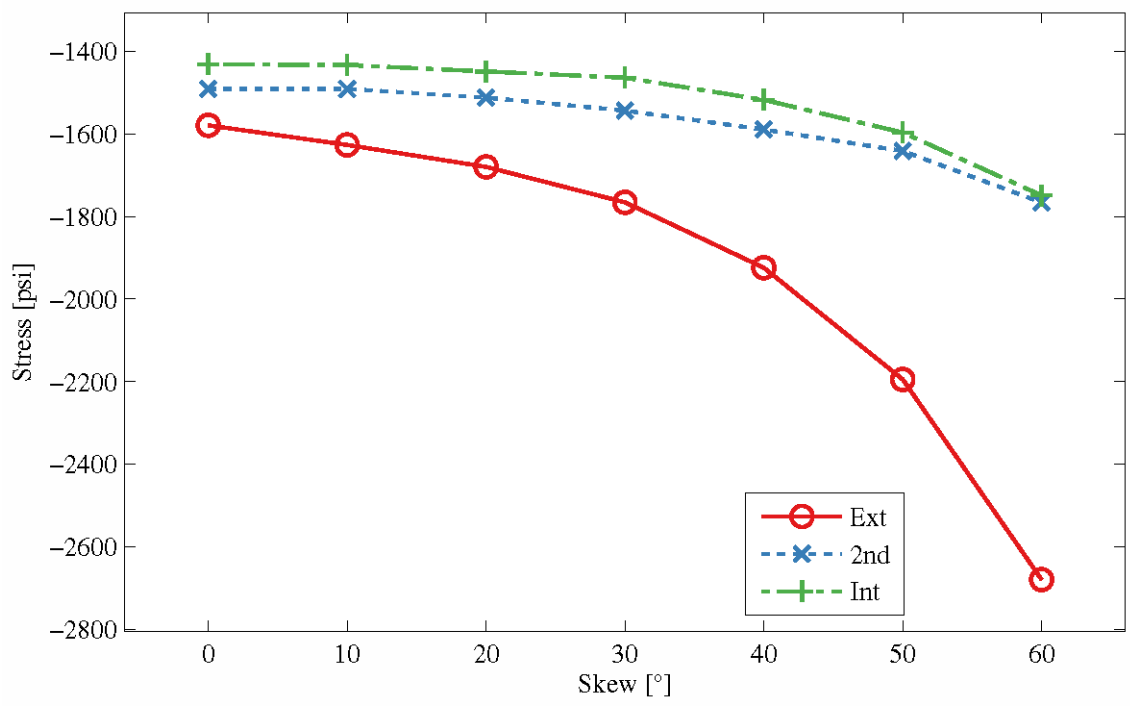

Figure D-13 - Effect of Skew Angle on Total Composite Section Stress

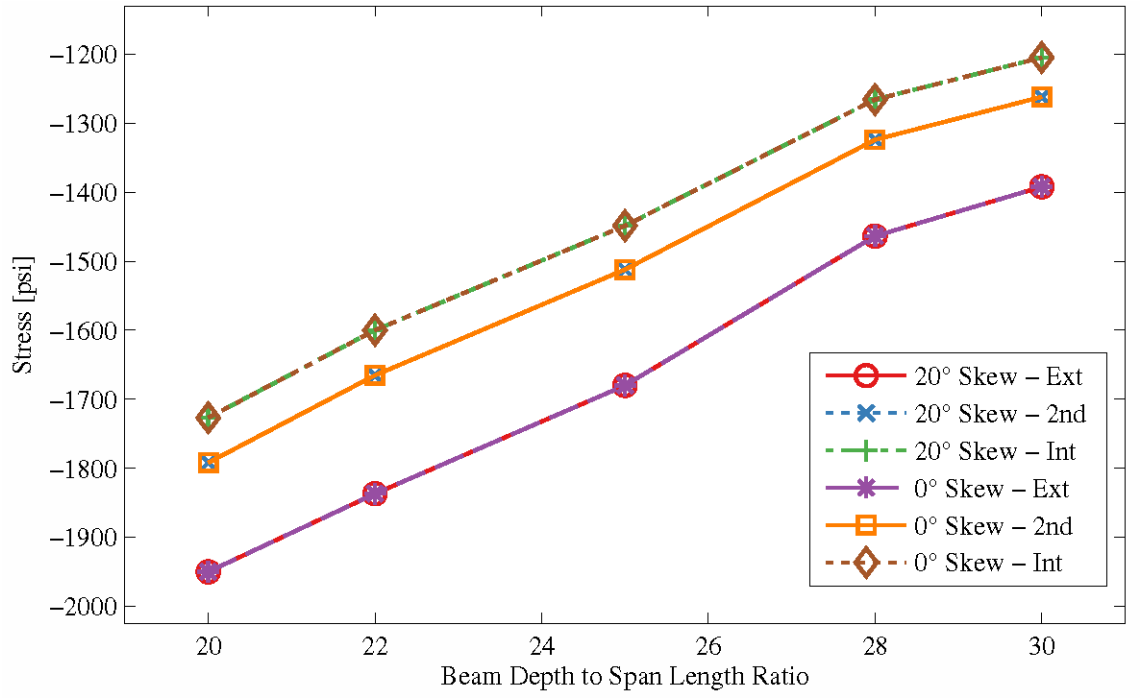

Figure D-14 - Effect of Span to Depth Ratio on Total Composite Section Stress

D.2 Deck Stress

D.2.1 Non-Structural Element Stiffness On

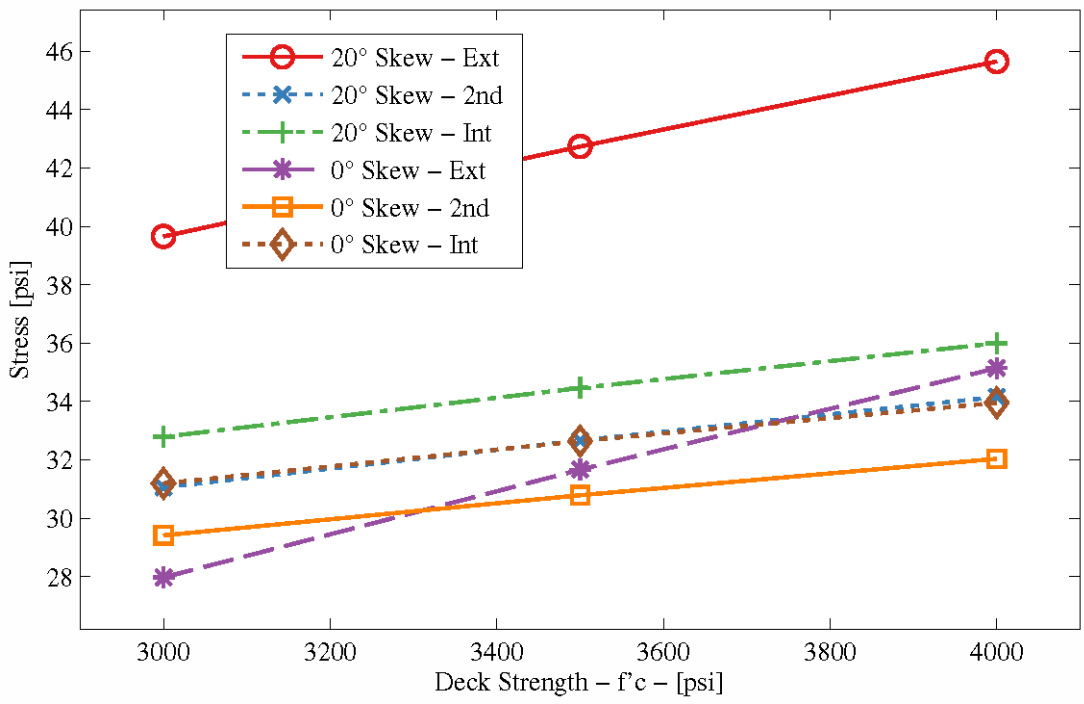

Figure D-15 - Effect of Deck Strength on Deck Stress

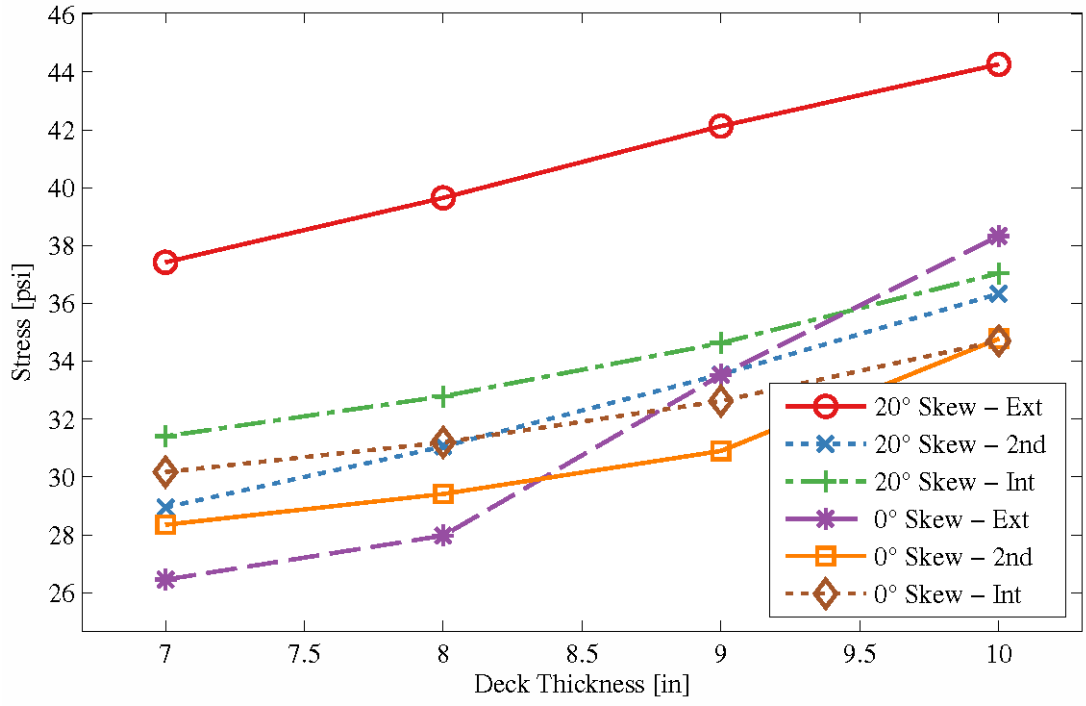

Figure D-16 - Effect of Deck Thickness on Deck Stress

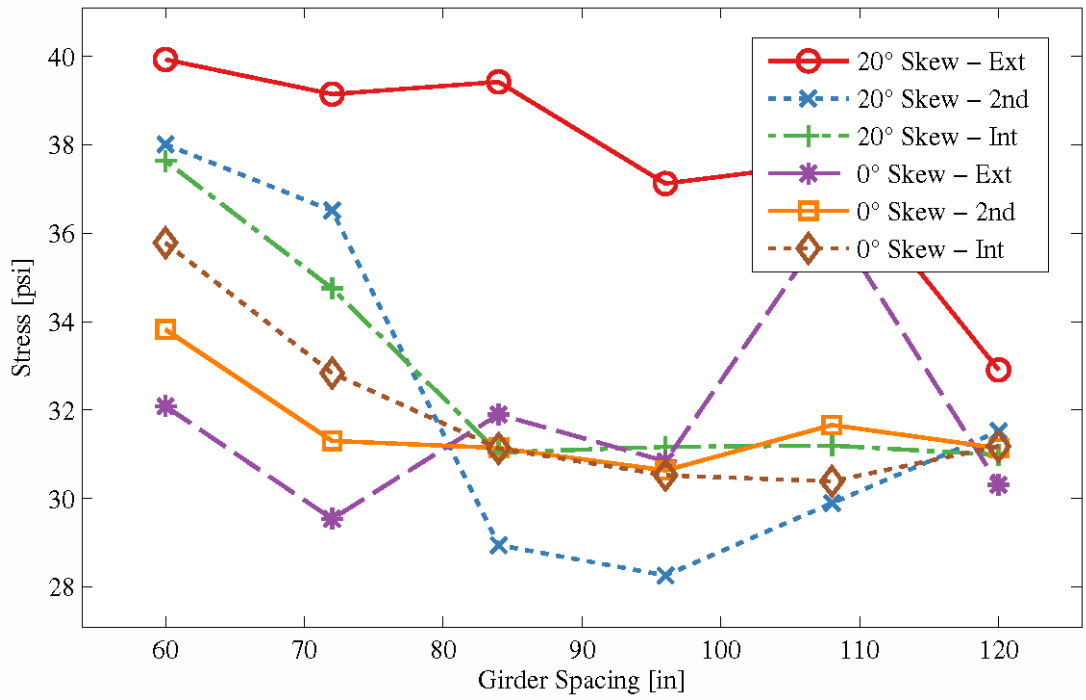

Figure D-17 - Effect of Girder Spacing on Deck Stress

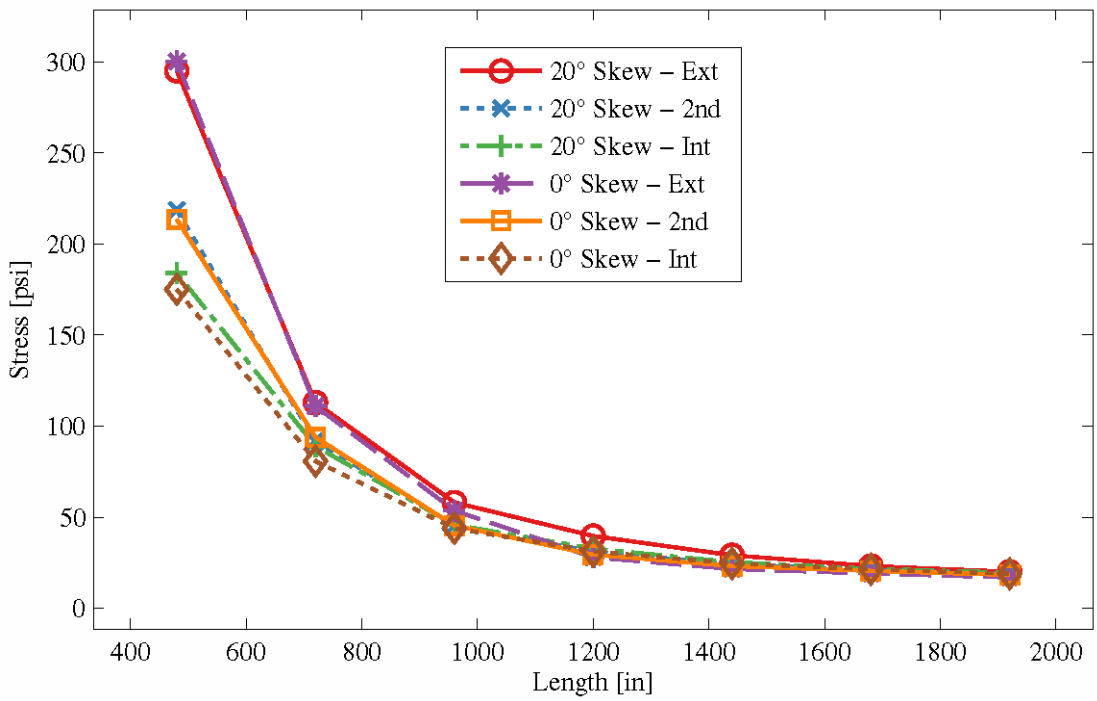

Figure D-18 - Effect of Span Length Normalized by Length on Deck Stress

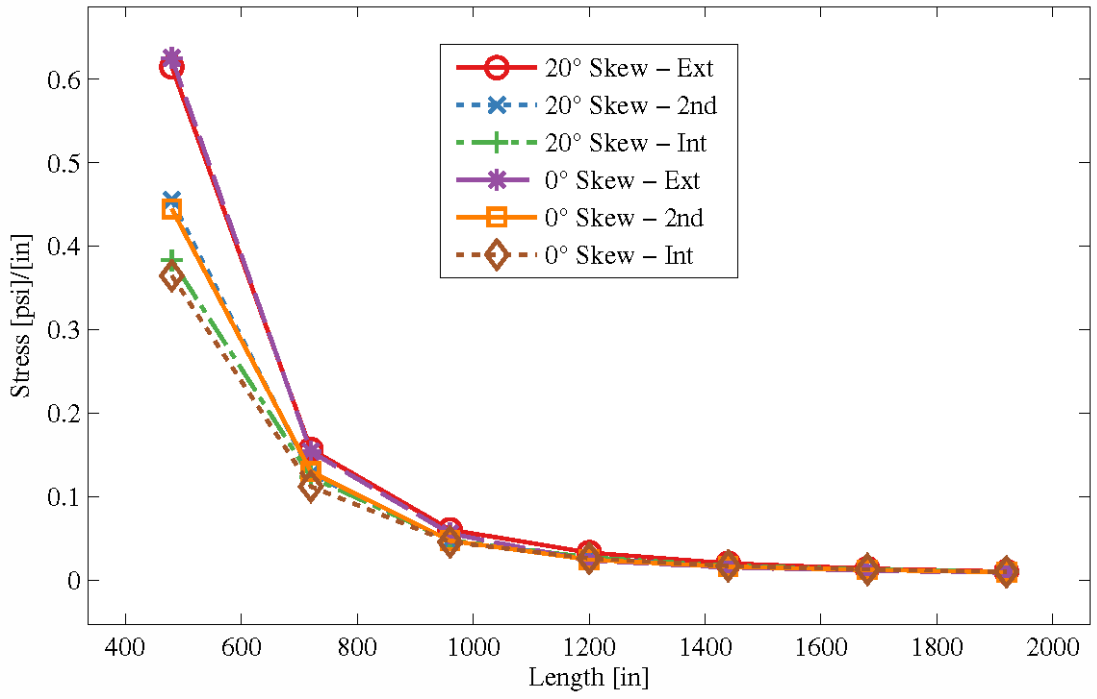

Figure D-19 - Effect of Span Length on Deck Stress

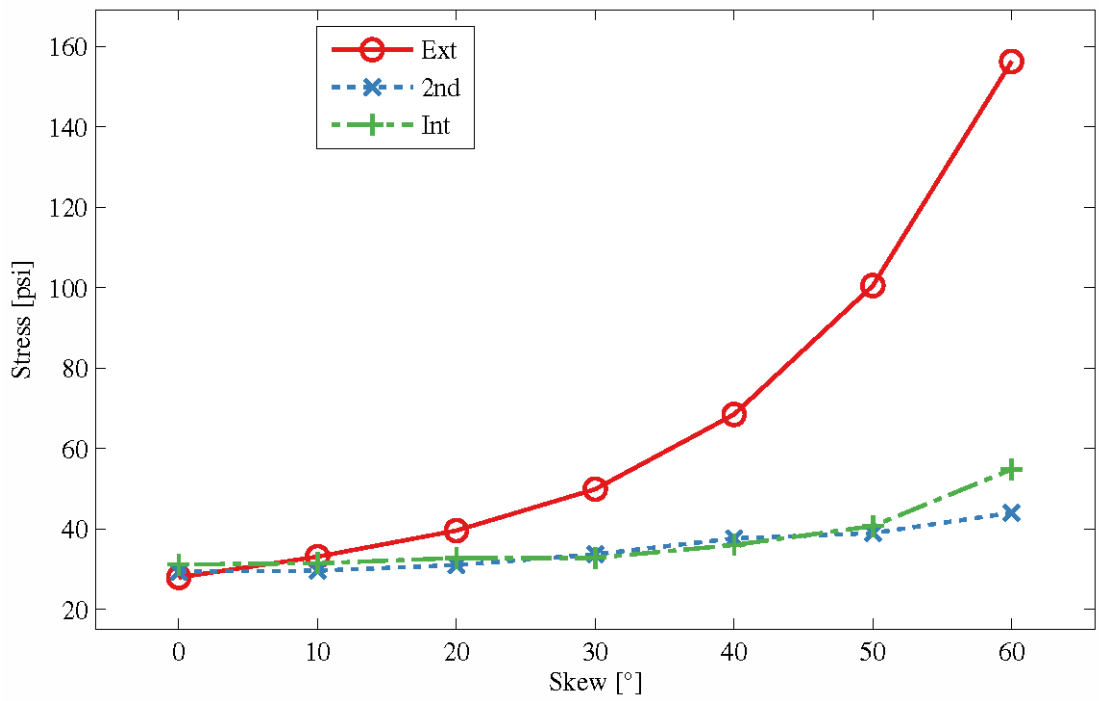

Figure D-20 - Effect of Skew Angle on Deck Stress

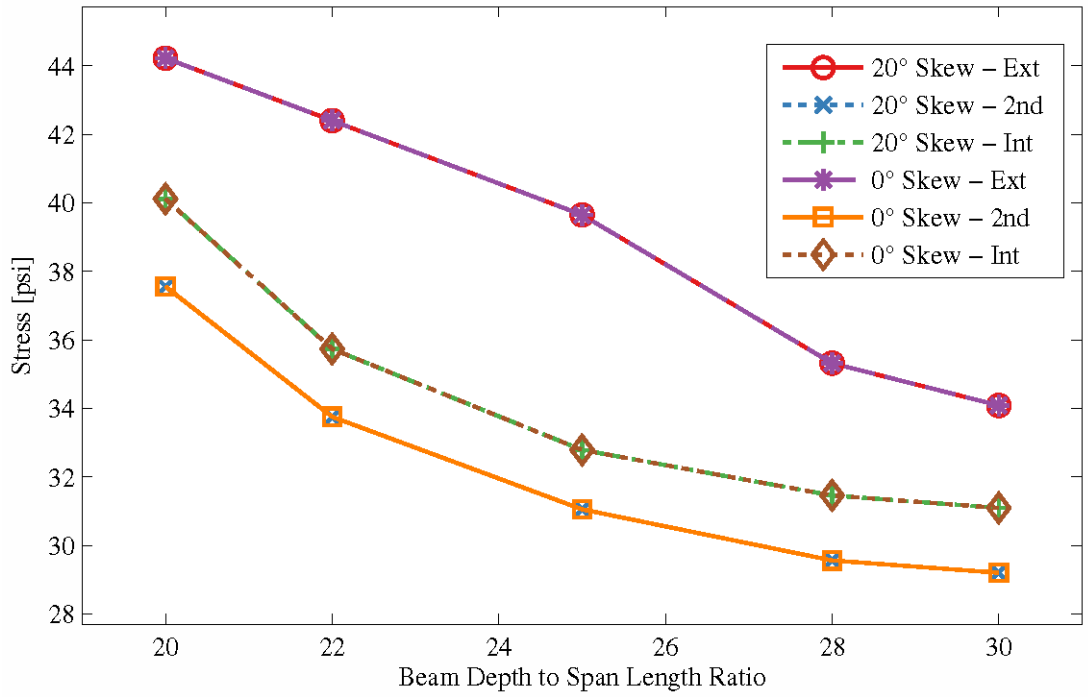

Figure D-21 - Effect of Span to Depth Ratio on Deck Stress

D.2.2 Non-Structural Element Stiffness Off

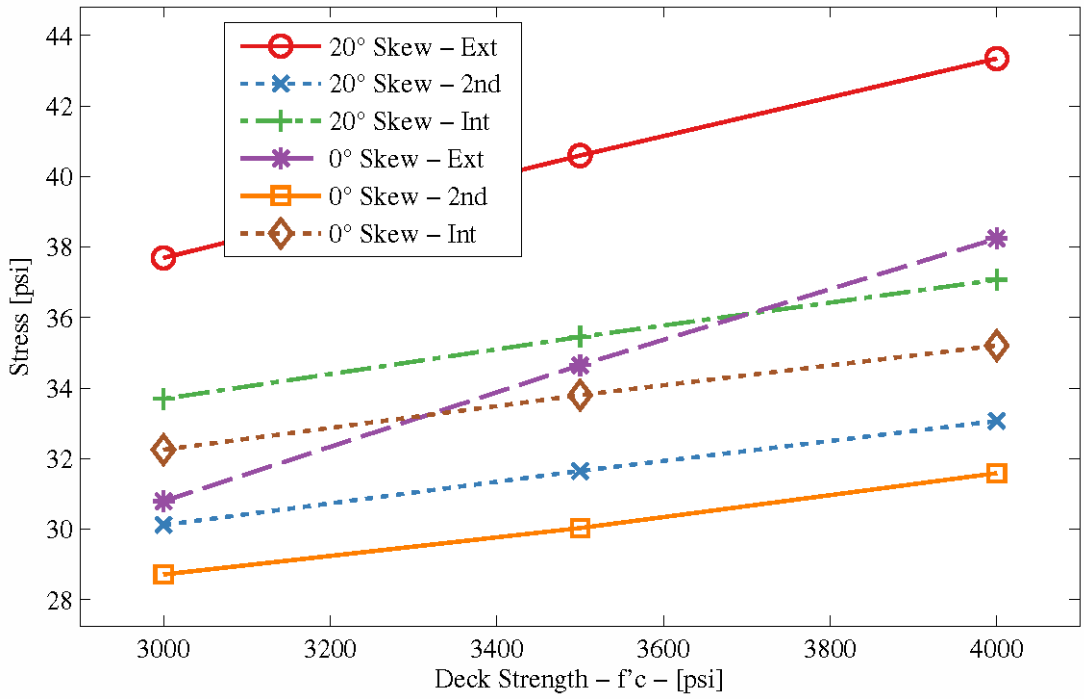

Figure D-22 - Effect of Deck Strength on Deck Stress

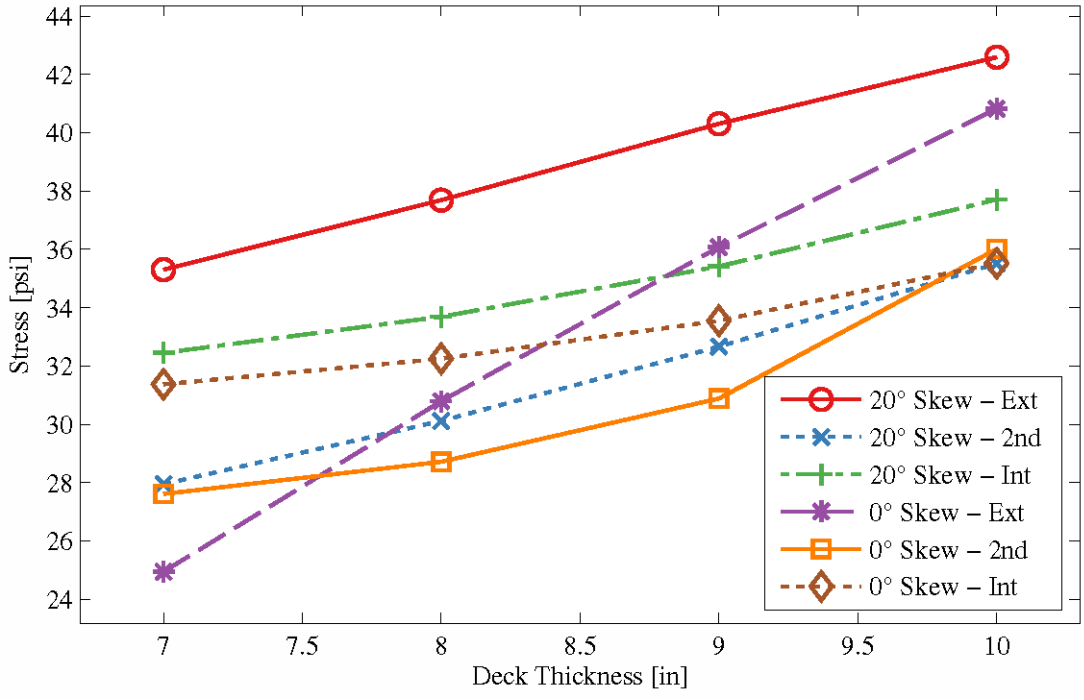

Figure D-23 - Effect of Deck Thickness on Deck Stress

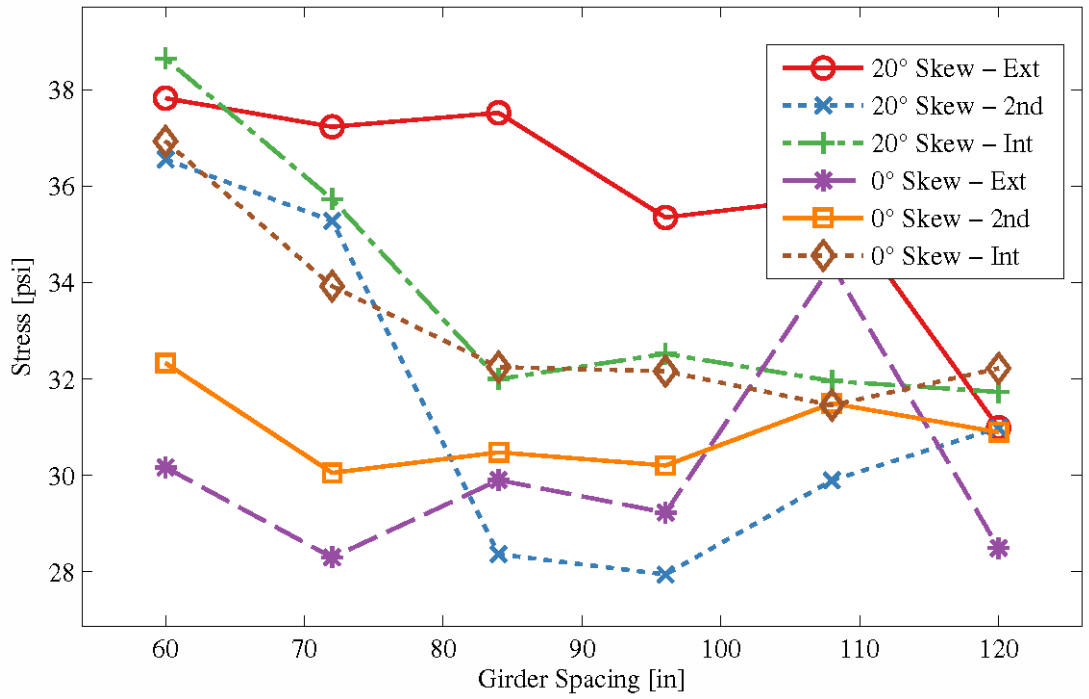

Figure D-24 - Effect of Girder Spacing on Deck Stress

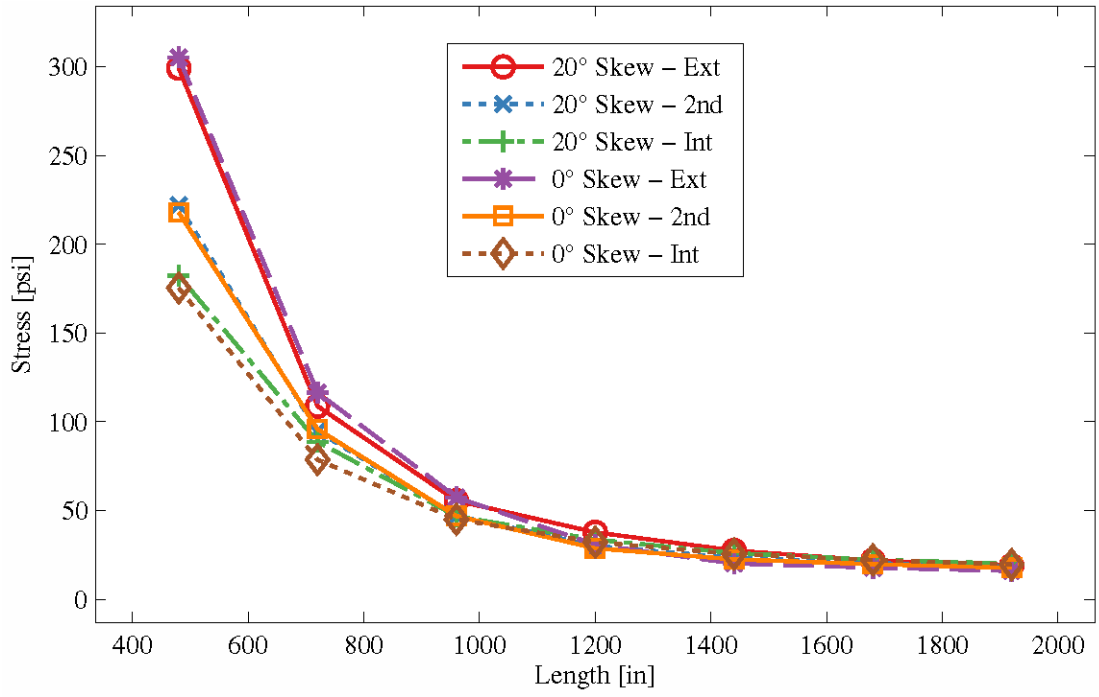

Figure D-25 - Effect of Span Length on Deck Stress

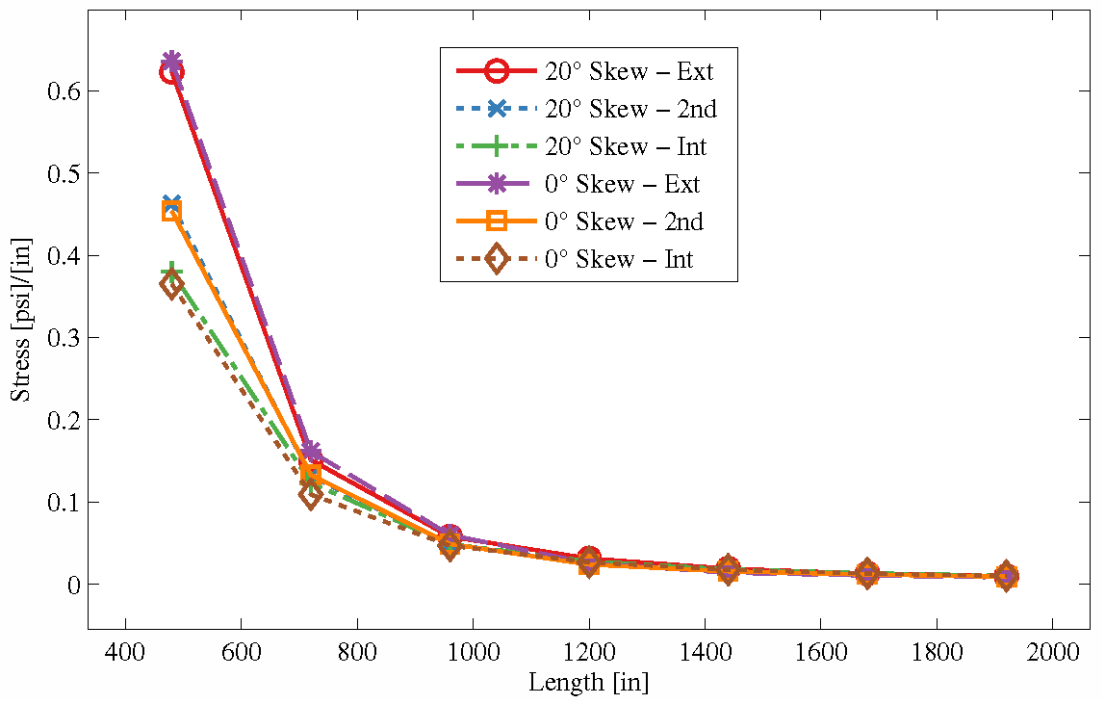

Figure D-26 - Effect of Span Length Normalized by Span Length on Deck Stress

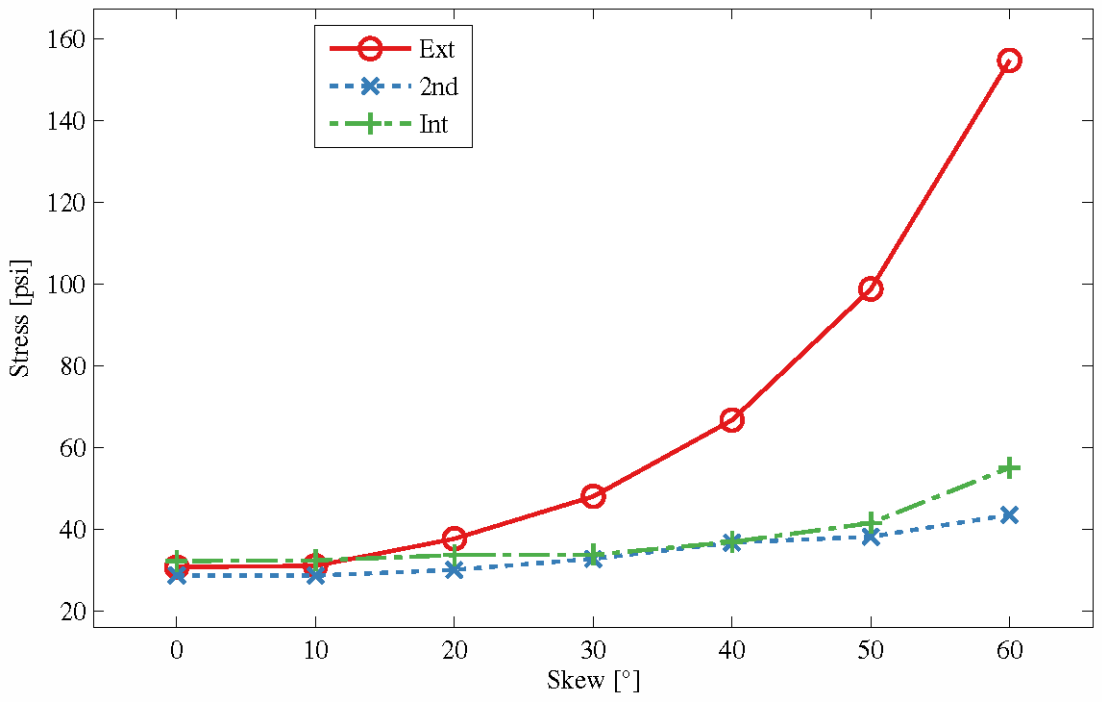

Figure D-27 - Effect of Skew Angle on Deck Stress

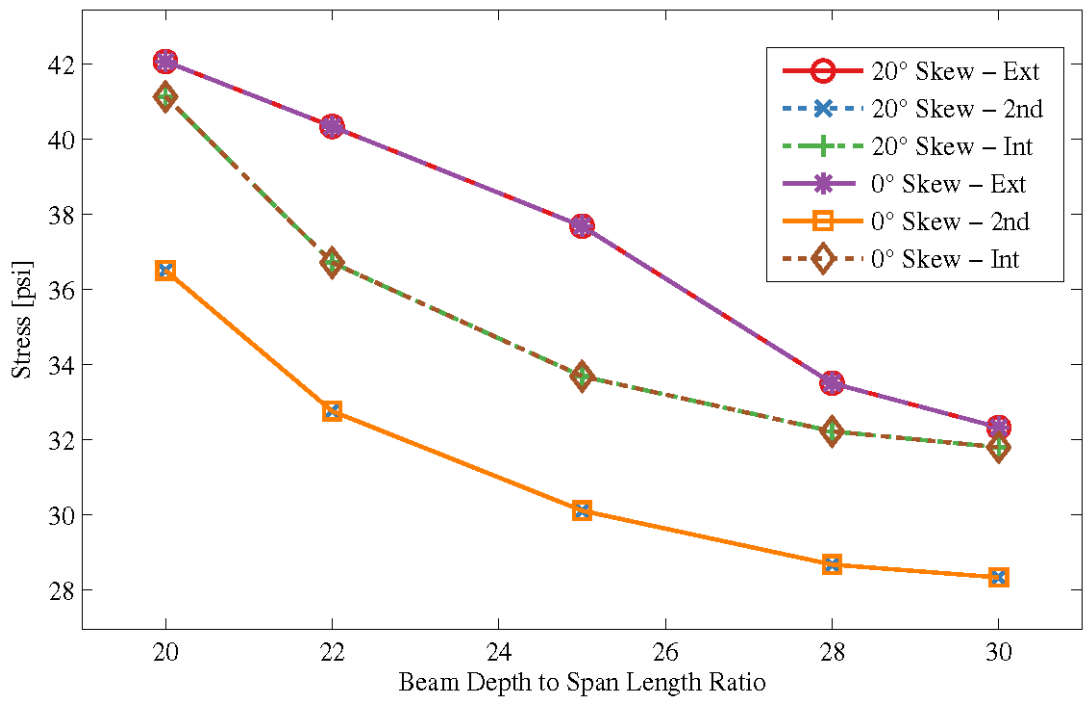

Figure D-28 - Effect of Beam Span on Deck Stress

\

D.3 Vertical Reaction at the Support

D.3.1 Non-Structural Element Stiffness On

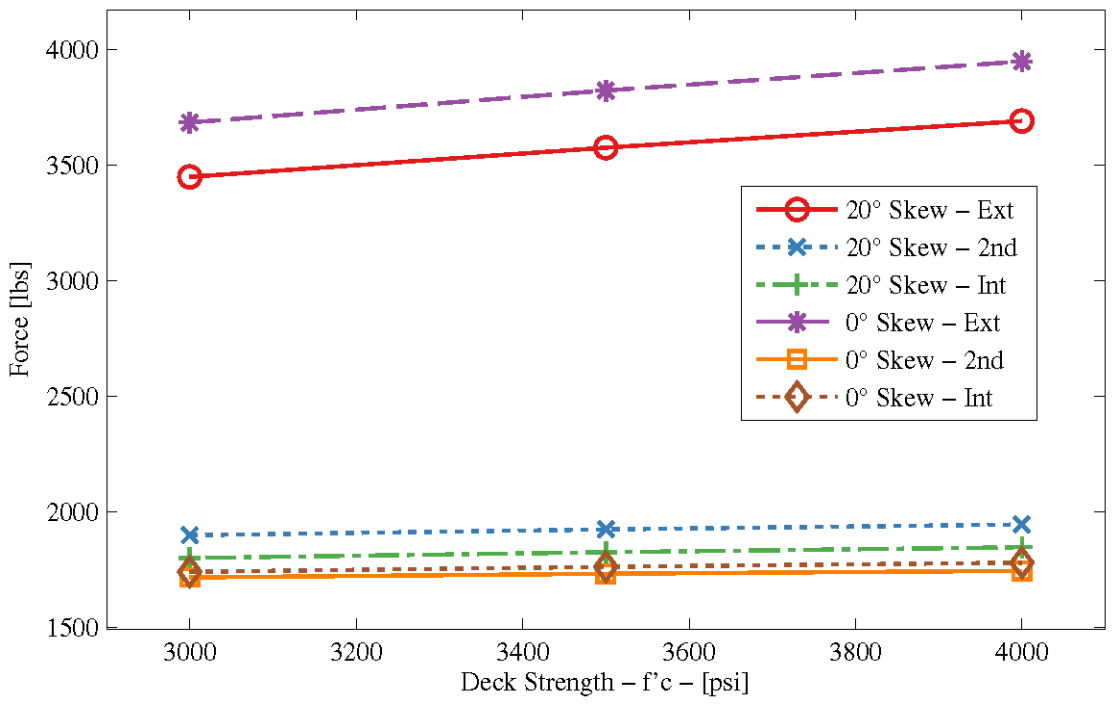

Figure D-29 - Effect of Deck Strength on Vertical Reaction at the Support

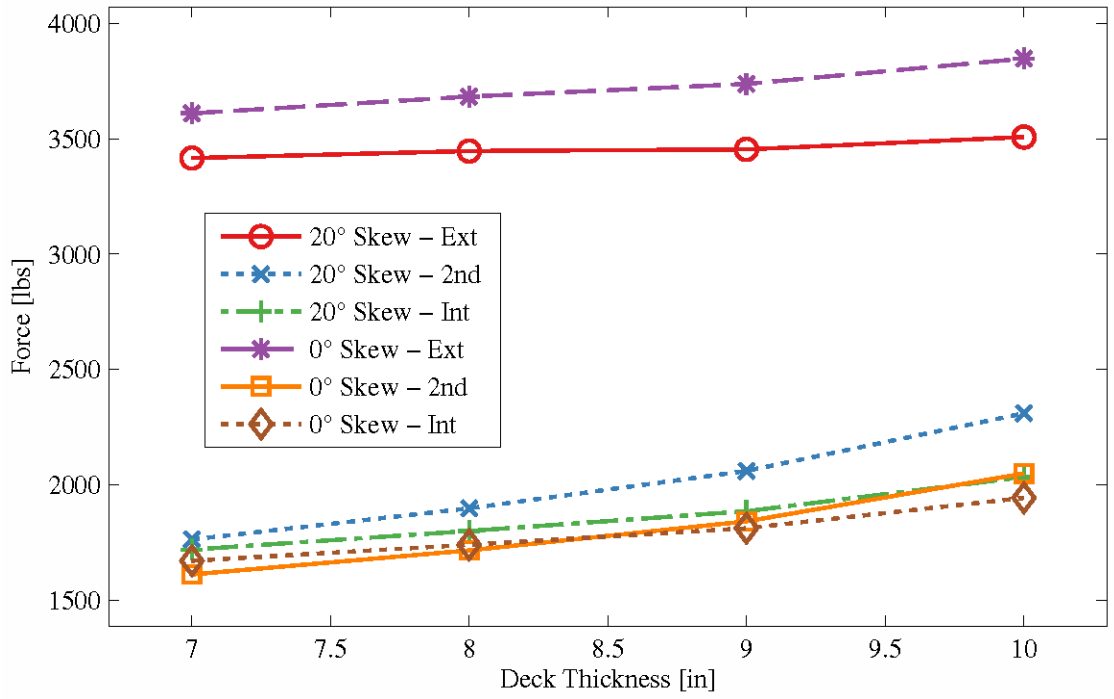

Figure D-30 - Effect of Deck Thickness on Vertical Reaction at the Support

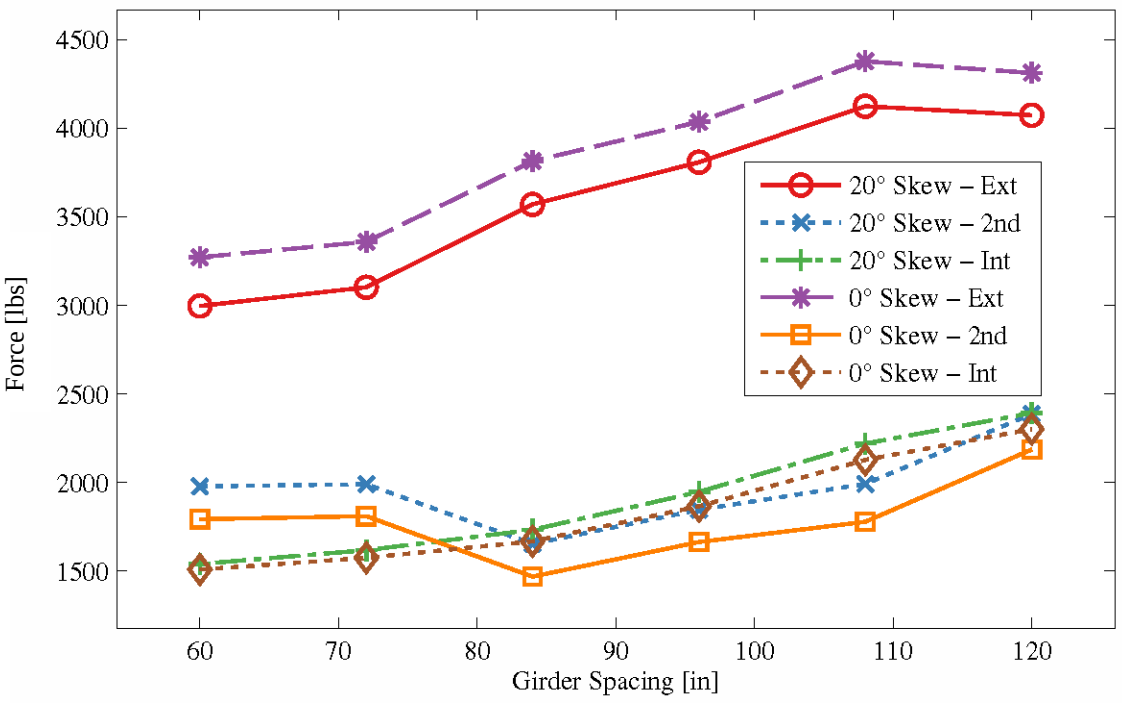

Figure D-31 - Effect of Girder Spacing on Vertical Reaction at the Support

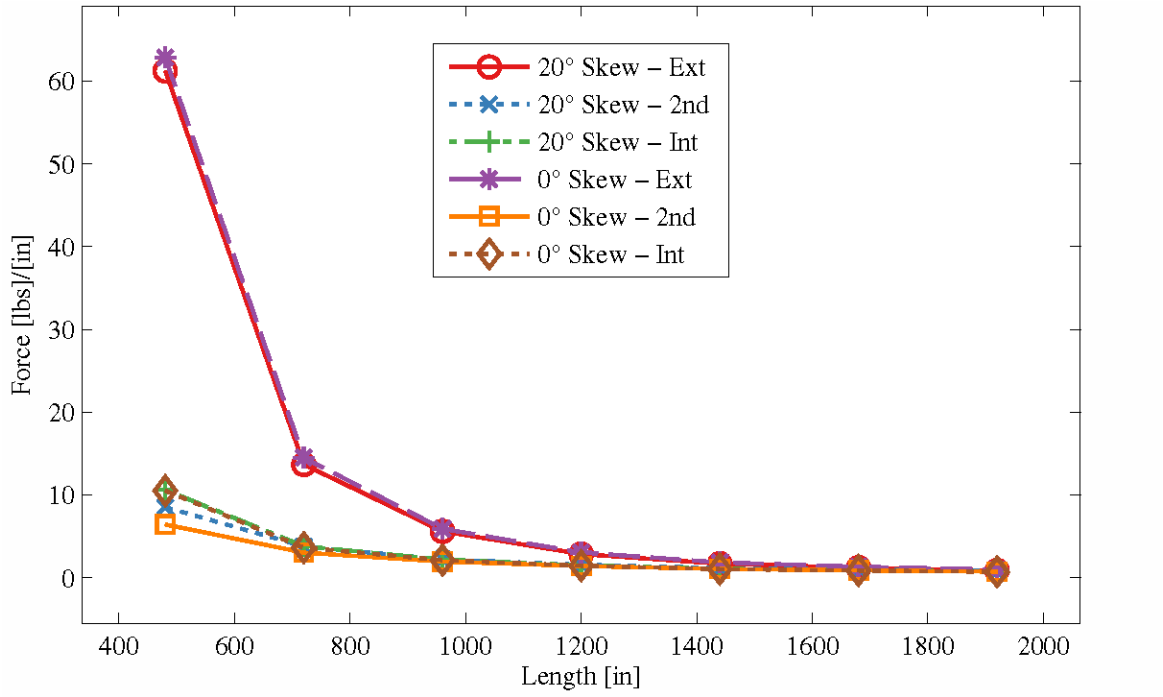

Figure D-32 - Effect of Span Length Normalized by Span Length on Vertical Reaction at the Support

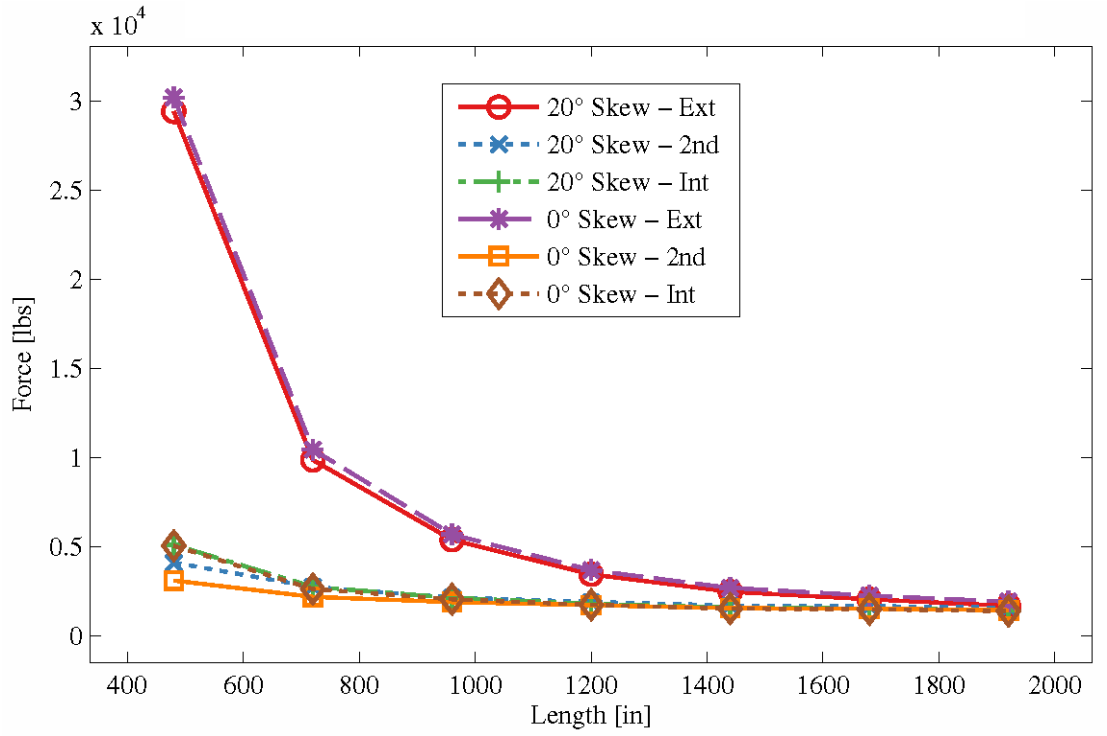

Figure D-33 - Effect of Span Length on Vertical Reaction at the Support

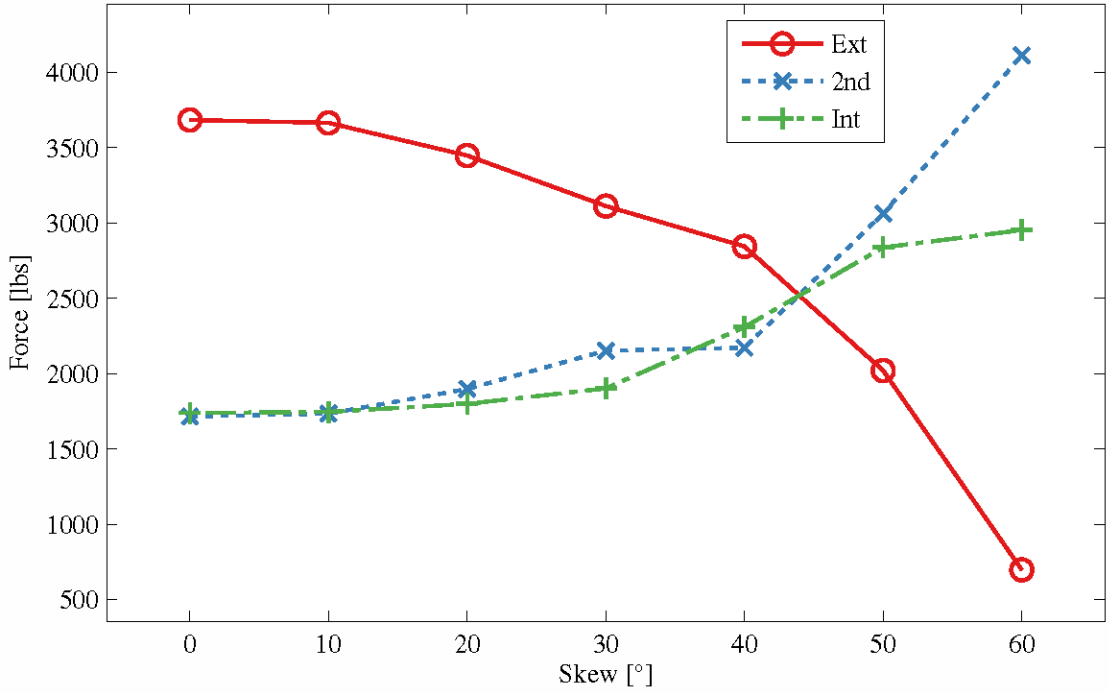

Figure D-34 - Effect of Skew Angle on Vertical Reaction at the Support

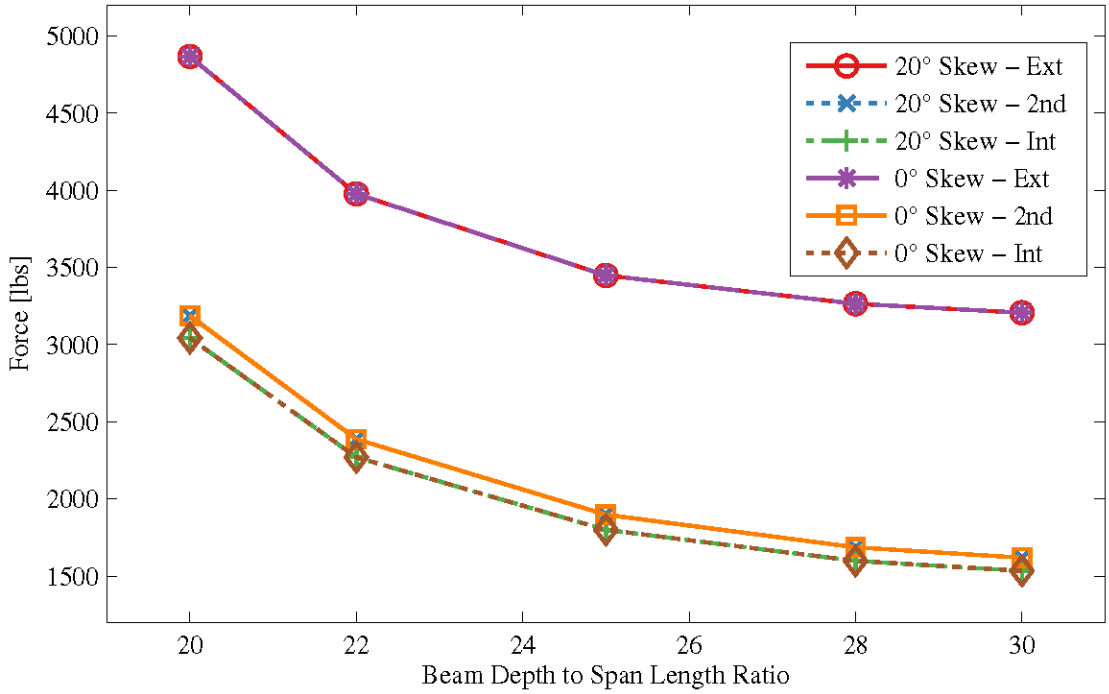

Figure D-35 - Effect of Span to Depth Ratio on Vertical Reaction at the Support

D.3.2 Non-Structural Element Stiffness Off

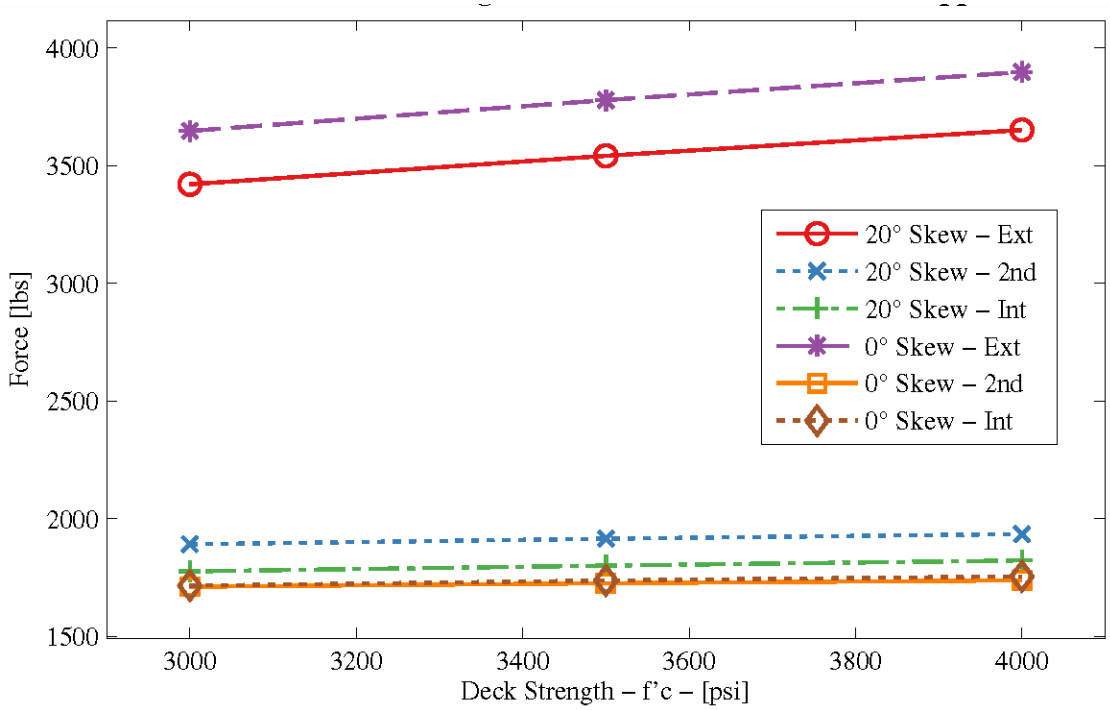

Figure D-36 - Effect of Deck Strength on Vertical Reaction at the Support

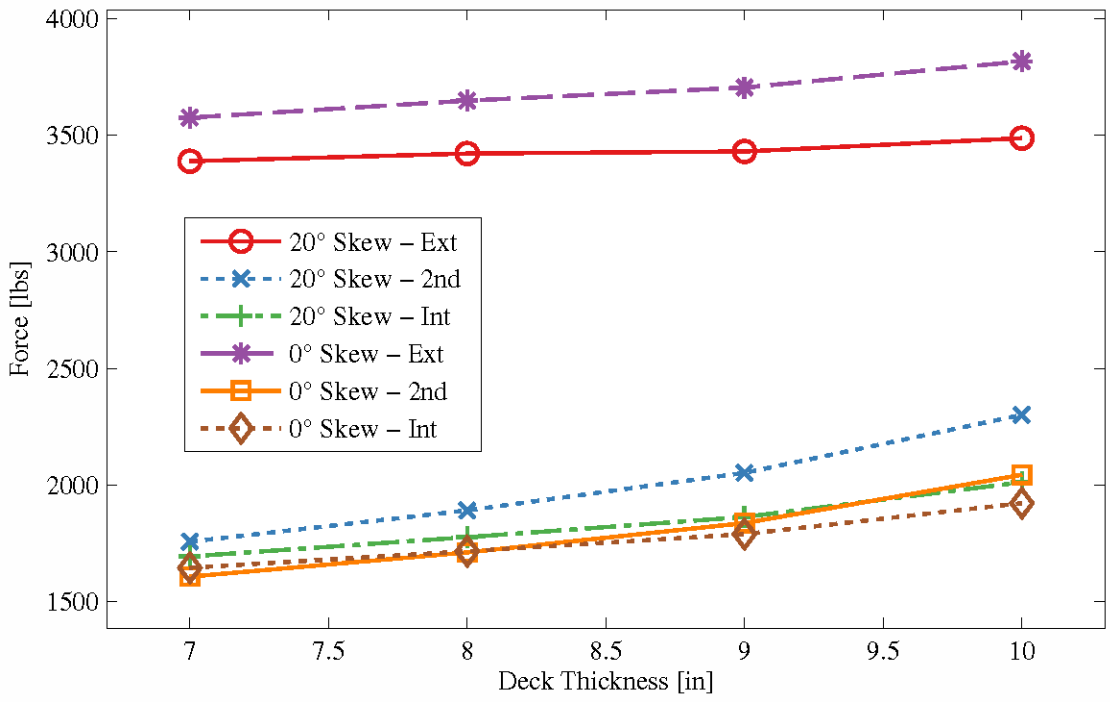

Figure D-37 - Effect of Deck Thickness on Vertical Reaction at the Support

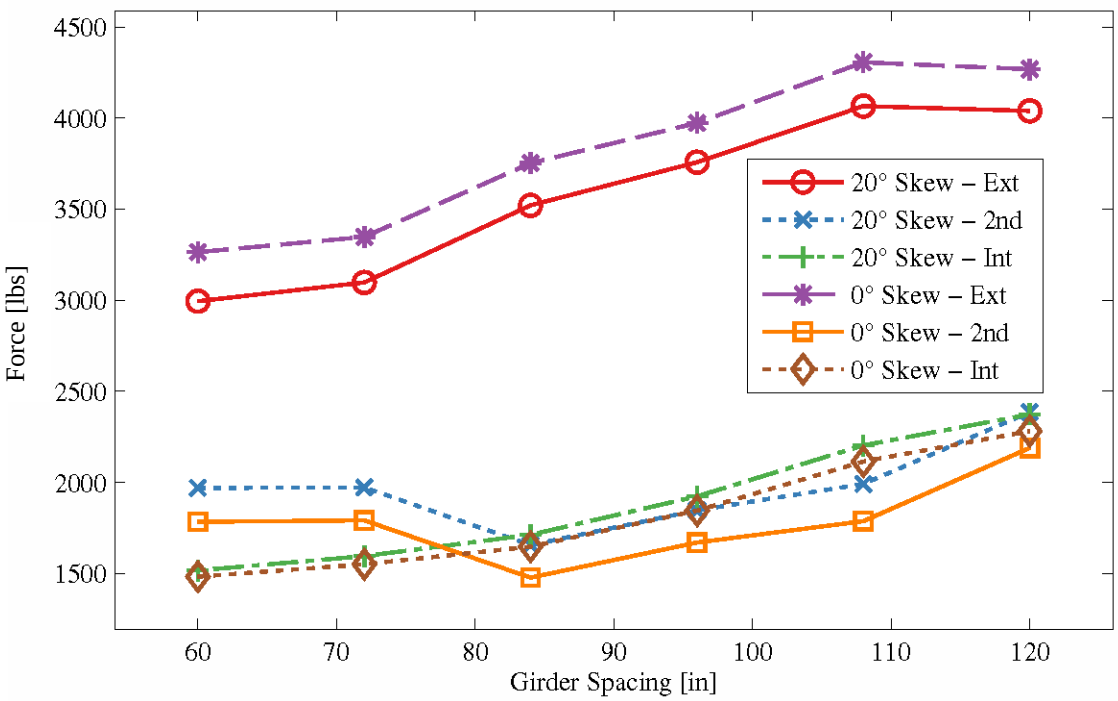

Figure D-38 - Effect of Girder Spacing on Vertical Reaction at the Support

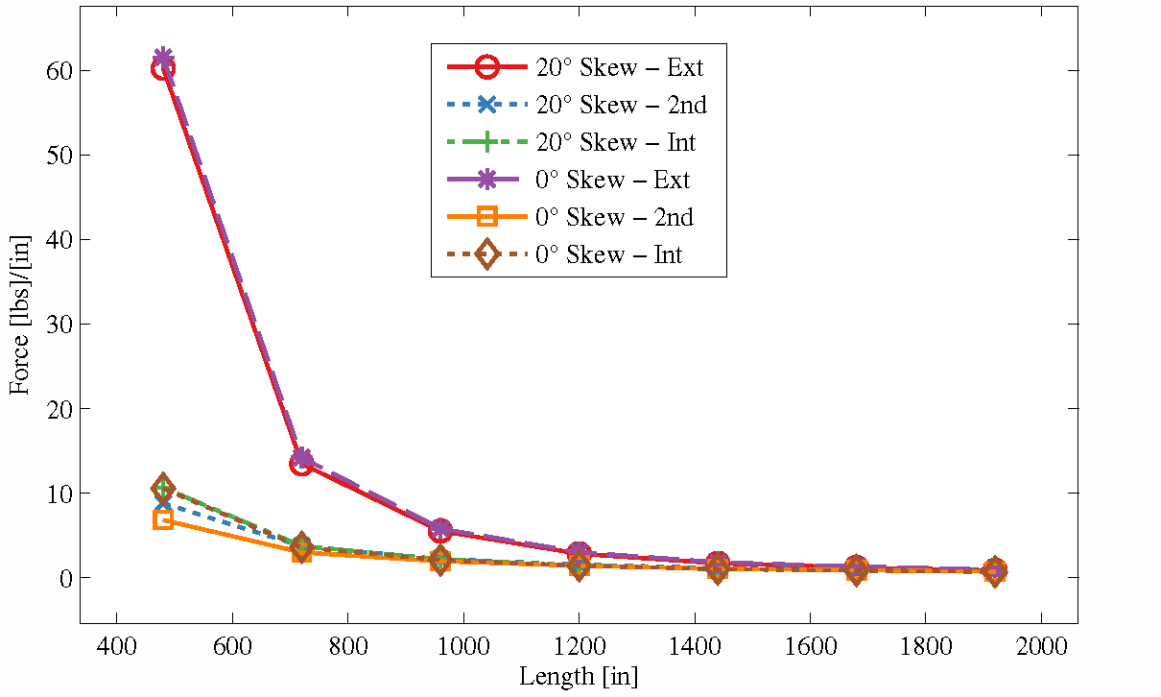

Figure D-39 - Effect of Span Length Normalized by Length on Vertical Reaction at the Support

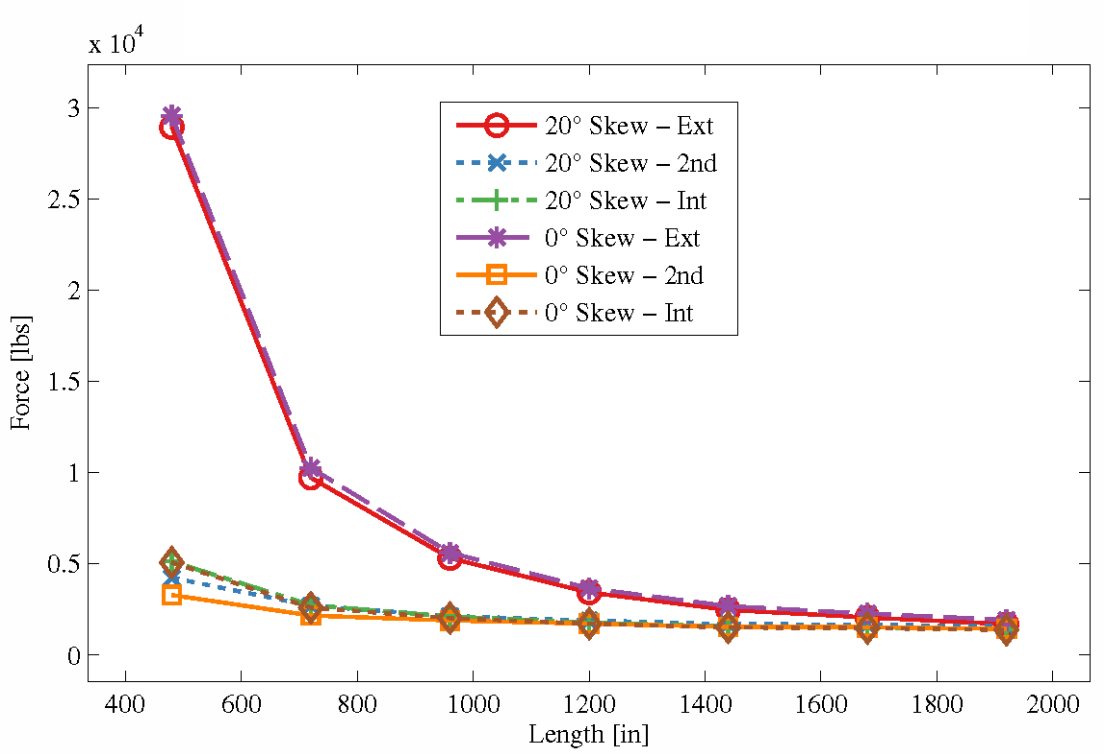

Figure D-40 - Effect of Span Length on Vertical Reaction at the Support

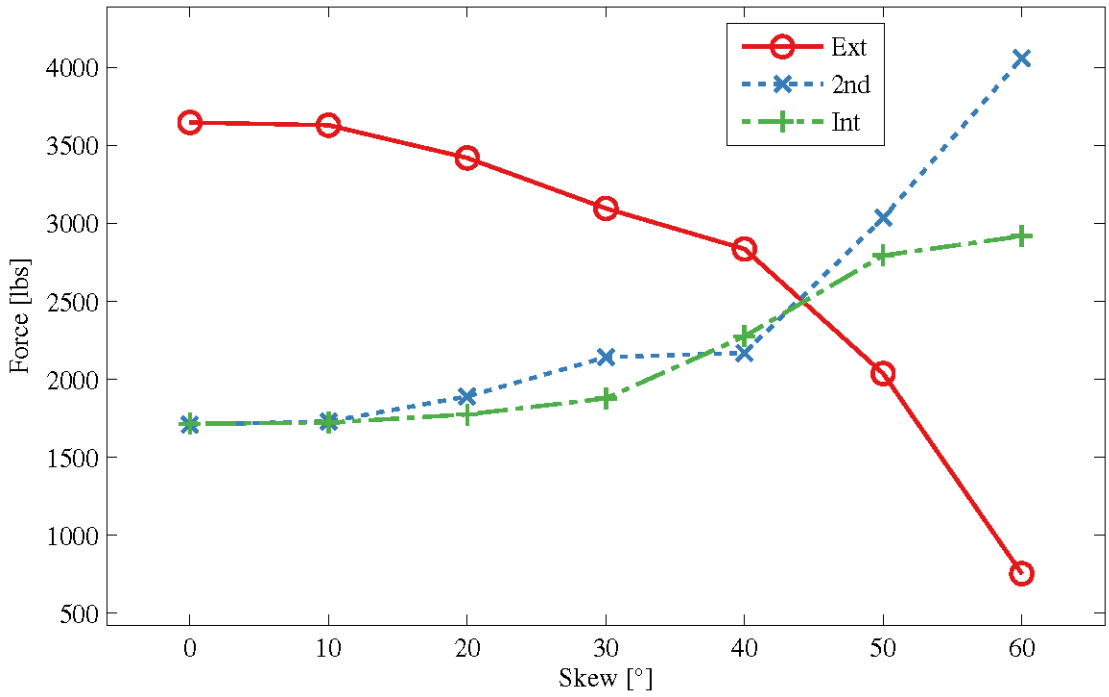

Figure D-41 - Effect of Skew Angle on Vertical Reaction at the Support

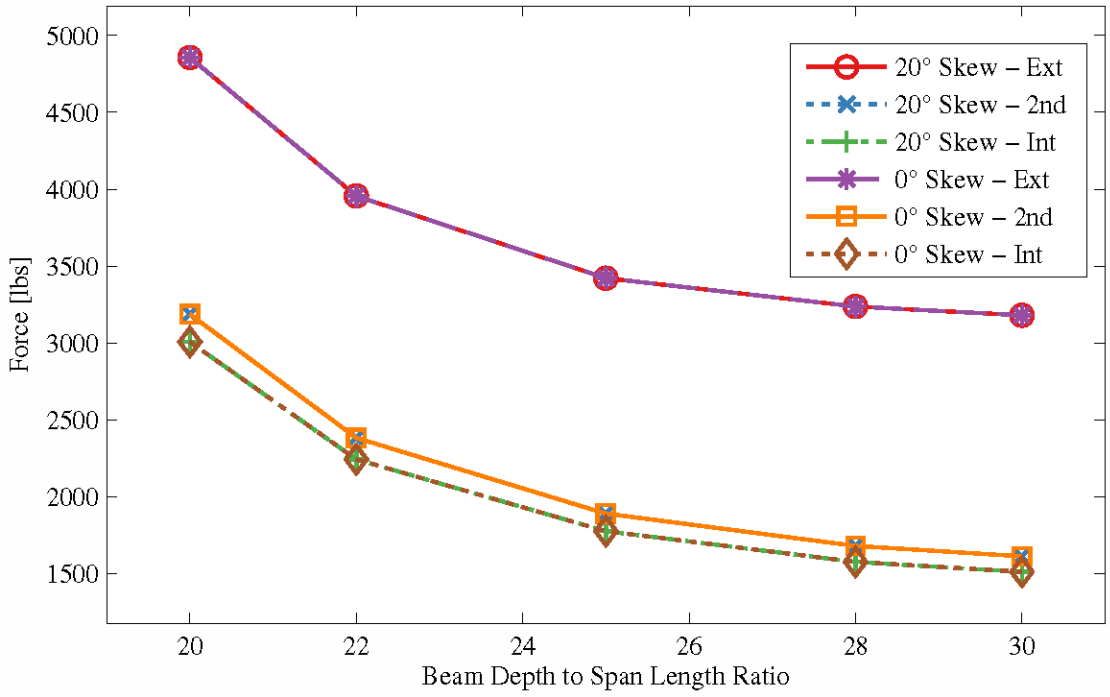

Figure D-42 - Effect of Span to Depth Ratio on Vertical Reaction at the Support